



National Library
of Canada

Acquisitions and
Bibliographic Services Branch

395 Wellington Street
Ottawa, Ontario
K1A 0N4

Bibliothèque nationale
du Canada

Direction des acquisitions et
des services bibliographiques

395, rue Wellington
Ottawa (Ontario)
K1A 0N4

Your file / Votre référence

Our file / Notre référence

AVIS

The quality of this microform is heavily dependent upon the quality of the original thesis submitted for microfilming. Every effort has been made to ensure the highest quality of reproduction possible.

If pages are missing, contact the university which granted the degree.

Some pages may have indistinct print especially if the original pages were typed with a poor typewriter ribbon or if the university sent us an inferior photocopy.

Reproduction in full or in part of this microform is governed by the Canadian Copyright Act, R.S.C. 1970, c. C-30, and subsequent amendments.

AVIS

La qualité de cette microforme dépend grandement de la qualité de la thèse soumise au microfilmage. Nous avons tout fait pour assurer une qualité supérieure de reproduction.

S'il manque des pages, veuillez communiquer avec l'université qui a conféré le grade.

La qualité d'impression de certaines pages peut laisser à désirer, surtout si les pages originales ont été dactylographiées à l'aide d'un ruban usé ou si l'université nous a fait parvenir une photocopie de qualité inférieure.

La reproduction, même partielle, de cette microforme est soumise à la Loi canadienne sur le droit d'auteur, SRC 1970, c. C-30, et ses amendements subséquents.

University of Alberta

Aspects of Radiative Corrections for Heavy Quark
Decays



by
Andrzej Prus Czarnecki

A thesis
presented to the Faculty of Graduate Studies and Research
in partial fulfilment of the requirements for the degree
of

Doctor of Philosophy
in
Theoretical Physics

Department of Physics

Edmonton, Alberta
Fall 1993



National Library
of Canada

Acquisitions and
Bibliographic Services Branch

395 Wellington Street
Ottawa, Ontario
K1A 0N4

Bibliothèque nationale
du Canada

Direction des acquisitions et
des services bibliographiques

395, rue Wellington
Ottawa (Ontario)
K1A 0N4

Your file: Votre référence

Our file: Notre référence

The author has granted an irrevocable non-exclusive licence allowing the National Library of Canada to reproduce, loan, distribute or sell copies of his/her thesis by any means and in any form or format, making this thesis available to interested persons.

L'auteur a accordé une licence irrévocable et non exclusive permettant à la Bibliothèque nationale du Canada de reproduire, prêter, distribuer ou vendre des copies de sa thèse de quelque manière et sous quelque forme que ce soit pour mettre des exemplaires de cette thèse à la disposition des personnes intéressées.

The author retains ownership of the copyright in his/her thesis. Neither the thesis nor substantial extracts from it may be printed or otherwise reproduced without his/her permission.

L'auteur conserve la propriété du droit d'auteur qui protège sa thèse. Ni la thèse ni des extraits substantiels de celle-ci ne doivent être imprimés ou autrement reproduits sans son autorisation.

ISBN 0-315-88336-7

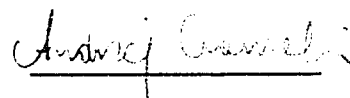
Canada

UNIVERSITY OF ALBERTA
RELEASE FORM

NAME OF AUTHOR: Andrzej Prus Czarnecki
TITLE OF THESIS: Aspects of Radiative Corrections for
Heavy Quark Decays
DEGREE: Doctor of Philosophy
YEAR THIS DEGREE GRANTED: 1993

Permission is hereby granted to the University of Alberta library to reproduce single copies of this thesis and to lend such copies for private, scholarly or scientific research purposes only.

The author reserves other publication rights, and neither the thesis or extensive extracts from it may be printed or otherwise reproduced without the author's written permission.



Andrzej Prus Czarnecki

10960 - 35A Ave.


Edmonton, Alberta, T6J 0A3

Date: August 26th, 1993

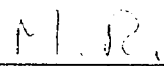
UNIVERSITY OF ALBERTA

FACULTY OF GRADUATE STUDIES AND RESEARCH

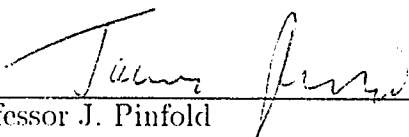
The undersigned certify that they have read, and recommend to the Faculty of Graduate Studies and Research for acceptance, a thesis entitled "Aspects of Radiative Corrections for Heavy Quark Decays" submitted by Andrzej Prus Czarnecki in partial fulfilment of the requirements for the degree of Doctor of Philosophy in Theoretical Physics



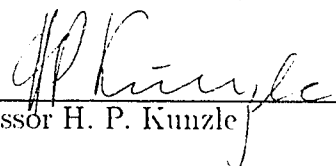
Professor A. N. Kamal, Supervisor



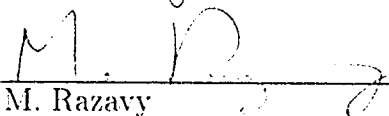
Professor S. Dawson



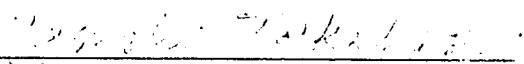
Professor J. Pinfold



Professor H. P. Kunzle



Professor M. Razavy



Professor Y. Takahashi

Date: August 22nd, 1992

Abstract

Various aspects of heavy quark decays are analyzed in the framework of the Standard Model, and its extension suggested by supersymmetry in which two Higgs doublets are present. Quantum chromodynamic corrections are calculated for the energy spectrum of hadronic products and for the angular distributions of charged leptons in semileptonic decays, as well as to the total rate of the decay of top quark into bottom quark and W boson. Both QCD and electroweak corrections are given for a decay in which the W boson is replaced by a charged Higgs boson. Similarities between QCD corrections in both channels are analyzed with help of the Equivalence Theorem. Finally, a recently proposed method for doing two loop calculations is illustrated with the example of the anomalous magnetic moment of an electron and a possibility of its application to a future calculation of two loop corrections to the top quark width is discussed.

Acknowledgments

I would like to express my gratitude to Professor A.N. Kamal for his constant help, encouragement and advice, for prompt reading and friendly criticism on my manuscripts, and for his kind support during my doctoral studies at the University of Alberta.

Special acknowledgment is due to Professor Marek Jeřabek for introducing me to the field of radiative corrections and supervising my work during a year of my doctoral studies at the Jagellonian University in Cracow.

I am also indebted to the members of the supervisory committee, especially to Professor M. Razavy and Professor Y. Takahashi, for their interest in my work and for many helpful discussions. I thank Professor J. Pinfeld for the opportunity to use the computing facilities of the Subatomic Research Center of the University of Alberta. I express sincere thanks to Professor H. Sherif for his help, advice, and interest in my doctoral studies. I am very grateful to all the members of the supervisory committee for careful reading of the draft of this thesis and suggesting many corrections.

It is a pleasure to acknowledge enjoyable collaboration with Professor J.H. Kühn, whom I also thank for the opportunity to visit Max Planck Institute in Munich, and with Dr. Sacha Davidson.

Finally, I would like to thank my parents for constant support and encouragement, and my wife Weronika for understanding and patience during the time when this thesis was being completed.

My research has been supported by Isaac Walton Killam Memorial Doctoral Scholarship and the University of Alberta Dissertation Fellowship. I am grateful to the University of Alberta Graduate Scholarship Committee for giving me these awards.

Contents

1	Introduction	1
1.1	About this thesis	1
1.2	Elements of perturbative QCD	3
1.2.1	QCD Lagrangian and quantization	3
1.2.2	BRST Symmetry and Slavnov-Taylor identities	5
1.2.3	Evaluation of Z_1 and Z_3	7
1.2.4	β function to one loop	9
2	Aspects of Semileptonic Decays of Heavy Quarks	13
2.1	QCD Corrections to Hadron Spectrum	14
2.1.1	Introduction	14
2.1.2	Born approximation	16
2.1.3	Virtual QCD corrections	18
2.1.4	Real gluon radiation	19
2.1.5	Total first order QCD effects	20
2.1.6	Discussion of the results	23
2.2	Lepton Spectra from Decays of Polarized Top Quarks	25
2.2.1	Introduction	25
2.2.2	Corrections to Decays of Polarized t Quarks	26
2.2.3	Discussion of the results	29
2.2.4	A formula for $\Delta H_2(x, y, z)$	31
2.2.5	Integration over Euler angles	32
2.2.6	Algebraic evaluation of the integrals	33
3	Total rate of the decay $t \rightarrow W^+ b$	36
3.1	Introduction	36
3.2	Limiting case of $m_b = m_W = 0$	38

3.3	Virtual corrections	39
3.4	Real gluon effects	40
4	Decay $t \rightarrow H^+ b$	46
4.1	Introduction	46
4.2	Limiting case of a very heavy top quark	47
4.3	Effects of b and H^+ masses	50
4.3.1	QCD Corrections	51
4.3.2	Discussion	54
4.3.3	Summary	58
4.3.4	Details of the calculation	58
4.4	QCD corrections to two body decays of the top	59
4.4.1	Structure of counterterms	60
4.4.2	Equivalence Theorem	61
4.4.3	Summary	64
5	Electroweak corrections to decays involving a charged Higgs boson	65
5.1	Introduction	65
5.2	Renormalization scheme	66
5.3	Remarks on cancellation of divergences	69
5.4	Vertex corrections	71
5.5	Real photon radiation	73
5.6	Results and discussion	76
5.7	Renormalization constants	78
6	On the calculation of the anomalous magnetic moment of the electron	84
6.1	Introduction	84
6.2	Integrals $M(\alpha_1, \alpha_2, \alpha_3, \alpha_4, \alpha_5)$	86
6.2.1	Relation M_1	88
6.2.2	Relation M_7	88
6.3	Integrals $N(\alpha_1, \alpha_2, \alpha_3, \alpha_4, \alpha_5)$ and a summary of recurrence relations	89
6.4	Analytic formulas for some of the integrals	89
6.5	Calculation of the anomalous magnetic moment	91
6.5.1	Vacuum polarization contribution	91

6.5.2	Two-photon contributions	95
6.6	On the two loop corrections to top decay	99
7	Conclusions and Outlook	101
	Bibliography	103

List of Tables

1.1	Contributions of diagrams in Figure 1.1	10
5.1	Particle contents of triangle diagrams. The last column shows the coefficient of $\frac{\alpha}{4\pi} \frac{2}{4-n}$ in δ_{Δ}^l and δ_{Δ}^r	74
6.1	Notation used for labeling the recurrence relations.	87
6.2	Useful relations for integrals N	90
6.3	Useful relations for integrals M	90
6.4	Contributions of diagrams in Figure 6.2 to the anomalous mag- netic moment of the electron.	98

List of Figures

1.1	Processes contributing to three gluon vertex to one loop	8
1.2	Processes contributing to gluon self interaction	10
2.1	Tree level process $t \rightarrow b\bar{l}\nu_l$	13
2.2	Real gluon radiation	14
2.3	Vertex correction	15
2.4	Normalized distribution of the total energy of hadrons shown for $m_t = 40, 60$ and 80 GeV in the Born approximation. . . .	17
2.5	First order QCD correction $R(x_h)$ to the distribution of the total energy of hadrons.	21
2.6	Normalized distribution of the total energy of hadrons for $m_t = 120$ GeV in the region of the peak.	25
2.7	The ratio R , see eq. (2.44), for $m_b = 5$ GeV and $m_t = 80, 120$ and 160 GeV (solid lines), and for $\epsilon = 0$, $m_t = 80$ and 160 GeV (dashed lines)	30
3.1	Tree level process $t \rightarrow W^+b$	37
4.1	Ratio of the first order correction to the Born rate for $\tan \beta = 1$ and $m_t = 150$ GeV: $m_b = 4.5$ GeV (Model I - solid, Model II - dotted), $m_b = 0$ (dash-dotted line).	55
4.2	Ratio of the branching ratios of $t \rightarrow bH^+$ and $t \rightarrow bW^+$ for $m_b = 4.5$ GeV: in the Model I with and without QCD corrections (solid and dashed lines, indistinguishable) and in the Model II (dotted and dash-dotted lines, respectively). . . .	56
4.3	Real gluon radiation amplitudes	62
4.4	Virtual one loop amplitudes	62

5.1	Types of tadpole diagrams in 2HDM	69
5.2	Mixing between the charged Higgs and the Goldstone boson	70
5.3	Momentum independent contributions to mixing	70
5.4	Mixing between the charged Higgs and the W boson	70
5.5	Vertex corrections to the decay of t quark	72
5.6	Vertex corrections to the charged Higgs boson decay	72
5.7	Real photon corrections to the decay of t quark	75
5.8	Real photon corrections to the charged Higgs boson decay	75
5.9	Bosonic contributions to corrections $\Delta\Gamma$ (solid line) and the fermionic contributions from which twice the value of universal corrections Δr was subtracted (dashed). Plotted as a function of m_{H^+} for $\tan\beta = 1.5$	81
5.10	Corrections $\overline{\Delta\Gamma}$ plotted as a function of m_{H^+} for various values of $\tan\beta$: $\tan\beta = 0.5$ (solid line), $\tan\beta = 1.5$ (long dash) and $\tan\beta = 5$ (short dash)	82
5.11	Corrections $\overline{\Delta\Gamma}$ plotted as a function of $\tan\beta$ for two different values of m_{H^+} : $m_{H^+} = 90$ GeV (solid line) and $m_{H^+} = 120$ GeV (dashed)	83
6.1	Vacuum polarization contribution to the anomalous magnetic moment	92
6.2	Two photon contributions to the anomalous magnetic moment	96

Chapter 1

Introduction

1.1 About this thesis

This thesis is devoted to the study of quantum corrections, especially in the context of top quark decay. Top quark decays have been studied theoretically for several years to find convenient, detectable signatures: a lot of work has been devoted to semileptonic decays [1, 2]. As the top has not yet been found, it is probably too heavy to be seen at present accelerators; there is now strong evidence that the top is actually substantially heavier than the weak gauge bosons. If this is the case, the dominant decay channel should be $t \rightarrow W^+b$. Since this is a two body decay, various corrections to its rate can be calculated with relatively little effort. Moreover, such calculations are of large practical importance, e.g., for a correct description of threshold phenomena in top production.

Once the QCD and electroweak corrections became known, non-standard possibilities for top decay were considered. The first effect coming to mind is an enlarged Higgs sector, which frequently includes a second doublet. This implies a charged Higgs, which, if it were heavier than the top quark, would contribute additional virtual corrections to the decay $t \rightarrow W^+b$. This effect has been studied in ref. [3, 4] and can be as large as 10% of the total decay rate. On the other hand, if the top quark is heavier than the charged Higgs, the decay $t \rightarrow H^+b$ becomes possible [5]. Various corrections to this reaction have been studied as well.

Original results concerning QCD corrections to top quark decays pre-

sented in this thesis are the following: energy spectrum of hadronic products of a semileptonic decay of the t quark, angular distribution and energy spectrum of a lepton produced in a decay of a polarized t quark and the total decay rate of the t quark into a b quark and a charged Higgs boson (in models with an extended Higgs sector). In the context of this last decay channel the electroweak corrections are also given. In addition, a few known results are rederived using improved methods: QCD corrections to the total decay rate of the t quark into a b quark and a W boson are calculated using dimensional regularization and the two-loop anomalous magnetic moment of the electron is computed using an algebraic method proposed recently by Broadhurst et al. This last result is included for the reason that a similar method might also be successful in estimating two-loop QCD corrections to the top decay in the limit of a large mass of the top.

Results presented in Chapter 2 were derived in collaboration with M. Jezabek and J.H. Kühn, and were published in ref. [6, 7]. Part of Chapter 3 appeared in ref. [8]. QCD corrections to the decay $t \rightarrow H^+b$ were calculated with Sacha Davidson and were partially published in ref. [9, 10, 11]. The two loop calculation of the anomalous magnetic moment of the electron was done with A.N. Kamal and appeared in ref. [12]. The material of Chapter 5 has been submitted for publication [13].

This thesis is organized as follows. In the reminder of the Introduction some elements of perturbative quantum chromodynamics are summarized in order to justify its application to the top decays. In Chapter 2 QCD corrections to semileptonic decays of the top are considered. The next Chapter is devoted to the application of the dimensional regularization to the corrections to the total decay rate of $t \rightarrow W^+b$ and in Chapter 4 total decay rate of $t \rightarrow H^+b$ is examined. Chapter 5 is devoted to the study of electroweak corrections to the decay $t \rightarrow H^+b$ in an extension of the Standard Model motivated by supersymmetry. In the last Chapter the algebraic method of Broadhurst et al. is applied to the calculation of the two-loop anomalous magnetic moment of the electron. The possible application of this method to the problem of the top quark width is discussed. The results obtained in this thesis are summarized in Conclusions and Outlook.

1.2 Elements of perturbative QCD

Effects of Quantum Chromodynamics in processes involving large momentum transfers, like decays of heavy quarks or deep inelastic scattering, can be calculated using perturbation theory. The following chapters will bring examples of calculations of various quantities in this framework, and here a justification of this procedure is given. The basic observation which will be made is that the effective coupling constant of QCD decreases with the momentum transfer. This is expressed in the following formula:

$$\alpha(Q^2) = \frac{1}{b_f \ln \frac{Q^2}{\Lambda_{QCD}^2}} \quad (1.1)$$

where Q^2 is the square of momentum transfer characteristic for a given process and Λ_{QCD} is energy scale of QCD, of the order of few hundred MeV. The dimensionless coefficient b_f can be calculated perturbatively and the one loop calculation will be given below. Much of this exposition is based on ref. [14, 15]. However, the calculation of b_f can be done in many ways (four different ways follow already from Slavnov-Taylor identities). The approach followed here is not the simplest one; it is based on the renormalization of the three gluon vertex, which was first calculated by Celmaster and Gonsalves [16] and cannot be found in standard textbooks due to the length of calculation. It will be presented to show various calculational techniques and usefulness of algebraic manipulation programs.

This section is organized as follows. First the Lagrangian of QCD is introduced. Second, BRS symmetry of the quantum version of the Lagrangian is examined and Slavnov-Taylor identities are derived. The set of renormalization constants of QCD is defined and two of them are calculated. Finally, the results are used to find the evolution equation of the effective coupling constant.

1.2.1 QCD Lagrangian and quantization

On the classical level the Lagrangian density of quantum chromodynamics, describing interaction of quark fields ψ with gluon field A_μ^a , is written in the following form (only one flavour of quarks is taken into consideration; space-time dependence is not shown explicitly, wherever this does not lead

to confusion):

$$\mathcal{L} = -\frac{1}{4}F_{\mu\nu}^a F^{a\mu\nu} + \bar{\psi}(i \not{D} - m)\psi, \quad (1.2)$$

where the field strength tensor is:

$$F_{\mu\nu}^a = \partial_\mu A_\nu^a - \partial_\nu A_\mu^a + gf^{abc} A_\mu^b A_\nu^c, \quad (1.3)$$

and the covariant derivative is:

$$D_\mu = \partial_\mu - igT^a A_\mu^a. \quad (1.4)$$

T^a are matrices of the $SU(3)$ algebra, which satisfy $[T^a, T^b] = if^{abc}T^c$, where f^{abc} are the structure constants of $SU(3)$. The quark fields belong to the fundamental, and the gluon fields to the adjoint representation. This Lagrangian is then invariant under the non-Abelian $SU(3)$ group of local transformations:

$$\begin{aligned} \psi &\rightarrow \psi' = U\psi \\ T^a A_\mu^a &\rightarrow T^a A_\mu^{a'} = U \left(T^a A_\mu^a - \frac{i}{g} U^{-1} \partial_\mu U \right) U^{-1}, \end{aligned} \quad (1.5)$$

where $U = \exp(-iT^a\Theta^a)$, with Θ^a being space-time dependent parameters of the transformation. It is because of this symmetry of the theory that one encounters difficulties with the quantization. The reason for these difficulties is the invariance of the Lagrangian under transformations containing an arbitrary space-time function [17]. The second Noether theorem [18] states that as a consequence of this invariance the equations of motion are not independent. Intuitively it is clear that we cannot describe in a canonical way the time evolution of a dynamical variable, which can be changed by an arbitrary time-dependent function without affecting the action. For this reason the classical Lagrangian (1.2) cannot serve as a basis for quantization. This is also seen if one tries to compute the canonical momenta, for it turns out that the one conjugate to A_0^a vanishes:

$$\Pi_0^a = \frac{\partial \mathcal{L}}{\partial \dot{A}^{a0}} = -F_{00}^a = 0, \quad (1.6)$$

thus contradicting the canonical commutation relations.

The way to deal with this difficulty is to specify the gauge by imposing a subsidiary condition $C_a = 0$, where C_a is some function of fields. This allows us to specify which variables in the Lagrangian are dynamical and proceed with quantization using this subset. In practice one can retain all the original variables but introduce additional anticommuting scalar fields obeying Fermi statistics (Faddeev-Popov ghosts) which cancel contributions from the non-physical degrees of freedom (called also zero modes; a good guide to the original literature in this problem is given in [19]; see also [20]). The same method of quantization can be used in theories with spontaneously broken symmetry. A procedure of obtaining the Lagrangian of the theory quantized in this way has been given by 't Hooft and Veltman [21, 22].

In practical calculations in QCD it is useful to take a subsidiary condition of the form $\partial^\mu A_\mu^a = 0$ which corresponds to the Lorentz gauge. With this choice the gauge fixing term which we add to the Lagrangian is $-(\partial^\mu A_\mu^a)^2/2\alpha$, with $(1/2\alpha)$ playing the role of a Lagrange multiplier.

1.2.2 BRST Symmetry and Slavnov-Taylor identities

After the addition of the gauge fixing term and compensating for its side effects by introducing Faddeev-Popov ghosts the QCD Lagrangian becomes:

$$\begin{aligned}
\mathcal{L} &= \mathcal{L}_G + \mathcal{L}_{GF} + \mathcal{L}_{FP} + \mathcal{L}_F \\
\mathcal{L}_G &= -\frac{1}{4}F_{\mu\nu}^a F^{a\mu\nu} \quad (\text{gauge term}), \\
\mathcal{L}_{GF} &= -\frac{1}{2\alpha} (\partial^\mu A_\mu^a)^2 \quad (\text{gauge fixing}), \\
\mathcal{L}_{FP} &= i(\partial^\mu \chi_1^a) D_\mu^{ab} \chi_2^b \quad (\text{Faddeev - Popov term}), \\
\mathcal{L}_F &= \bar{\psi}^i (i \not{D}^{ij} - m \delta^{ij}) \psi^j \quad (\text{fermion term}). \tag{1.7}
\end{aligned}$$

As opposed to its classical version (1.2), the quantum Lagrangian of QCD is no longer invariant under gauge transformation. However, it possesses another symmetry, which has been discovered by Becchi, Rouet and Stora [23, 24] and, independently, by Tyutin [25], and is called BRST symmetry. It consists in the invariance under the local gauge transformation with $\Theta^a(x) = -g\omega\chi_2^a(x)$ with ω being a constant anticommuting quantity (Grassman number), so that $\{\omega, \omega\} = \{\psi, \omega\} = \{\chi_i, \omega\} = 0$ [26]. The transformation rule of the ghost fields is adjusted so that the Lagrangian remains

invariant, up to a total derivative:

$$\begin{aligned}
\psi_i &\rightarrow \psi'_i = \psi_i + \frac{i}{2} g \omega \lambda_{ij}^a \lambda_2^a \psi_j, \\
\bar{\psi}_i &\rightarrow \bar{\psi}'_i = \bar{\psi}_i - \frac{i}{2} g \bar{\psi}_j \omega \lambda_{ji}^a \lambda_2^a, \\
A_\mu^a &\rightarrow A'^a_\mu = A_\mu^a + g \omega f^{abc} A_\mu^b \lambda_2^c + \omega \partial_\mu \lambda_2^a, \\
\lambda_1^a &\rightarrow \lambda'^a_1 = \lambda_1^a + i \frac{\omega}{\alpha} \partial^\mu A_\mu^a, \\
\lambda_2^a &\rightarrow \lambda'^a_2 = \lambda_2^a - \frac{\omega}{2} g f^{abc} \lambda_2^b \lambda_2^c.
\end{aligned} \tag{1.8}$$

Since this is a particular case of a gauge transformation, the classical part of Lagrangian remains invariant, whereas the variations of the gauge fixing and ghost terms combine to give a total derivative:

$$\delta(\mathcal{L}_{GF} + \mathcal{L}_{FP}) = -\frac{\omega}{\alpha} \partial^\mu \left[(\partial^\nu A_\nu^a) D_\mu^{ab} \lambda_2^b \right]. \tag{1.9}$$

BRST symmetry of the quantum Lagrangian plays a very important role in the canonical quantization of QCD. In fact an approach different to the Faddeev-Popov method is possible: one begins with the requirement of BRST symmetry and then constructs the general Lagrangian dependent on classical fields as well as ghosts [27].

As a particular application of BRST one can derive Slavnov-Taylor identities - relations between Green's functions which are a generalization of Ward-Takahashi identities of QED [28, 29] to the non-Abelian case [30, 31]. These identities ensure "charge universality" in QCD. We observe that in the quantum Lagrangian of QCD there are four types of terms containing the strong coupling constant g ; they are responsible for triple and quartic gluon interactions and for ghost-gluon and fermion-gluon vertices. However, quantum effects result in the necessity of renormalization. The question arises whether or not the corrections to the above four vertices lead to the same renormalization of the coupling constant. In perturbation theory the infinities arising in the process of renormalization can be factored out explicitly in renormalization constants. One writes the bare quantities in the form $\phi = Z_\phi^{1/2} \phi_r$ and $n = Z_n n_r$, where ϕ denotes gluon, ghost and quark fields and n - parameters like masses, coupling constant or the gauge parameter α .

Consistent renormalization of all four types of interactions is necessary to preserve the BRST invariance of the Lagrangian. This imposes restrictions

on the number of independent counterterms. A set consistent with BRST turns out to be sufficient to render all diagrams finite to an arbitrary order in perturbation theory (for an elegant proof see [19]). It follows that we can calculate the charge renormalization constant Z_g in four different ways:

$$Z_g = \frac{Z_1}{Z_3^{3/2}} = \frac{Z_4^{1/2}}{Z_3} = \frac{\tilde{Z}_1}{\tilde{Z}_3 Z_3^{1/2}} = \frac{Z_{1F}}{Z_2 Z_3^{1/2}}. \quad (1.10)$$

Z_1 , \tilde{Z}_1 , Z_4 and Z_{1F} are counterterms for the four types of vertices mentioned above, in the respective order. Z_2 , Z_3 and \tilde{Z}_3 are wave function renormalization constants fermions, gluons and ghosts respectively. Our aim now will be to calculate Z_g , which will be used later to derive an evolution equation for the coupling constant. We will employ the first relation in (1.10).

1.2.3 Evaluation of Z_1 and Z_3

We first calculate the one-loop renormalization constant Z_1 . We have to evaluate the divergent parts of diagrams shown in Figure 1.1. Since the result has dimension 1, the divergent terms have to be constructed using one four-vector. The most general form of the contribution of the n th diagram can be parametrized by three unknowns:

$$\Lambda_{\mu\nu\lambda}^{(n)abc}(p, q, r) = -\frac{ig_r^3}{(4\pi)^2} f^{abc} [A(p-q)_\lambda g_{\mu\nu} + B(q-r)_\mu g_{\nu\lambda} + C(r-p)_\nu g_{\mu\lambda}]. \quad (1.11)$$

A simple method of doing this calculation consists in multiplying each amplitude by the three tensors on the RHS of the above equation and solving the system of three linear equations obtained in this way for the coefficients A , B , C . This procedure will be illustrated with an example of the gluon triangle loop (see Figure 1.1(c)).

Using the notation of [14] Feynman rule for the three gluon vertex is:

$$-igf^{abc}V_{\mu\nu\lambda}(p, q, r), \quad (1.12)$$

where

$$V_{\mu\nu\lambda}(p, q, r) = (p-q)_\lambda g_{\mu\nu} + (q-r)_\mu g_{\nu\lambda} + (r-p)_\nu g_{\mu\lambda}. \quad (1.13)$$

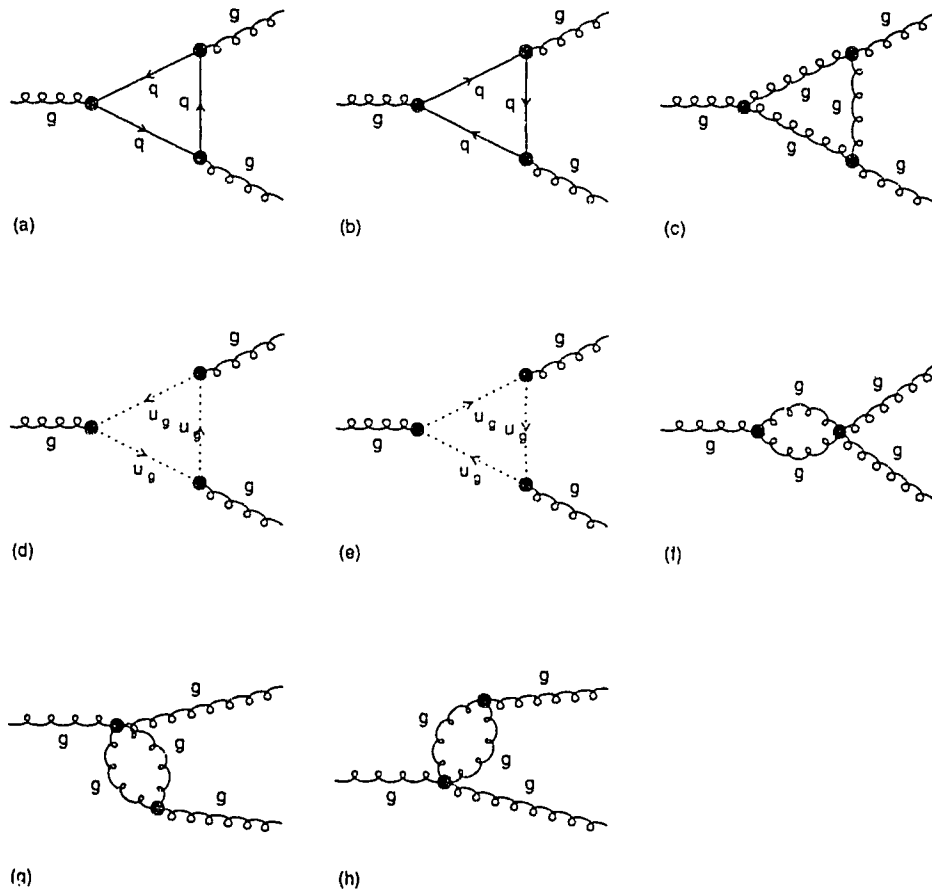


Figure 1.1: Processes contributing to three gluon vertex to one loop

For simplicity the Feynman gauge is used in this calculation. Although renormalization constants are gauge dependent, this dependence cancels out in β function, which we want to find. Using this notation the amplitude corresponding to the diagram 1.1(c) is:

$$\begin{aligned} \Lambda_{\mu\nu\lambda}^{(n)abc}(p, q, r) = & (-ig_r)^3 f^{aij} f^{ibl} f^{lck} \int \frac{d^D k}{(2\pi)^D} \frac{1}{k^2(k+p)^2(k+p+r)^2} \\ & V_{\mu\alpha\beta}(p, k, -k-p) V_{\alpha\nu\gamma}(-k, -r-p, k+r+p) V_{\gamma\omega\beta}(-k-r-p, r, k+p), \end{aligned} \quad (1.14)$$

where the integration is performed in $D = 4 - 2\varepsilon$ dimensional space. It is at this stage that the algebraic manipulation program FORM [32] greatly simplifies the task at hand. By contracting this expression with the three tensorial structures and extracting the ultraviolet pole of the integral we obtain contribution of the gluon triangle:

$$\Lambda_{\mu\nu\lambda}^{(c)abc}(p, q, r) = -\frac{ig_r^3}{16\pi^2} \frac{39}{8} f^{abc} V_{\mu\nu\lambda}(p, q, r). \quad (1.15)$$

Contributions of the remaining diagrams are evaluated in the same way and the results are listed in Table 1.1 (N_F denotes the number of quark flavors). What remains to be calculated is the gluon wave-function renormalization constant Z_3 . Contributions arise from diagrams shown in Figure 1.2. As result we obtain to one loop:

$$\begin{aligned} Z_1 &= 1 - \frac{g_r^2}{(4\pi)^2} \left(\frac{2}{3} N_F - 2 \right) \frac{1}{\varepsilon}, \\ Z_3 &= 1 - \frac{g_r^2}{(4\pi)^2} \left(\frac{2}{3} N_F - 5 \right) \frac{1}{\varepsilon}. \end{aligned} \quad (1.16)$$

1.2.4 β function to one loop

Infinites which arise in calculation of quantum corrections are the reason for introducing counterterms. In a renormalizable theory the structure of counterterms is determined by the types of vertices present in the unrenormalized Lagrangian; a so-called renormalization scheme is a prescription: calculate loop corrections to the given vertex and subtract from the result the value of this vertex when external momenta assume certain values. The order of magnitude of these prescribed momenta is called the renormalization scale and

Table 1.1: Contributions of diagrams in Figure 1.1

Diagram	Coefficient of $-\frac{ig_s^3}{16\pi^2} f^{abc} V_{\mu\nu\lambda}(p, q, r)$
(a)+(b)	$\frac{2}{3}N_F$
(c)	$\frac{39}{8}$
(d)+(e)	$-\frac{1}{8}$
(f)+(g)+(h)	$-\frac{27}{4}$
Total	$\frac{2}{3}N_F - 2$

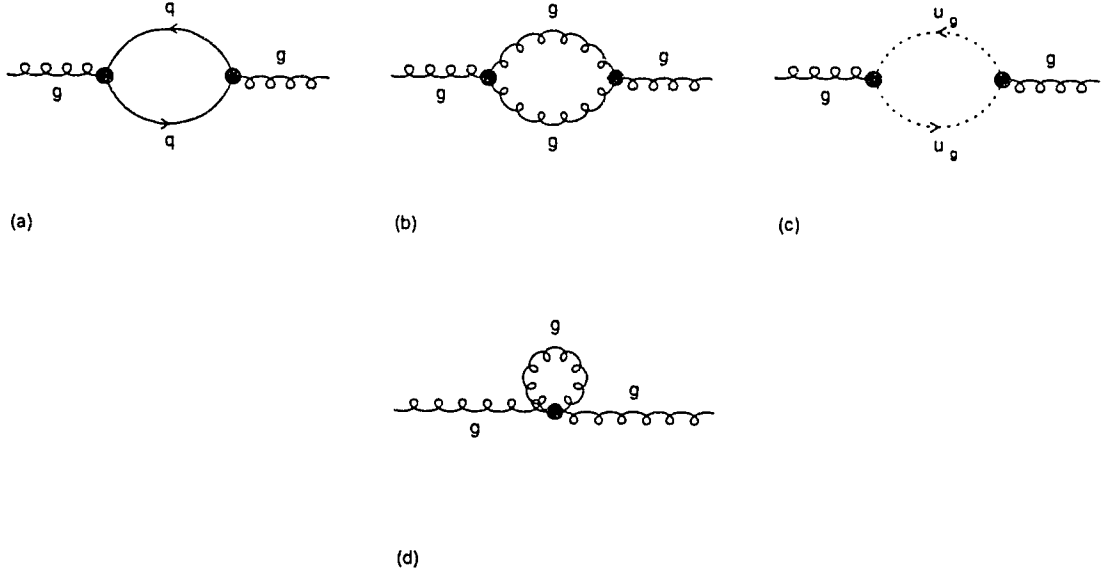


Figure 1.2: Processes contributing to gluon self interaction

we shall denote it by μ . In this way the renormalized parameters of the theory depend explicitly on renormalization scale. The magnitude of μ should be chosen to represent the typical size of momenta present in the process under consideration; otherwise there may arise terms dependent on the large ratio of the two scales which could destroy the validity of the perturbation theory. By examining the functional dependence of the coupling constant on the renormalization scale we can predict its behaviour at large momentum transfers, e.g. in decays of heavy quarks. This behaviour is governed by the β function which we will define and examine below. It has to be noted that the counterterms (1.16) calculated in the previous section are also dependent on the renormalization scale, although it was not shown explicitly. This dependence is contained in the coupling constant: in dimensional regularization the coupling constant acquires an infinitesimal dimension of mass. We now write down the bare and the renormalized coupling constant g and g_r with the mass dimension factored out explicitly. For the bare coupling constant we introduce an arbitrary scale μ_0 , and for the renormalized one it is the renormalization scale:

$$g \equiv g_0 \mu_0^\varepsilon, \quad g_r \equiv g_R \mu^\varepsilon. \quad (1.17)$$

The dimensionless constant g_R depends on μ both through the term $\mu^{-\varepsilon}$ and through the renormalization constant $Z_g(\mu)$. We now introduce the function β (in the minimal subtraction (MS) scheme):

$$\beta(g_R) \equiv \mu \frac{dg_R}{d\mu} = -\varepsilon g_R - \frac{\mu}{Z_g} \frac{dZ_g}{d\mu} g_R. \quad (1.18)$$

Recalling that $Z_g = Z_1 Z_3^{-3/2}$ we obtain:

$$Z_g = 1 - \frac{g_R^2}{(4\pi)^2} \left(-\frac{1}{3} N_F + \frac{11}{2} \right) \frac{1}{\varepsilon}, \quad (1.19)$$

so that the following equation can be written for the function β :

$$\beta(g_R) = -\varepsilon g_R + \frac{1}{\varepsilon} \frac{1}{(4\pi)^2} \left(-\frac{2}{3} N_F + 11 \right) g_R^2 \beta(g_R), \quad (1.20)$$

which can be solved iteratively to give:

$$\beta(g_R) = -\frac{1}{(4\pi)^2} \left(11 - \frac{2}{3} N_F \right) g_R^3 + o(g_R^3) \equiv -\beta_0 g_R^3 + \dots \quad (1.21)$$

We now want to find the value of the coupling constant for a process with a characteristic momentum scale Q^2 . From the definition of the β function we have

$$\frac{d\mu}{\mu} = \frac{dg_R}{\beta(g_R)}, \quad (1.22)$$

or, after integrating both sides from μ to $\sqrt{Q^2}$ and taking only the contributions of lowest order in g_R :

$$\ln \frac{Q}{\mu} = \int_{g_R(\mu)}^{g_R(Q)} \frac{dg_R}{\beta(g_R)} \equiv \frac{1}{2\beta_0} \left(\frac{1}{g_R^2(\mu)} - \frac{1}{g_R^2(Q)} \right). \quad (1.23)$$

with $Q \equiv \sqrt{Q^2}$. Now we obtain the desired formula (1.1):

$$g_R^2(Q) = \frac{1}{g_R^{-2}(\mu) + 2\beta_0 \ln(Q/\mu)} \equiv \frac{1}{\beta_0 \ln(Q^2/\Lambda^2)}, \quad (1.24)$$

where in the last step we have introduced a new dimensional parameter $\Lambda = \mu \exp[-1/(2\beta_0 g_R^2(\mu))]$. The value of this parameter has to be extracted from experiments. Currently known results (see [33] for a review) indicate that the strong coupling constant $\alpha_s = g_s^2/4\pi$ is of the order of 0.1 for the expected mass of the top quark between 90 and 200 GeV. This justifies applying perturbative QCD to calculations of radiative corrections to decays of the top. Several such calculations will be presented in the following chapters.

Chapter 2

Aspects of Semileptonic Decays of Heavy Quarks

In this chapter two aspects of QCD corrections in semileptonic decays of heavy quarks will be studied with the example of the decay $t \rightarrow b\bar{l}\nu_l$. The first one will be the energy spectrum of all hadronic products of such decay. Here QCD corrections are important as they open a new kinematically allowed region in which hadrons can be produced. This is because the tree level process shown in the Figure 2.1 is a three body reaction and hadrons produced from the quark b can carry energy not larger than half the mass of the decaying t quark (neglecting masses of the b quark and of the leptons; effects of the b quark mass (m_b) will be treated in detail later). If the first order QCD corrections are included we have to take into account real gluon radiation, shown in Figure 2.2, and the effects of vertex loops in Figure 2.3,

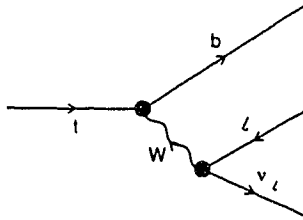


Figure 2.1: Tree level process $t \rightarrow b\bar{l}\nu_l$

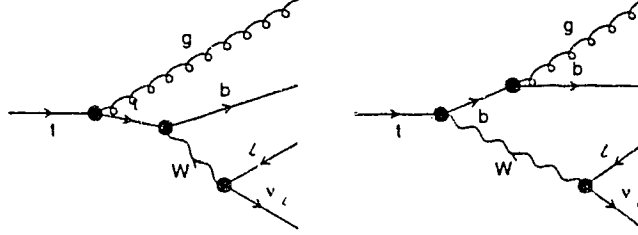


Figure 2.2: Real gluon radiation

together with counterterms. Now that the four body channel is open it is possible for the hadrons to carry away all the energy of the decaying quark. The second effect to be examined is the angular distribution of leptons produced in a decay of a polarized top quark. It is important to know the impact of QCD corrections in this case, because the angular distribution of leptons provides important means of observing CP violation in $t\bar{t}$ production [34]. In this chapter all calculations will be done using Pauli-Villars regularization. Infrared divergences will be dealt with by introducing a small mass λ of the gluon. Of course final results are independent of λ .

2.1 QCD Corrections to Hadron Spectrum

2.1.1 Introduction

Semileptonic decays of the top quark were studied in detail by Jezabek and Kühn in papers [1, 2, 35]. These authors have studied total rates and energy distributions of leptons. Those calculations were performed in the framework of the QCD improved parton model up to the first order in α_s . As is well known, the lepton spectra in semileptonic decays are free from QCD infrared divergences. In the present section the distribution of the total energy of hadrons E_h is calculated, another quantity free from infrared divergences. Infrared finiteness of this distribution follows from energy conservation and

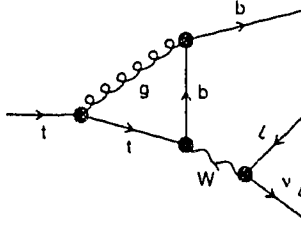


Figure 2.3: Vertex correction

infrared finiteness of the energy distribution for the virtual W .

In contrast to the case of lepton spectra the kinematic boundaries are different for the final states with and without hard gluons. Thus, studying energy distribution of hadrons or, equivalently, of the virtual W , one can obtain non-trivial information on the masses of the quarks involved as well as on α_s .

The top quark has not been discovered yet. However there are some indirect indications that its mass m_t should be between 90 and 200 GeV (for a recent review see e.g. [36]). Thus, the effects of the W propagator are of crucial importance in the case of the top quark decay. In particular, if m_t is large enough, production of real W dominates and in Born approximation the decay becomes quasi two-body. In this case the shape of the E_h distribution reflects the shape of the W and QCD corrections modify the corresponding Breit-Wigner distribution.

The formulas to be presented describe decays of free quarks. In order to compare them with the experiment one has to include bound state effects, for example the Fermi motion, see e.g. [37, 38, 1].

2.1.2 Born approximation

In the Born approximation the energy distribution of hadrons is given by:

$$\frac{d\Gamma^{(0)}}{dE_b} = \frac{1}{(2\pi)^3} \frac{1}{8m_t} \int_{E_l^{min}}^{E_l^{max}} |\mathcal{M}|^2 dE_l \quad (2.1)$$

with E_b , E_l denoting energies of the b quark and the charged lepton respectively. The limits of the integration over lepton energy are:

$$\begin{aligned} E_l^{min} &= \frac{1}{2} \left(m_t - E_b - \sqrt{E_b^2 - m_b^2} \right) \\ E_l^{max} &= \frac{1}{2} \left(m_t - E_b + \sqrt{E_b^2 - m_b^2} \right) \end{aligned} \quad (2.2)$$

It is practical to introduce dimensionless variables by taking mass of the top quark as the unit of energy [1]:

$$x_l = \frac{2E_l}{m_t}, \quad x_h = \frac{E_h}{m_t}, \quad \epsilon = \frac{m_b}{m_t}. \quad (2.3)$$

Here E_h denotes the total energy of hadronic products of the decay. On the level of the Born approximation, i.e., in the absence of gluons, this is just the energy the b quark. In the following the values of all kinematical variables for the vanishing four-momentum of the gluon in the final state (or, in the absence of the gluon) will be denoted by a bar: for example $\bar{x}_h = E_b/m_t$ in the case at hand. Four-momenta of the top quark, bottom quark, W boson, gluon, charged lepton and of its neutrino will be denoted by Q , q , W , G , l and ν respectively. It is also useful to define a four-vector $P = q + G$ representing the hadronic part of the final state. Following [1] further kinematical variables are defined:

$$y = \frac{W^2}{m_t^2}, \quad z = \frac{P^2}{m_t^2}, \quad \xi = \frac{m_t^2}{m_W^2}, \quad \gamma = \frac{\Gamma_W}{m_W}. \quad (2.4)$$

In the rest frame of the decaying quark the energy, three-momentum and rapidity of the hadrons are:

$$\begin{aligned} p_0 &= x_h, \\ p_3 &= \sqrt{x_h^2 - z}, \\ p_{\pm} &= p_0 \pm p_3, \\ Y_p &= \frac{1}{2} \ln \frac{p_+}{p_-}. \end{aligned} \quad (2.5)$$

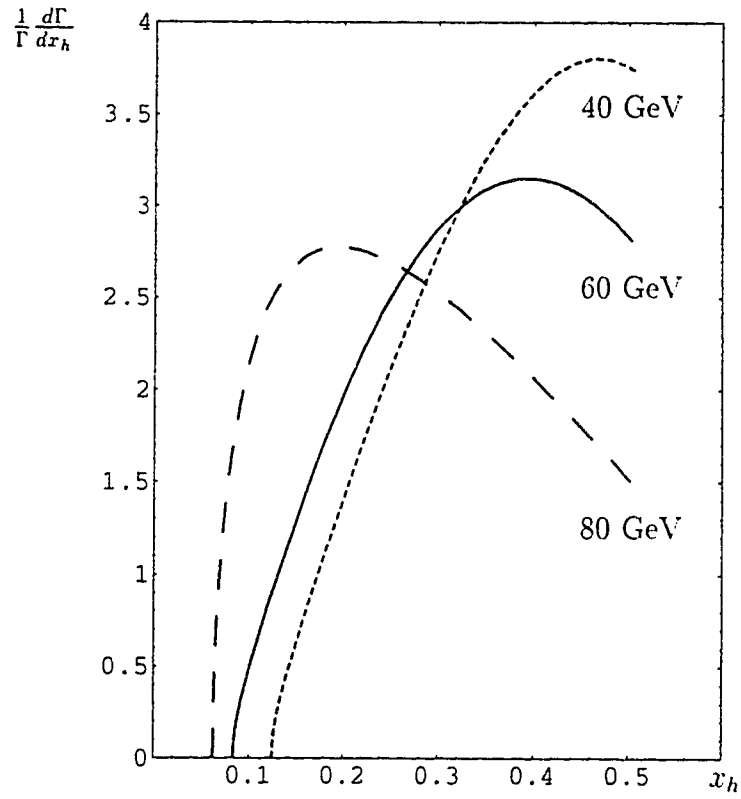


Figure 2.4: Normalized distribution of the total energy of hadrons shown for $m_t = 40, 60$ and 80 GeV in the Born approximation.

and for the leptons:

$$\begin{aligned}
w_0 &= 1 - x_h, \\
w_3 &= p_3, \\
w_{\pm} &= w_0 \pm w_3, \\
Y_w &= \frac{1}{2} \ln \frac{w_+}{w_-}.
\end{aligned} \tag{2.6}$$

Values of these variables for $G = 0$ are obtained by putting $z = \epsilon^2$ in the above formulas. For example $\bar{p}_3 = \sqrt{x_h^2 - \epsilon^2}$.

Since masses of leptons can safely be neglected in this calculation, the square of the invariant matrix element can be written as:

$$|\mathcal{M}|^2 = \frac{64G_F^2}{(1 - \xi\bar{y})^2 + \gamma^2} (Q \cdot l)(q \cdot \nu), \tag{2.7}$$

where the finite width of the W boson has been taken into account. Upon integration over lepton energy this leads to the hadron energy distribution:

$$\frac{d\Gamma^{(0)}}{dx_h} = -\frac{G_F^2 m_l^5}{12\pi^3} \frac{\bar{p}_3 \bar{u}}{(1 - \xi\bar{y})^2 + \gamma^2}, \tag{2.8}$$

where

$$y(x_h, z) = 1 + z - 2x_h, \tag{2.9}$$

$$u(x_h, z) = -x_h(3 - 4x_h) - z(3x_h - 2). \tag{2.10}$$

and $\bar{y} = y(x_h, \epsilon^2)$, $\bar{u} = u(x_h, \epsilon^2)$. This result is shown in Figure 2.4.

2.1.3 Virtual QCD corrections

The contribution of virtual gluons arises from the interference of the process depicted in Figure 2.3 with the Born amplitude (Figure 2.1). The vertex correction is ultraviolet as well as infrared divergent. The ultraviolet divergence is cancelled by wave function renormalization of the external quark legs.

In Pauli-Villars regularization this amplitude can be calculated in the same manner as the QED virtual correction to the muon decay [39, 40, 41]. The resulting contribution to the decay rate is:

$$\frac{d\Gamma_V^{(1)}}{dx_h} = \frac{1}{(2\pi)^5} \frac{2\alpha_s}{3\pi} \frac{64G_F^2}{(1-\xi\bar{y})^2 + \gamma^2} \int H_{\alpha\beta} L^{\alpha\beta} dR_2(Q; q, W) dR_2(W; l, \nu),$$

where $dR_2(P; p_1, p_2)$ is a two body phase space element:

$$dR_2(P; p_1, p_2) = \delta^4(P - p_1 - p_2) \frac{d^3p_1}{2p_1^0} \frac{d^3p_2}{2p_2^0}. \quad (2.11)$$

$L^{\alpha\beta}$ stands for the leptonic tensor for which we have:

$$\begin{aligned} \int L^{\alpha\beta} dR_2(W; l, \nu) &\equiv \int \nu^\alpha l^\beta dR_2(W; l, \nu) \\ &= \frac{\pi}{24} (\bar{y} g^{\alpha\beta} + 2W^\alpha W^\beta), \end{aligned} \quad (2.12)$$

and $H^{\alpha\beta}$ is the renormalized hadronic tensor given in [1].

The final formula for the virtual correction is:

$$\begin{aligned} \frac{d\Gamma_V^{(1)}}{dx_h} = & -\frac{2\alpha_s}{3\pi} \frac{G_F^2 m_l^5}{12\pi^3} \frac{1}{(1-\xi\bar{y})^2 + \gamma^2} \left\{ -2x_h \bar{u} \left[\text{Li}_2 \left(1 - \frac{\bar{p}_- \bar{w}_-}{\bar{p}_+ \bar{w}_+} \right) \right. \right. \\ & - \text{Li}_2 \left(1 - \frac{\bar{w}_-}{\bar{w}_+} \right) \left. \right] + \bar{p}_3 \left[\frac{1}{y} \ln \epsilon \left(2x_h^2 (\epsilon^2 - 1) - \bar{u} (1 - \epsilon^2 - 2\bar{y}) \right) - 4\bar{u} \right] \\ & + \bar{Y}_p \left[\epsilon^2 (-12x_h + 4\epsilon^2 + 6) + x_h^2 (\epsilon^2 + 1) + 2x_h \bar{u} \right. \\ & - \frac{1}{y} \left(x^2 (\epsilon^2 - 1)^2 + 2\bar{u} (x^2 - \epsilon^2) \right) - 2x \bar{u} \left(\bar{Y}_p + 2\bar{Y}_w + 2 \ln \epsilon \right) \left. \right] \\ & \left. - 4x \bar{u} \ln \epsilon \bar{Y}_w + \left(x \frac{\bar{Y}_p}{\bar{p}_3} - 1 \right) \ln \lambda \right\}, \end{aligned} \quad (2.13)$$

where Li_2 denotes the dilogarithm [42].

2.1.4 Real gluon radiation

The contribution of the real gluon radiation in the first order in α_s is described by two Feynman diagrams, see Figure 2.2, which yield:

$$d\Gamma_4^1 = \frac{1}{2} \frac{1}{(2\pi)^8} |\mathcal{M}|^2 dR_4(Q; q, G, l, \nu). \quad (2.14)$$

The four-body phase-space is factorized in the following way:

$$dR_4(Q; q, G, l, \nu) = 2dx_h dz dR_2(t; P, W) dR_2(W; l, \nu) dR_2(P; b, G). \quad (2.15)$$

The integration over the phase space of leptons $dR_2(W; l, \nu)$ is carried out in analogy to eq. (2.12). The integration over $dR_2(t; q, G)$ gives the volume of the two body phase space equal $\pi p_3(z)$. The only non-trivial integration is the one over the phase-space of hadrons, and is performed using algebraic manipulation program REDUCE. The final result will be given in form of an integral over dz , which in principle could also be done in terms of polylogarithms, but because of the full W -boson propagator the result would be very lengthy. For the purpose of obtaining numerical values for the spectrum it is easier to perform one-dimensional integration, rather than to compute a number of higher polylogarithmic functions.

The square of the matrix element in eq. 2.14 is given by:

$$|\mathcal{M}|^2 = \frac{2^{13}}{3} \frac{G_F^2 \alpha_s \pi}{(1 - \xi y)^2 + \gamma^2} \left(\frac{B_1}{D_1^2} + \frac{B_2}{D_1 D_2} + \frac{B_3}{D_2^2} \right). \quad (2.16)$$

and the amplitudes B_i and propagators D_i can be found from the expressions derived in section 2.2.2 for the case of a polarized top quark. Terms in the formulas for B_i which do not contain the gluon four-momentum lead to infrared divergences. For these terms the integration over z is performed analytically and the divergence is regularized by introducing a small mass λ of the gluon. It has to be stressed that this procedure requires doing some very complicated integrals and is greatly simplified if one uses dimensional regularization instead. This approach will be taken in the following chapter in which it is applied to the calculation of the total decay rate $t \rightarrow bW$.

2.1.5 Total first order QCD effects

Adding the contributions of the real and virtual gluons we find the formula for the first order QCD correction:

$$\frac{d\Gamma^{(1)}}{dx_h} = \frac{G_F^2 m_t^5}{12\pi^3} \frac{2\alpha_s}{3\pi} \mathcal{G}_1(x_h), \quad (2.17)$$

where $\mathcal{G}_1(x_h)$ has to be given separately for the two kinematical regions, as explained in section 2.1.6. For $\epsilon \leq x \leq (1 + \epsilon^2)/2$

$$\begin{aligned}
\mathcal{G}_1(x) = & \left\{ \bar{Y}_p \left[F_1 - 4x\bar{u} \ln \frac{4(x^2 - \epsilon^2)}{\epsilon^2} \right] + \bar{p}_3 \left[F_2 \ln \epsilon + F_3 + 4\bar{u} \ln 4(x^2 - \epsilon^2) \right] \right. \\
& + x\bar{u} \left[2\text{Li}_2 \left(1 - \frac{\bar{p}_- \bar{w}_-}{\bar{p}_+ \bar{w}_+} \right) - 2\text{Li}_2 \left(1 - \frac{\bar{w}_-}{\bar{w}_+} \right) - 3\text{Li}_2 \left(\frac{2\bar{p}_3}{\bar{p}_3 - x} \right) \right. \\
& \left. \left. + 3\text{Li}_2 \left(\frac{2\bar{p}_3}{\bar{p}_3 + x} \right) + 4\bar{Y}_w \ln \epsilon \right] \right\} \frac{1}{(1 - \xi\bar{y})^2 + \gamma^2} \\
& + \int_{\epsilon^2}^{x^2} \frac{dz}{(1 - \xi y)^2 + \gamma^2} \left\{ h(x, z) \right. \\
& \left. + \frac{4\xi u [2 - \xi(y + \bar{y})]}{(1 - \xi\bar{y})^2 + \gamma^2} [p_3(z)(1 + \epsilon^2/z)/2 - xY_p(z)] \right\} \quad (2.18)
\end{aligned}$$

where

$$\begin{aligned}
F_1 &= 2[x\bar{u}(2\bar{Y}_w + \bar{Y}_p) + 6x^2(2 - 3x) + \epsilon^2(8x - 3 - 3\epsilon^2)] \\
F_2 &= 3[x(5 - 8x) + \epsilon^2(7x - 4)] \\
F_3 &= 2/3[x(12x^2 - 20x + 9) + 11\epsilon^2(3x - 2)] \\
h(x, z) &= \frac{1}{2}Y_p(z)[2z^2 + (3 - 12x - \epsilon^2)z + 4x(2x + 1) - \epsilon^2(3 + \epsilon^2)] \\
&+ \frac{1}{2z^2}p_3(z)\{8z^3 + 2(1 - 9x + \epsilon^2)z^2 + [3x(4x - 3) \\
&+ \epsilon^2(2 - x + 2\epsilon^2)]z + x\epsilon^2(4x - 3 - \epsilon^2)\} \quad , \quad (2.19)
\end{aligned}$$

whereas for $(1 + \epsilon^2)/2 < x \leq 1$

$$\mathcal{G}_1(x) = \int_{2x-1}^{x^2} \frac{dz}{(1 - \xi y)^2 + \gamma^2} \left\{ h(x, z) + \frac{2u}{z - \epsilon^2} \left[p_3(z) \left(1 + \frac{\epsilon^2}{z} \right) - 2xY_p(z) \right] \right\} \quad (2.20)$$

We checked the absence of mass singularities ($\epsilon \rightarrow 0$) for $\mathcal{G}_1(x_h)$. As another cross check we compared the results for total semileptonic decay rates following from Eqs. (2.17), (2.18) and (2.20) with those given in [2]. We found that they are in perfect numerical agreement.

In the four fermion limit $m_W \rightarrow \infty$, i.e. $\xi, \gamma \rightarrow 0$, the integrals in (2.18) and (2.20) can be calculated analytically. For $\epsilon \leq x \leq (1 + \epsilon^2)/2$ we obtain:

$$\begin{aligned}
\mathcal{G}_1(x) = & \bar{Y}_p \left[\tilde{F}_1 + 2x\bar{u} \left(2\bar{Y}_w + \bar{Y}_p - 2 \ln \frac{4(x^2 - \epsilon^2)}{\epsilon^2} \right) \right] \\
& + \bar{p}_3 \left[\tilde{F}_2 \ln \epsilon + \tilde{F}_3 + 4\bar{u} \ln 4(x^2 - \epsilon^2) \right] \\
& + x\bar{u} \left[2\text{Li}_2 \left(1 - \frac{\bar{p}_- \bar{w}_-}{\bar{p}_+ \bar{w}_+} \right) - 2\text{Li}_2 \left(1 - \frac{\bar{w}_-}{\bar{w}_+} \right) - 3\text{Li}_2 \left(\frac{2\bar{p}_3}{\bar{p}_3 - x} \right) \right. \\
& \left. + 3\text{Li}_2 \left(\frac{2\bar{p}_3}{\bar{p}_3 + x} \right) + 4\bar{Y}_w \ln \epsilon \right] \quad (2.21)
\end{aligned}$$

where

$$\begin{aligned}
\tilde{F}_1 &= \frac{1}{12} [36x^2(5 - 8x) - 6\epsilon^2(10x^2 - 28x + 9) \\
&\quad + 3\epsilon^4(20x - 19) + 5\epsilon^6] \\
\tilde{F}_2 &= 3[x(5 - 8x) + \epsilon^2(7x - 4)] \\
\tilde{F}_3 &= \frac{1}{180} [32x^5 - 168x^4 + 1170x^3 - 3720x^2 + 2430x \\
&\quad - \epsilon^2(14x^3 - 36x^2 - 4905x + 3120) - 3\epsilon^4(31x + 256)] \quad (2.22)
\end{aligned}$$

and for $(1 + \epsilon^2)/2 < x \leq 1$

$$\begin{aligned}
\mathcal{G}_1(x) = & \frac{1}{180} (1 - x) [32x^5 - 136x^4 + 1034x^3 - 2946x^2 + 1899x + 312 \\
& - 15\epsilon^2(2x^3 - 6x^2 - 267x + 208) - 90\epsilon^4(x + 4)] \\
& + \frac{1}{2} \epsilon^2 x(x - 1)(3 - 4x + \epsilon^2)/(2x - 1) \\
& + \frac{1}{24} \ln(2x - 1) [320x^3 - 240x^2 + 24x + 5 - 3\epsilon^2(8x + 1) - 36\epsilon^4 x] \\
& + 2\bar{u} \left\{ 2\bar{p}_3 \ln \left(\frac{\bar{p}_3 + 1 - x}{\bar{p}_3 - 1 + x} \right) + x \left[\ln(2x - 1) \ln \left(\frac{\epsilon^2}{2x - 1 - \epsilon^2} \right) \right. \right. \\
& \left. \left. - \text{Li}_2 \left(\frac{2x - 1}{\bar{p}_-} \right) - \text{Li}_2 \left(\frac{2x - 1}{\bar{p}_+} \right) + \text{Li}_2 \left(\frac{1}{\bar{p}_-} \right) + \text{Li}_2 \left(\frac{1}{\bar{p}_+} \right) \right] \right\} \quad (2.23)
\end{aligned}$$

In the massless limit ($\epsilon \rightarrow 0$) we obtained for $0 \leq x \leq 1/2$:

$$\begin{aligned} \mathcal{G}_1(x) = & x^2 \left\{ \frac{1}{90}(16x^4 - 84x^3 + 585x^2 - 1860x + 1215) \right. \\ & \left. + (8x - 9) \ln 2x + 2(4x - 3) \left[\frac{\pi^2}{2} + \text{Li}_2(1 - 2x) \right] \right\} \quad (2.24) \end{aligned}$$

and for $1/2 < x \leq 1$:

$$\begin{aligned} \mathcal{G}_1(x) = & \frac{1}{180}(1 - x)(32x^5 - 136x^4 + 1034x^3 - 2946x^2 + 1899x + 312) \\ & - \frac{1}{24} \ln(2x - 1)(64x^3 - 48x^2 - 24x - 5) \\ & + x^2(3 - 4x)[- \pi^2 + 4\text{Li}_2(2x) + \ln^2(2x - 1)]. \quad (2.25) \end{aligned}$$

2.1.6 Discussion of the results

In Figure 2.4 the normalized distribution of the total energy of hadrons is shown for $m_b = 5$ GeV and $m_t = 40, 60$ and 80 GeV in the Born approximation. These distributions vanish outside the kinematical boundaries $\epsilon \leq x \leq (1 + \epsilon^2)/2$. The first order QCD correction

$$\frac{d\Gamma^{(1)}}{dx_h} = \frac{2\alpha_s}{3\pi} \Gamma_b R(x_h), \quad (2.26)$$

where Γ_b denotes the total semileptonic width in Born approximation, is shown in Figure 2.5 for the same three values of m_t . In the region $\epsilon \leq x_h \leq (1 + \epsilon^2)/2$ both real and virtual gluons contribute and the combined correction to the differential rate is negative. In the region $(1 + \epsilon^2)/2 < x_h \leq 1$ only configurations with at least one real gluon are allowed and thus the correction to the width is positive there. The gluon cannot be soft unless x_h is very close to $(1 + \epsilon^2)/2$, where the correction has a logarithmic singularity. If the top quark is so heavy that real W production is possible the shape of the hadron energy distribution reflects the shape of the W boson. A few GeV above the threshold real W production becomes the dominant decay mode. In Figure 2.6 the distribution of the energy of hadrons is shown for $m_t = 120$ GeV (solid line). The Born approximation (dashed line) and $O(\alpha_s)$ correction (dotted line) are also plotted. In the region below the peak the correction is negative, and above it is positive.

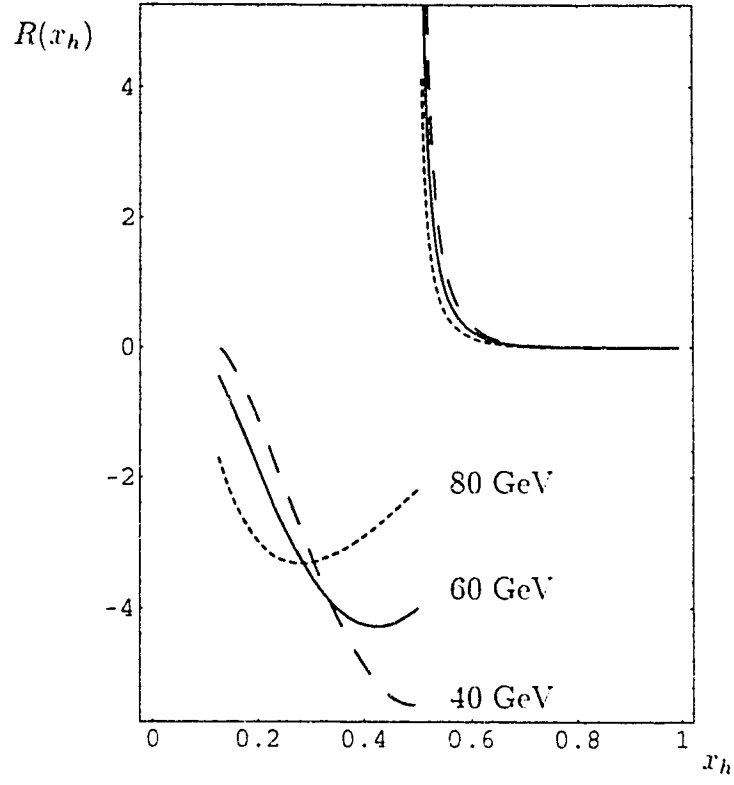


Figure 2.5: First order QCD correction $R(x_h)$ to the distribution of the total energy of hadrons.

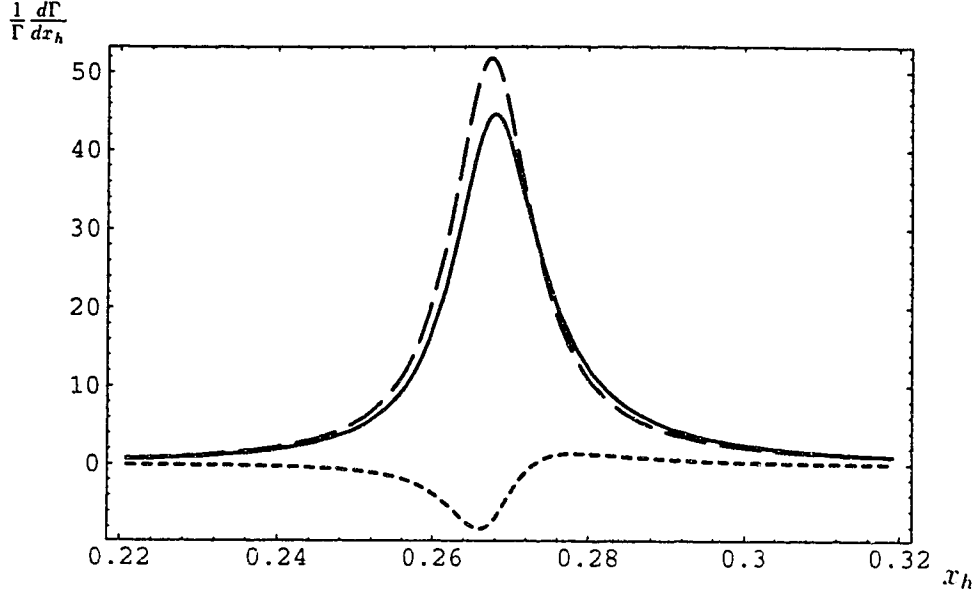


Figure 2.6: Normalized distribution of the total energy of hadrons for $m_t = 120$ GeV in the region of the peak.

2.2 Lepton Spectra from Decays of Polarized Top Quarks

2.2.1 Introduction

Similarly to the case of electromagnetic corrections for muon decay $\mu \rightarrow e + \bar{\nu}_e + \nu_\mu$ [41], also the angular distribution of leptons from the decay $t \rightarrow \bar{l} + \nu_l + b$ of polarized top quarks will be affected by QCD corrections. However, an important difference is observed already in the Born term: the lepton spectrum in the top decay can be factorized [2, 43] into an energy-dependent function and a factor $(1 + \cos \theta)/2$, where θ denotes the angle between the lepton direction and the top spin. The angular distribution of leptons thus serves to analyze the spin of t -quarks produced in e^+e^- annihilation and the factorization has evident implications also for the search of the top at hadron colliders [43]. With this motivation in mind QCD corrections are evaluated to the double differential distribution

$$\frac{d\Gamma_{pol}}{dx_l d\cos\theta} = \frac{d\Gamma_{pol}^{(0)}}{dx_l d\cos\theta} + \frac{d\Gamma_{pol}^{(1)}}{dx_l d\cos\theta}. \quad (2.27)$$

The notation has already been explained in the previous sections. θ is the angle between the direction of the charged lepton and the vector \vec{s} describing the polarization of the top quark in its rest frame. As in the analysis of the hadron spectra we neglect the masses of the leptons in the final state. In the Born approximation

$$\frac{d\Gamma_{pol}^{(0)}}{dx_l d\cos\theta} = \frac{d\Gamma^{(0)}}{dx_l} \frac{(1 + |\vec{s}| \cos\theta)}{2}, \quad (2.28)$$

where $d\Gamma^{(0)}/dx_l$, the energy distribution for the decays of unpolarized t quarks has been given in eq. (2.20) of the ref. [1]. In section 2.2.2 the first order QCD correction is derived in the form of a one-dimensional integral:

$$\frac{d\Gamma_{pol}^{(1)}}{dx_l d\cos\theta} = -\frac{2\alpha_s}{3\pi} \frac{G_F^2 m_t^5}{16\pi^3} \int_0^{y_m} \frac{dy F_1^{pol}}{(1 - \xi y)^2 + \gamma^2}. \quad (2.29)$$

Contributions to F_1^{pol} arise from both virtual and real gluon emission. It is shown that virtual gluons and a dominant part of real emission lead to a separable form analogous to eq. (2.28) for the Born term. Thus the double differential distribution $d\Gamma_{pol}/dx_l d\cos\theta$ can be written to a good approximation as a product of energy and angular distributions also after corrections of order α_s are included. This claim will be substantiated by studying the function ΔF_1 defined by the equation:

$$F_1^{pol} = \frac{1}{2}(1 + |\vec{s}| \cos\theta) F_1 + \frac{1}{2} |\vec{s}| \cos\theta \Delta F_1 \quad (2.30)$$

where F_1 describes decays of unpolarized quarks, see eq. (3.2) of ref. [1]. $|\Delta F_1/F_1|$ will be shown to be of the order of few percent. For m_t above 70 GeV ΔF_1 can be reasonably well approximated by $\Delta \tilde{F}_1$, i.e. its limit for the vanishing mass of the down type quark. The general formula, which is much lengthier, is provided for the sake of completeness in section 2.2.4. Some details of the calculation are explained in sections 2.2.5 and 2.2.6.

2.2.2 Corrections to Decays of Polarized t Quarks

In the Born approximation the differential rate for the decay $t \rightarrow b + e^+ + \nu$ reads, (cf. (2.14) of [1]):

$$d\Gamma_{pol}^{(0)} = \frac{1}{2m_t} \frac{64G_F^2}{(1 - \xi y)^2 + \gamma^2} |M_0^{pol}|^2 \frac{dR_3}{(2\pi)^5}, \quad (2.31)$$

where

$$|M_0^{pol}|^2 = (q\nu)(Rl), \quad R = Q - m_t s. \quad (2.32)$$

and s is the polarization four vector of the t quark. For $s = 0$ $|M_0^{pol}|^2$ coincides with $|M_0|^2$, the matrix element squared for unpolarized t quarks, (cf. equation (2.16) of [1]). It is remarkable that one can obtain $|M_0^{pol}|^2$ from $|M_0|^2$ by replacing (Ql) by (Rl) . Equation 2.28 is an immediate consequence of this observation.

Virtual gluon exchange gives the following contribution to the differential rate:

$$d\Gamma_{3,pol}^{(1)} = \frac{1}{2m_t} \frac{2\alpha_s}{3\pi} \frac{64G_F^2}{(1-\xi y)^2 + \gamma^2} M_3^{pol} \frac{dR_3}{(2\pi)^5} \quad (2.33)$$

where

$$\begin{aligned} M_3^{pol} = & - \left\{ H_0(q\nu)(Rl) + \epsilon^2 H_+(Q\nu)(Rl) \right. \\ & + H_-(q\nu) \left((ql) + [(Rl)(Qq) - (Ql)(Rq)] / Q^2 \right) \\ & \left. + \frac{1}{2} \epsilon^2 (H_+ + H_-) \left(Q^2(\nu l) + (Q\nu)(Rl) - (R\nu)(Ql) \right) \right\} \end{aligned} \quad (2.34)$$

and the functions H_0, H_{\pm} have been defined in eqs. (2.29-30) in ref. [1]. By putting $s = 0$ we can rederive eq. (2.28) of that paper for the ‘unpolarized’ case. The three-body phase space is parametrized as follows:

$$dR_3 = \frac{1}{32} Q^2 dx_l dy d(\cos\theta) d\alpha d\beta \quad (2.35)$$

After integration over two Euler angles, cf. section 2.2.5, we obtained a formula for the contribution of virtual gluons:

$$\frac{d\Gamma_{v,pol}^{(1)}}{dx_l d\cos\theta} = - \frac{G_F^2 m_t^5}{16\pi^3} \frac{2\alpha_s}{3\pi} \frac{(1 + |\vec{s}| \cos\theta)}{2} \int_0^{y_m} dy \frac{1}{(1-\xi y)^2 + \gamma^2} F_v(x_l, y, \epsilon^2). \quad (2.36)$$

The function F_v has been introduced¹ in ref. [1] and reads:

$$\begin{aligned} F_v(x_l, y, \epsilon^2) = & \left(H_0 x_l (x_M - x_l) + \epsilon^2 H_+ x_l (x_M - x_l - y) \right. \\ & \left. + H_-(x_l - y)(x_M - x_l) + \epsilon^2 y \frac{\bar{Y}_p}{\bar{p}_3} \right). \end{aligned} \quad (2.37)$$

¹An extra factor of 2 in the last term in eq. (2.33) of ref. [1] when compared to this formula is due to a typographic error in ref. [1].

The contribution from real gluon emission is given by:

$$d\Gamma_{4,pol}^{(1)} = \frac{1}{2m_t} \frac{2\alpha_s\pi}{3} \frac{64G_F^2}{(1-\xi y)^2 + \gamma^2} |M_4^{pol}|^2 \frac{dR_4}{(2\pi)^8}, \quad (2.38)$$

$$|M_4^{pol}|^2 = 32 \left(\frac{B_1^{pol}}{D_1^2} + \frac{B_2^{pol}}{D_1 D_2} + \frac{B_3^{pol}}{D_2^2} \right), \quad (2.39)$$

where

$$\begin{aligned} B_1^{pol} &= (q\nu)[(Rl)(QG - Q^2) + (Gl)(RQ) - (Ql)(RG) + (Gl)(RG)], \\ B_2^{pol} &= (q\nu)\{(Gl)(Rq) - (ql)(RG) + (Rl)[(qG) - (QG) - 2(qQ)]\} \\ &\quad + (Rl)[(Q\nu)(qG) - (G\nu)(qQ)], \\ B_3^{pol} &= (Rl)[(G\nu)(qG) - \nu(q+G)q^2], \\ D_1 &= -2(QG), \\ D_2 &= 2(qG), \end{aligned} \quad (2.40)$$

This equation coincides for $s = 0$ with the corresponding formulae from ref. [1], eqs. (2.33-36). The term $\sim B_3^{pol}$ has a structure which leads to a form analogous to (2.28). The terms $\sim B_{1,2}^{pol}$ do not have this feature. However, those parts of B_1^{pol} and B_2^{pol} which do not lead to separable expressions of the form (2.28) contain at least one four momentum G_μ . Since the denominators D_1 and D_2 are small for $G_\mu \approx 0$ (in Q rest frame) we expect that

$$\frac{d\Gamma_{4,pol}^{(1)}}{dx_l d\cos\theta} \approx \frac{d\Gamma_4^{(1)}}{dx_l} \frac{(1 + |\vec{s}| \cos\theta)}{2}. \quad (2.41)$$

In particular the infrared divergent piece of $|M_4^{pol}|^2$ is exactly factorizable, so we calculate it by multiplying the result for the unpolarized t quark by the angular factor $(1 + |\vec{s}| \cos\theta)/2$. The evaluation of the infrared finite piece proceeds as follows. The four-body phase space is parametrized by

$$dR_4(Q; l, \nu, q, G) = Q^2 dz dR_3(Q; l, \nu, P) dR_2(P; q, G) \quad (2.42)$$

The integrations over the two body phase space of the quark-gluon system are performed first. A method for algebraic evaluation of corresponding integrals

is sketched in the section 2.2.6. Using the parametrization (2.35) for the three body phase space one integrates over the Euler angles α and β , see section 2.2.5. The remaining integral over z , the mass squared of the quark-gluon system, can be solved by using recursion relations listed in the Appendix B of ref. [1].

2.2.3 Discussion of the results

Combined contributions from real and virtual gluons and the $O(\alpha_s)$ corrections to the charged lepton spectrum are written in the form (2.29 and 2.30), where

$$\Delta F_1(x_l, y, \epsilon^2) = \Delta H_2(x_l, y, \epsilon^2) - \Delta H_2(x_l, y, z_m) \quad (2.43)$$

and the function $\Delta H_2(x, y, z)$ is given in the section 2.2.4. The ratio

$$R = \int_0^{y_m} \frac{dy \Delta F_1}{(1 - \xi y)^2 + \gamma^2} / \int_0^{y_m} \frac{dy F_1}{(1 - \xi y)^2 + \gamma^2} \quad (2.44)$$

is plotted in Figure 2.7 for $m_b = 5$ GeV, $m_W = 82$ GeV, $\Gamma_W = 2.2$ GeV, and $m_t = 80, 120$ and 160 GeV (solid lines). Since R is small we conclude that to a good approximation the double differential decay rate for the charged lepton can be written as a product of the energy distribution times the angular factor $\frac{1}{2}(1 + |\vec{s}| \cos \theta)$. In the limit $\epsilon = 0$ our formula for ΔF_1 simplifies considerably:

$$\begin{aligned} \Delta \tilde{F}_1 &\equiv \Delta F_1(x, y, \epsilon^2 = 0) \\ &= 2x[\text{Li}_2(x) + \text{Li}_2(y/x) - \text{Li}_2(y) - \text{Li}_2(1)] \\ &\quad + \frac{1}{x}[(1 - 3x)(1 - x) \ln(1 - x) + (4x - y - 1)(1 - y) \ln(1 - y)] \\ &\quad + (y - 3x)(1 - y/x) \ln(1 - y/x) + (1 - x)(1 - y/x)(1 + x - y) \end{aligned} \quad (2.45)$$

Also shown in Figure 2.7 is the ratio R for $\epsilon = 0$. Those curves correspond to transitions $t \rightarrow s$ (or d). They show also that for the transition $t \rightarrow b$, ΔF_1 is well approximated by $\Delta \tilde{F}_1$.

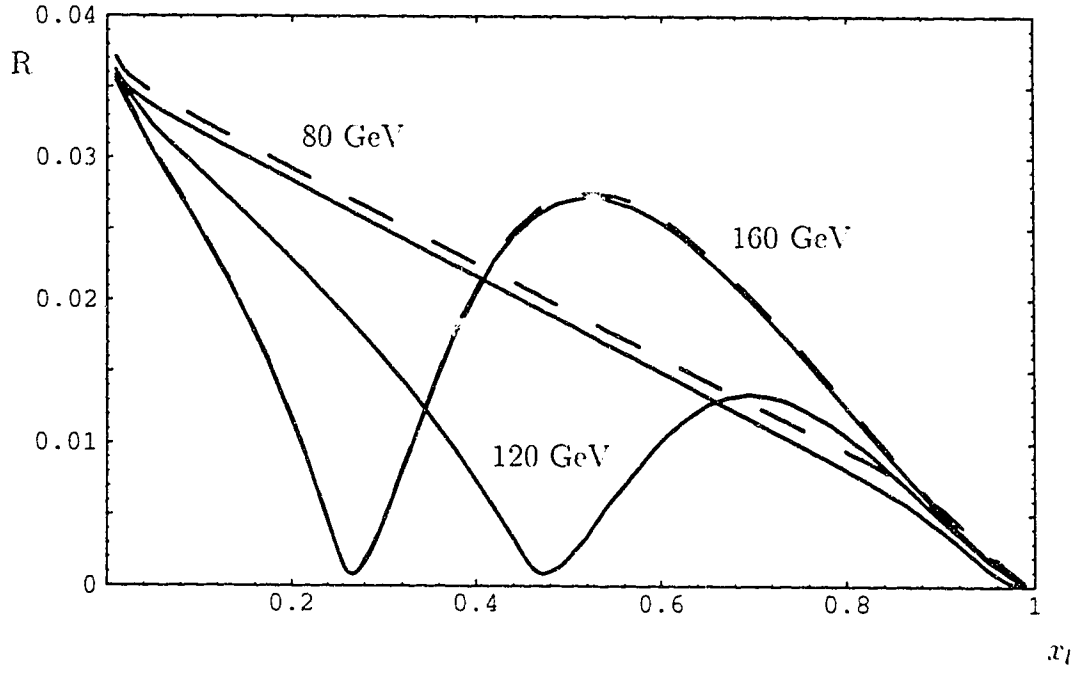


Figure 2.7: The ratio R , see eq. (2.44), for $m_b = 5$ GeV and $m_t = 80, 120$ and 160 GeV (solid lines), and for $\epsilon = 0$, $m_t = 80$ and 160 GeV (dashed lines)

2.2.4 A formula for $\Delta H_2(x, y, z)$

$$\begin{aligned}\Delta H_2(x, y, z) = & [h_1 + zh_2]/[2p_3(z)]^4 + [h_3 + zh_4]/[2p_3(z)]^2 \\ & + \frac{\bar{Y}_p}{\bar{p}_3} z \{ [h_5 + zh_6]/[2p_3(z)]^4 + [h_7 + zh_8]/[2p_3(z)]^2 + h_9 + zh_{10} \} \\ & + h_{11} \ln z + h_{12} [Li_2(w_+) + Li_2(w_-)]/2 + h_{13}/[2p_3(z)]^4/z + \epsilon^2 h_{14}/z\end{aligned}\quad (2.46)$$

where

$$\begin{aligned}h_1 = & \{-6y(1-y)^2[x^2(3+2x) + y(1+6x+3x^2) + y^2] \\ & + 12\epsilon^2 y(1-y)^2(3x^2+y) + \epsilon^4[x^2(1-x) + yx(-3-13x+10x^2) \\ & + y^2(-4+30x-13x^2-x^3) + y^3(-4-3x+x^2)]\}/x \\ h_2 = & \{12y[x^2(3+4x) + y(1+12x+18x^2+4x^3) + 3y^2(2+4x+x^2) + y^3] \\ & - 24\epsilon^2 y[x^2(3+2x) + y(1+6x+3x^2) + y^2] \\ & + \epsilon^4[-x^2(1-x) + yx(3+32x+x^2) + y^2(10+3x-x^2)]\}/(2x) \\ h_3 = & \{(1-y)[-x^2(x+3) + y(-1-6x+24x^2+14x^3) \\ & + y^2(9+48x+15x^2-x^3) + 3y^3(1-2x) + y^4] \\ & + 2\epsilon^2(1-y)[x^2(3-x) + y(1-4x-19x^2) + y^2(-6+x+x^2)] \\ & - \epsilon^4[2x^2(1-x) + y(1-11x+3x^2) + y^2x(9-x) - y^3]\}/[x(1-y)] \\ h_4 = & \{(1-y)[6x^2(1+x) + 2y(1+18x+24x^2+2x^3) + 2y^2(5+9x) - 2y^3] \\ & - 4\epsilon^2(1-y)[x^2(3+x) + y(1+8x+x^2)] \\ & + \epsilon^4[x^2(5-x) + y(2-x-3x^2) - 2y^2]\}/[2x(1-y)] \\ h_5 = & 6(1-y)y\{(1-y)(1+x)[y(1+x)^2 + 3(x+y)^2] \\ h_6 = & 6y\{y^3(-3x-5) + y^2(-x^3-15x^2-30x-10) \\ & + y(-10x^3-30x^2-15x-1) + x^2(-5x-3) \\ & + \epsilon^2 2(1+x)[y(1+x)^2 + 3(x+y)^2] + \epsilon^4[y(-3x-1) + x^2(-x-3)]\}/x \\ h_7 = & \{y^4 + y^3(9x^2-6x-19) + y^2(-4x^3-69x^2-78x-7) \\ & + y(-22x^3-15x^2+12x+1) + x^2(2x+3) \\ & + \epsilon^2[2y^3(-2x-1) + 2y^2(-3x^2+22x+8) + 2y(6x^3+24x^2-2x-1) \\ & - 6x^2] + \epsilon^4[y^2(4x-3) + y(-7x^2-8x+1) + x^2(-2x+3)]\}/x\end{aligned}$$

$$\begin{aligned}
h_8 &= \{-y^3 + 3y^2(-5x^2 - 14x - 4) + y(-10x^3 - 48x^2 - 24x - 1) \\
&\quad + x^2(-4x - 3) + \epsilon^2[2y^2(2x + 3) + 2y(11x^2 + 14x + 1) + 2x^2(2x + 3)] \\
&\quad + \epsilon^4[y(-4x - 1) - 3x^2]\}/x \\
h_9 &= \{-y^3 + y^2(4x - 1) - y(32x + 18x^2 + 1) - 4x^3 - 6x^2 + 4x - 1 \\
&\quad + 2\epsilon^2[y(-x^2 + 6x + 1) + 7x^2 - 2x + 1] - \epsilon^4(y + 1)\}/(2x) \\
h_{10} &= [y^2 - 4xy - 10x^2 - 4x + 1 + 2\epsilon^2(x^2 + 2x - 1) + \epsilon^4]/(2x) \\
h_{11} &= [y^2 - 4xy + 4x - 1 + 2\epsilon^2(x - 1)^2 - \epsilon^4]/(2x) \\
h_{12} &= -2x \\
h_{13} &= \epsilon^4(x - 1)(y - 1)^2(y - x)(2y - yx - x)/(2x) \\
h_{14} &= \epsilon^2(1 - x)(y - x)/[2(1 - y)]
\end{aligned} \tag{2.47}$$

The following relations, derived from the condition that $\Delta H_2(x, y, z)$ has no singularity at $p_3(z) = 0$, have been used as non-trivial cross checks of calculations:

$$\begin{aligned}
h_5 &= [(y - 1)h_1 + (y - 1)^2h_2 + (y + 3)h_{13}/(y - 1)]/2 \\
h_6 &= [-h_1 - (y + 3)h_2 + h_{13}/(1 - y)]/2 \\
h_7 &= \{(y + 3)h_1/[4(1 - y)] - (y + 11)h_2/4 + 3(y - 1)h_3 \\
&\quad + 3(y - 1)^2h_4 - h_{13}(y^2 - 14y - 19)/[4(y - 1)^3]\}/6 \\
h_8 &= \{h_1/(y - 1) - [-h_2 + 12h_3 + 12(y + 3)h_4 + (9 - y)/(y - 1)^3h_{13}]\}/24
\end{aligned} \tag{2.48}$$

2.2.5 Integration over Euler angles

Units are chosen so that $Q^2 = 1$. In the Q rest frame the following four-momenta are considered: l , $P = q + G$, ν and s , together with the corresponding three-vectors

$$\vec{l} + \vec{P} + \vec{\nu} = 0, \tag{2.49}$$

and the unit three-vectors \hat{l} , \hat{s} and

$$\hat{w} = \frac{\vec{l} \times \vec{s}}{|\vec{l} \times \vec{s}|}. \tag{2.50}$$

The three Euler angles α , β and θ , describe the orientation of \vec{l} and \vec{P} with respect to an orthogonal system of coordinates with the z -axis directed along \hat{s} . Let θ denote the angle between \hat{s} and \hat{l} , α the angle between \hat{w} and \vec{P}_T (the projection of \vec{P} onto the plane perpendicular to \hat{l}) and β the angle between \hat{w} and the y -axis. It is clear that all the scalar products which appear in M_3^{pol} and $|M_4^{pol}|^2$ do not depend on β . Thus, the integration over β is trivial and gives an overall factor of 2π . Integration over α is non-trivial because (sP) and $(s\nu)$ depend on α . Using the decomposition

$$\vec{P} = P_L \hat{l} + |\vec{P}_T| \cos \alpha \hat{w} - |\vec{P}_T| \sin \alpha \hat{w} \times \hat{l} \quad (2.51)$$

one derives:

$$\int d\alpha (sP) = 2\pi |\vec{s}| \cos \theta \left[\frac{1}{2}(1 + y - z) - \frac{y}{x_l} \right]. \quad (2.52)$$

Then, from energy-momentum conservation,

$$Q = P + l + \nu \quad (2.53)$$

it follows that

$$\int d\alpha (s\nu) = 2\pi |\vec{s}| \cos \theta \left[\frac{y}{x_l} - \frac{1}{2}(1 + y - z - x_l) \right], \quad (2.54)$$

because $(Qs) = 0$ and

$$(ls) = -\frac{1}{2}x_l |\vec{s}| \cos \theta. \quad (2.55)$$

2.2.6 Algebraic evaluation of the integrals

In this section formulae are listed which allow algebraic evaluation of the integrals

$$\begin{aligned} I_n &= \int dR_2(P; q, G)(QG)^n \\ J_n^\alpha &= \int dR_2(P; q, G)(QG)^n G^\alpha \\ K_n^{\alpha\beta} &= \int dR_2(P; q, G)(QG)^n G^\alpha G^\beta \\ L_n^{\alpha\beta\gamma} &= \int dR_2(P; q, G)(QG)^n G^\alpha G^\beta G^\gamma \end{aligned} \quad (2.56)$$

for $n \geq -2$. It is easy to show that only integrals of this form appear when one integrates $|M_4^{pol}|^2$. Since we are interested in infrared finite pieces we put $G^2 = 0$. For I_n we take, (cf. eq. (A.8) of ref. [1]):

$$\begin{aligned} I_{-2} &= \frac{\pi}{(PG)Q^2} \\ I_{-1} &= \frac{\pi}{\sqrt{\Delta}} Y_p \\ I_n &= \pi \frac{(PG)^{n+1} (PQ)^n}{(P^2)^{n+1}} \quad (n \geq 0) \end{aligned} \tag{2.57}$$

where

$$\begin{aligned} (PG) &= \frac{1}{2}(P^2 - q^2), \\ Y_p &= \frac{1}{2} \ln \frac{(QP) + \sqrt{\Delta}}{(QP) - \sqrt{\Delta}}, \\ \Delta &= Q^2 P^2 - (QP)^2. \end{aligned} \tag{2.58}$$

Using Lorentz invariance one derives:

$$J_n^\alpha = a_n^{(1)} Q^\alpha + b_n^{(1)} P^\alpha. \tag{2.59}$$

where

$$\begin{aligned} a_n^{(1)} &= \frac{1}{\Delta} (P^2 I_{n+1} - (PG)(QP) I_n), \\ b_n^{(1)} &= \frac{1}{\Delta} (Q^2 (PG) I_n - (QP) I_{n+1}). \end{aligned} \tag{2.60}$$

It is evident that $K_n^{\alpha\beta}$ is symmetric:

$$K_n^{\alpha\beta} = a_n^{(2)} g^{\alpha\beta} + b_n^{(2)} Q^\alpha Q^\beta + c_n^{(2)} P^\alpha P^\beta + d_n^{(2)} [Q^\alpha P^\beta + P^\alpha Q^\beta] \tag{2.61}$$

It must be also traceless. By contracting $K_n^{\alpha\beta}$ with P^α and Q^α we obtain a system of linear equations. The solution is

$$a_n^{(2)} = -a_{n+1}^{(1)} - \frac{P^2}{2(QP)} b_{n+1}^{(1)} + \frac{Q^2(PG)}{2(QP)} a_n^{(1)}$$

$$\begin{aligned}
b_n^{(2)} &= \frac{1}{2\Delta(QP)} \\
&\quad -(PG)[2(QP)^2 + P^2Q^2]a_n^{(1)}\} \\
c_n^{(2)} &= \frac{1}{2\Delta(QP)} \{4Q^2(QP)a_{n+1}^{(1)} + [3Q^2P^2 - 2(QP)^2] \\
&\quad -3(PG)(Q^2)^2a_n^{(1)}\} \\
d_n^{(2)} &= \frac{1}{2\Delta} \{-4(QP)a_{n+1}^{(1)} - P^2b_{n+1}^{(1)} + 3(PG)Q^2a_n^{(1)}\} \quad (2.62)
\end{aligned}$$

In a similar way we obtain the following formula for $L_n^{\alpha\beta\gamma}$:

$$\begin{aligned}
L_n^{\alpha\beta\gamma} &= a_n^{(3)}(g^{\alpha\beta}Q^\gamma + g^{\alpha\gamma}Q^\beta + g^{\beta\gamma}Q^\alpha) + b_n^{(3)}(g^{\alpha\beta}P^\gamma + g^{\alpha\gamma}P^\beta + g^{\beta\gamma}P^\alpha) \\
&\quad + d_n^{(3)}P^\alpha P^\beta P^\gamma + e_n^{(3)}(Q^\alpha Q^\beta P^\gamma + Q^\alpha P^\beta Q^\gamma + P^\alpha Q^\beta Q^\gamma) \\
&\quad + P^\alpha P^\beta Q^\gamma \quad (2.63)
\end{aligned}$$

where

$$\begin{aligned}
a_n^{(3)} &= \frac{1}{\Delta} (P^2a_{n+1}^{(2)} - (QP)(PG)a_n^{(2)}) \\
b_n^{(3)} &= \frac{1}{\Delta} (Q^2(PG)a_n^{(2)} - (QP)a_{n+1}^{(2)}) \\
c_n^{(3)} &= \frac{1}{\Delta} (P^2b_{n+1}^{(2)} - (QP)(PG)b_n^{(2)}) - \frac{2P^2a_n^{(3)}}{\Delta} \\
d_n^{(3)} &= \frac{1}{\Delta} (Q^2(PG)c_n^{(2)} - (QP)c_{n+1}^{(2)}) - \frac{2Q^2b_n^{(3)}}{\Delta} \\
e_n^{(3)} &= \frac{1}{\Delta} (Q^2(PG)b_n^{(2)} - (QP)b_{n+1}^{(2)}) + \frac{2(QP)a_n^{(3)}}{\Delta} \\
f_n^{(3)} &= \frac{1}{\Delta} (P^2c_{n+1}^{(2)} - (QP)(PG)c_n^{(2)}) + \frac{2(QP)b_n^{(3)}}{\Delta}. \quad (2.64)
\end{aligned}$$

Chapter 3

Total rate of the decay $t \rightarrow W^+ b$

3.1 Introduction

Although one-loop radiative corrections to most reactions within the Standard Model have been computed, it remains an important task to develop better and more efficient techniques for doing loop calculations. Recent applications include for example decays of heavy quarks and non-standard processes like charged Higgs decay. There has recently been much progress in developing algorithms for doing multiloop calculations using dimensional regularization (see chapter 6 and references therein). The basic idea of dimensional regularization is to calculate integrals, which diverge in 4 dimensions, in an arbitrary number of dimensions D and obtain the result in terms of a Laurent expansion around $D = 4$. The use of dimensional regularization for labelling ultraviolet divergences has become a standard technique. On the other hand, to regularize infrared divergences many researchers still assign a small mass to the gluon, even though it was shown long ago [44, 45, 46] that dimensional regularization can also be applied to this problem resulting in a simplification of calculations. The purpose of this Chapter is to calculate QCD corrections to the total decay rate of the decay of a top quark into a bottom quark and a W boson. Advantages of using dimensionally regularized phase space integrals will be demonstrated explicitly.

Recent CDF results suggest that the top quark is heavier than 89 GeV [47]. Even higher limit can be obtained from analysis of shape of the Z peak [48, 49]. This high top mass opens the possibility of its decay into a b

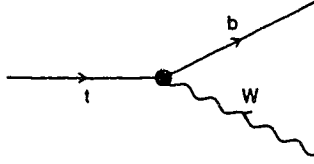


Figure 3.1: Tree level process $t \rightarrow W^+ b$

quark and a real W , depicted in Figure 3.1. As this will be the dominant decay channel, it is crucial to know its exact width together with QCD corrections [50]. The relevant formula was first derived by Jeřabek and Kühn [2]. However all the existing results were obtained by assigning a mass to the gluon in order to regularize the infrared divergences. In this Chapter dimensional regularization is adopted for both ultraviolet [51] and infrared [45] divergences. It turns out that this method leads to much simpler calculations than the method requiring the introduction of a gluon mass. A technique for doing phase space integrals is presented in detail. Effects of the b quark mass are accounted for. The final formula confirms the results of ref. [2].

Other properties of real W production, such as hadron energy spectrum, can be obtained from the results for semileptonic decays [6], described in the previous chapter. To this end an integration in a narrow-width approximation has to be carried out.

The notation to be used is adopted from the analysis of semileptonic decays [2] and has been explained in the previous Chapter. We define following symbols for scaled masses:

$$\epsilon = \frac{m_b}{m_t}, \quad w = \frac{m_W}{m_t}. \quad (3.1)$$

All four-momenta are scaled by taking m_t as a unit of energy and are denoted by Q, q, G, W for the top quark, bottom quark, gluon and W -boson respectively. For the value of kinematic variables for $z = \epsilon^2$ we use the abbreviations

$$\bar{p}_0 \equiv p_0(\epsilon^2) \quad \bar{p}_3 \equiv p_3(\epsilon^2) \quad etc. \quad (3.2)$$

The width of the decay $t \rightarrow Wb$ in the Born approximation reads:

$$\Gamma^{(0)}(t \rightarrow Wb) = \frac{G_F m_t^3}{4\sqrt{2}\pi} f \bar{p}_3 \quad (3.3)$$

where

$$f = (1 - \epsilon^2)^2 + w^2(1 + \epsilon^2) - 2w^4. \quad (3.4)$$

To evaluate the corrections from virtual gluons we work in D dimensional space, where $D = 4 - 2\varepsilon$, ε being an arbitrary complex number, which we will take to be 0 at the end of the calculation.

3.2 Limiting case of $m_b = m_W = 0$

In order to illustrate the technique of dimensional regularization with a simple example, the decay rate is first calculated in the simple limiting case where top is treated as much heavier than W -boson, in which case we can neglect masses m_W and m_b .

First the tree level decay rate has to be calculated in D dimensions. This is important, because terms proportional to ε can combine with poles from loop corrections to the vertex and external legs giving finite contribution. If we take m_t as the unit of mass we obtain:

$$\Gamma_B = \frac{2G_F}{\sqrt{2}}(2\pi)^{2-D} \int dR_2(t; W, q). \quad (3.5)$$

with the n -body phase space in D dimensions defined as follows:

$$dR_n(P; p_1, p_2, \dots, p_n) = \delta^D(P - \sum_{i=1}^n p_i) \prod_{i=1}^n \frac{d^{D-1}p_i}{2E_i} \quad (3.6)$$

We introduce spherical coordinates in a $(D - 1)$ -dimensional space, so that the volume element is:

$$\frac{d^{D-1}k}{2E} = \frac{E^{D-2}dE}{2E} (\sin \theta_1)^{D-3} (\sin \theta_2)^{D-2} \dots (\sin \theta_{D-3}) \prod_{i=1}^{D-2} d\theta_i \quad (3.7)$$

where $E = k^0$. The angular variables can be integrated out with help of the formula:

$$\int_0^\pi (\sin \theta)^n d\theta = \sqrt{\pi} \frac{\Gamma(\frac{n+1}{2})}{\Gamma(\frac{n+2}{2})} \quad (3.8)$$

and this gives:

$$\frac{d^{D-1}k}{2E} \rightarrow \frac{\pi^{\frac{D-1}{2}}}{\Gamma(\frac{D-1}{2})} E^{D-3} dE \quad (3.9)$$

The volume of the two-body phase space can now be easily calculated:

$$\begin{aligned}
\int \mathcal{R}_2((t; W, b)) &= \int \frac{d^{D-1}W}{2E_W} \frac{d^{D-1}b}{2E_b} \delta^{D-1}(\vec{W} + \vec{b}) \delta(1 - E_W - E_b) \\
&= \int \frac{d^{D-1}W}{4E_W^2} \delta(1 - 2E_W) \\
&= 2^{-1} \pi^{\frac{D-2}{2}} \frac{\Gamma(\frac{D-2}{2})}{\Gamma(D-2)}
\end{aligned} \tag{3.10}$$

In the last step we have used $\Gamma(D-2) = 2^{D-3} \pi^{-\frac{1}{2}} \Gamma(\frac{D-2}{2}) \Gamma(\frac{D-1}{2})$.

Calculation of the QCD corrections to the decay rate proceeds in analogy to the case of the decay $t \rightarrow H^+ b$ which will be treated in greater detail in the following chapter. Only the final result is quoted here:

$$\Gamma(t \rightarrow W^+ b) = \frac{G_F}{8\sqrt{2}\pi} m_t^3 |V_{tb}|^2 \left[1 + \frac{\alpha_s}{3\pi} \left(5 - \frac{4\pi^2}{3} \right) \right]. \tag{3.11}$$

3.3 Virtual corrections

We return now to the calculation including effects of b quark and W boson masses. First the one loop virtual corrections are evaluated. From the on-shell renormalization condition

$$\left. \frac{\partial \Sigma(p)}{\partial \not{p}} \right|_{p=m_q} = 0 \tag{3.12}$$

we determine the wave function renormalization constant for a quark of mass m_q :

$$Z_2 = 1 + \frac{\alpha_s}{3\pi} \left(-\frac{3}{\varepsilon} + 3\gamma - 3 \ln \frac{4\pi\mu^2}{m_q^2} - 4 \right) \tag{3.13}$$

We take the renormalization mass scale $\mu = m_t$ and thus absorb μ into the scaled masses. In calculating the vertex correction we take γ_5 anticommuting with all γ_μ . The total $O(\alpha_s)$ virtual correction is given by:

$$\begin{aligned}
\Gamma_V^{(1)} &= \frac{G_F m_t^3}{4\sqrt{2}\pi} \frac{2\alpha_s}{3\pi} \bar{p}_3 \left\{ f \left[\frac{2\bar{p}_0}{\bar{p}_3} \left(\text{Li}_2 \left(1 - \frac{\bar{w}_-}{\bar{w}_+} \right) - \text{Li}_2 \left(1 - \frac{\bar{p}_- \bar{w}_-}{\bar{p}_+ \bar{w}_+} \right) + \bar{Y}_p^2 \right. \right. \right. \\
&\quad \left. \left. - 2(\ln \epsilon + \bar{Y}_p)(\bar{Y}_w + \bar{Y}_p) - 4 + 4 \left(\frac{\bar{p}_0}{\bar{p}_3} \bar{Y}_p - 1 \right) \left(\frac{1}{2\varepsilon} - \ln \frac{\bar{p}_3}{2\pi} - \gamma - 1 \right) \right] \right. \\
&\quad \left. + 12w^2 \bar{Y}_p \bar{p}_3 - \ln \epsilon [1 + 4\epsilon^2 - 5\epsilon^4 - w^2(5 - \epsilon^2) + 4w^4] \right\}
\end{aligned} \tag{3.14}$$

3.4 Real gluon effects

To first order in α_s the remaining QCD effects to be calculated are emission of a gluon from the top or from the bottom quarks. The contribution to the total rate is:

$$\Gamma(t \rightarrow bWG) = \frac{1}{2(2\pi)^5} \int |M|^2 dR_3(Q; W, q, G). \quad (3.15)$$

We can factorize the three-body phase space into a product of two-body phase spaces:

$$dR_3(Q; W, q, G) = dP^2 dR_2(Q; W, P) dR_2(P; q, G) \quad (3.16)$$

where $P = q + G$ is the four-momentum of outgoing hadrons. Let us denote the square of the invariant mass of hadrons by z :

$$z \equiv P^2 \in [\epsilon^2, z_m = (1 - w)^2] \quad (3.17)$$

We will later have to integrate over z , but for now we can assume that the top quark decays into W (which is a real particle of specified mass) and a particle of mass \sqrt{z} . This is a two body decay, so the phase space integration is easy:

$$\begin{aligned} \int dR_2(Q; W, P) &= \int \frac{d^{D-1}W}{2W_0} \frac{d^{D-1}P}{2P_0} \delta^D(Q - P - W) \\ &= \int \frac{d^{D-1}P}{4W_0 P_0} \delta(Q_0 - P_0 - W_0). \end{aligned} \quad (3.18)$$

We use the factorization

$$d^{D-1}P = P^{D-2} dP d\Omega_{D-1} \quad (3.19)$$

where $d\Omega_{D-1}$ is a solid angle element in the $D - 1 = 3 - 2\varepsilon$ dimensional space. The integration over the angles gives:

$$\int d\Omega_{D-1} = \frac{2\pi^{\frac{3}{2}-\varepsilon}}{\Gamma(\frac{3}{2}-\varepsilon)} \quad (= 4\pi \text{ for } \varepsilon = 0). \quad (3.20)$$

The delta function is used up by the momentum integration and we obtain

$$\int dR_2(Q; W, P) = \frac{\pi^{\frac{3}{2}-\varepsilon}}{2\Gamma\left(\frac{3}{2}-\varepsilon\right)} p_3(z)^{1-2\varepsilon} \quad (3.21)$$

where $p_3(z)$ is the three-momentum of outgoing hadrons in the rest frame of the decaying quark.

We now turn our attention to the decay of our “particle of mass \sqrt{z} ” into a light quark and a gluon. We must stress here that it is an artificial object and in fact the gluon can be radiated either by the initial or by the final quark. To calculate corrections from the real gluon radiation we have to evaluate phase space integrals containing infrared divergences. There are two kinds of quark propagators in our process:

$$\frac{1}{(Q-G)^2-1} = -\frac{1}{2(QG)}, \quad (3.22)$$

$$\frac{1}{(q+G)^2-\epsilon^2} = \frac{1}{2(qG)}.$$

This leads to three types of divergent integrals:

$$C_1 = (2\pi)^{-5+4\varepsilon} \int dR_3(Q; W, q, G) \frac{1}{4(qG)^2}, \quad (3.23)$$

$$C_2 = -(2\pi)^{-5+4\varepsilon} \int dR_3(Q; W, q, G) \frac{1}{4(qG)(QG)}, \quad (3.24)$$

$$C_3 = (2\pi)^{-5+4\varepsilon} \int dR_3(Q; W, q, G) \frac{1}{4(QG)^2}. \quad (3.25)$$

Since the product (qG) depends only on z :

$$(qG) = \frac{z-\epsilon^2}{2}, \quad (3.26)$$

we pull it out of the integral over $dR_2(P; q, G)$ and write

$$C_n = \frac{2^{-8+4\varepsilon} \pi^{-\frac{7}{2}+3\varepsilon}}{\Gamma\left(\frac{3}{2}-\varepsilon\right)} \int_{\epsilon^2}^{z_m} dz p_3^{1-2\varepsilon} \left(\frac{-2}{z-\epsilon^2}\right)^{3-n} I_{1-n}, \quad (3.27)$$

with

$$I_n = \int dR_2(P; q, G)(QG)^n, \quad n = -2, -1, 0. \quad (3.28)$$

First we calculate the three integrals I_n . We work in the rest frame of $P = q + G$. Evaluation of I_0 is again trivial, leading to the volume of the quark-gluon phase space:

$$I_0 = \frac{\pi^{\frac{3}{2}-\varepsilon} E_G^{1-2\varepsilon}}{2\sqrt{z}\Gamma\left(\frac{3}{2}-\varepsilon\right)}, \quad (3.29)$$

where E_G denotes energy of the gluon:

$$E_G = \frac{z - \epsilon^2}{2\sqrt{z}}. \quad (3.30)$$

To proceed further we define a new integration variable $s = \cos \angle(\vec{Q}, \vec{G})$:

$$(QG) = \frac{E_G}{\sqrt{z}}(p_0 - p_3 s). \quad (3.31)$$

We will now calculate an integral over the hadronic phase space of the square of the first of the above propagators. This will illustrate the technique of doing phase space integrals in D dimensions.

Let us first have a closer look at spherical coordinates in a D-dimensional space. We choose one radius r and $D - 1$ angles $\theta_1 \dots \theta_{D-1}$ in analogy to the 3-dimensional space. The volume element in this system of coordinates is

$$d^D r = (r^{D-1} dr)(d\theta_1)(\sin \theta_2 d\theta_2) \dots (\sin^{D-2} \theta_{D-1} d\theta_{D-1}). \quad (3.32)$$

Standard spherical coordinates are recovered for $D = 3$ with θ_1 corresponding to ϕ and θ_{D-1} to θ .

We now want to do the integral

$$I_{-2} = \int dR_2(P; q, G) \frac{1}{(QG)^2}. \quad (3.33)$$

It is convenient to work in the rest frame of P . Energy and momentum of the heavy quark will be denoted by E_Q and P_Q , and energy of the gluon by

E_G . We take the z -axis to be along the three momentum of the heavy quark \vec{P}_Q . Then we have

$$\begin{aligned} I_{-2} &= \int \frac{d^{D-1}q}{2E_q} \frac{d^{D-1}G}{2E_G} \frac{\delta^D(P - q - G)}{E_G^2(E_Q - P_Q \cos \theta_{D-1})^2} \\ &= \int \frac{d^{D-1}G}{4E_q E_G^3} \frac{\delta(\sqrt{z} - E_q - E_G)}{(E_Q - P_Q \cos \theta_{D-1})^2}. \end{aligned} \quad (3.34)$$

The integration over E_G uses up the delta function. Since the integrand depends only on the angle θ_{D-1} , other angular variables can be integrated out and we get:

$$I_{-2} = \frac{\pi^{1-\varepsilon}}{2\Gamma(1-\varepsilon)} \frac{E_G^{-1-2\varepsilon}}{\sqrt{z}} \int_0^\pi \frac{\sin^{1-2\varepsilon} \theta_{D-1} d\theta_{D-1}}{(E_Q - P_Q \cos \theta_{D-1})^2}. \quad (3.35)$$

This integral can be done by a change of variable $s = \cos \theta_{D-1}$ and an expansion around $\varepsilon = 0$. We obtain:

$$\begin{aligned} I_{-2} &= \frac{\pi^{1-\varepsilon}}{2\Gamma(1-\varepsilon)} \frac{E_G^{-1-2\varepsilon}}{\sqrt{z}} \int_{-1}^1 \frac{(1-s^2)^{-\varepsilon} ds}{(E_Q - P_Q s)^2} \\ &= \frac{\pi^{1-\varepsilon}}{2\Gamma(1-\varepsilon)} \frac{E_G^{-1-2\varepsilon}}{\sqrt{z}} \left[\int_{-1}^1 \frac{ds}{(E_Q - P_Q s)^2} - \varepsilon \int_{-1}^1 \frac{\ln(1-s^2) ds}{(E_Q - P_Q s)^2} \right] \end{aligned} \quad (3.36)$$

Both these integrals are elementary. As a result we obtain:

$$I_{-2} = \frac{\pi^{1-\varepsilon}}{\Gamma(1-\varepsilon)} \frac{E_G^{-1-2\varepsilon}}{\sqrt{z}} \left[1 - 2\varepsilon \left(\ln 2 - \frac{p_0}{p_3} Y_p(z) \right) \right]. \quad (3.37)$$

In the same manner we can also get:

$$\begin{aligned} I_{-1} &= \frac{\pi^{1-\varepsilon} E_G^{-2\varepsilon}}{2\Gamma(1-\varepsilon)} \int_{-1}^1 \frac{(1-s^2)^{-\varepsilon}}{p_0 - p_3 s} ds \\ &= \frac{\pi^{1-\varepsilon}}{2\Gamma(1-\varepsilon)} \frac{E_G^{-2\varepsilon}}{p_3} \left[2Y_p(z) - \varepsilon \left(\text{Li}_2 \left(\frac{p_-}{p_+} \right) \right. \right. \\ &\quad \left. \left. - \text{Li}_2 \left(\frac{p_+}{p_-} \right) - 4Y_p(z) \ln \frac{p_3}{\sqrt{z}} \right) \right] \end{aligned} \quad (3.38)$$

We are now left with one dimensional integrals C_n which to the order $O(1)$ can be done in terms of elementary functions and dilogarithms:

$$\begin{aligned}
C_1 &= \frac{1}{2\bar{\tau}\pi^3\epsilon^2} \left[2\bar{p}_3 \left(-\frac{1}{2\epsilon} + \gamma - 2 + \ln \frac{2\bar{p}_3^3}{\pi\epsilon w} \right) + 2(w^2 - 1)\bar{Y}_p \right. \\
&\quad \left. - (1 - w^2 - \epsilon^2)\bar{Y}_w \right] \\
C_2 &= -\frac{1}{2\bar{\tau}\pi^3} \left[2\bar{Y}_p \left(-\frac{1}{2\epsilon} + \gamma - 1 + \ln \frac{2\bar{p}_3^3(z_m - \epsilon^2)}{\pi\epsilon} \right) \right. \\
&\quad + \text{Li}_2(1 - \bar{p}_-) - \text{Li}_2(1 - \bar{p}_+) - 3\text{Li}_2\left(1 - \frac{\bar{p}_-}{\bar{p}_+}\right) - 3\bar{Y}_p^2 \\
&\quad \left. + 2\ln\bar{p}_- \ln(1 - w - \bar{p}_-) - 2\ln\bar{p}_+ \ln(\bar{p}_+ - 1 + w) \right] \\
C_3 &= \frac{1}{2\bar{\tau}\pi^3} \left[2\bar{p}_3 \left(-\frac{1}{2\epsilon} + \gamma - 2 + \ln \frac{2\bar{p}_3^3}{\pi\epsilon w} \right) \right. \\
&\quad \left. - (1 - w^2 + \epsilon^2)\bar{Y}_p - (1 + w^2 - \epsilon^2)\bar{Y}_w \right] \tag{3.39}
\end{aligned}$$

These formulas are similar to those that can be obtained by the introduction of a finite gluon mass λ , but instead of $\ln \lambda$ we have a combination

$$\frac{1}{2\epsilon} - \gamma + 1 - \ln \frac{\bar{p}_3}{2\pi} \tag{3.40}$$

Integrals C_n are the only ones encountered in this calculation which contain poles $1/\epsilon$. All others are finite and can be easily done in 4-dimensional space. Evaluation of the real gluon radiation rate is now straightforward and after adding virtual corrections we obtain the total first order QCD correction to the total decay width:

$$\begin{aligned}
\Gamma^{(1)} &= \frac{G_F m_l^3}{8\sqrt{2}\pi} \frac{2\alpha_s}{3\pi} \left\{ 4f(1 - w^2 + \epsilon^2) \left[\text{Li}_2(\bar{p}_+) - \text{Li}_2(\bar{p}_-) - 2\text{Li}_2\left(1 - \frac{\bar{p}_-}{\bar{p}_+}\right) \right. \right. \\
&\quad \left. \left. + \bar{Y}_p \ln \frac{4\bar{p}_3^2 \bar{w}_-}{\bar{p}_+^2} - \bar{Y}_w \ln \bar{p}_- \right] + 4(1 - \epsilon^2)[(1 - \epsilon^2)^2 + w^2(1 + \epsilon^2) - 4w^4]\bar{Y}_w \right. \\
&\quad + [3 - \epsilon^2 + 11\epsilon^4 - \epsilon^6 + w^2(6 - 12\epsilon^2 + 2\epsilon^4) - w^4(21 + 5\epsilon^2) + 12w^6]\bar{Y}_p \\
&\quad + 8f\bar{p}_3 \ln \frac{w}{4\bar{p}_3^2} + 6[1 - 4\epsilon^2 + 3\epsilon^4 + w^2(3 + \epsilon^2) - 4w^4]\bar{p}_3 \ln \epsilon \\
&\quad \left. + [5 - 22\epsilon^2 + 5\epsilon^4 + 9w^2(1 + \epsilon^2) - 6w^4]\bar{p}_3 \right\} \tag{3.41}
\end{aligned}$$

We see that terms containing $\ln \bar{p}_3/2\pi$ have disappeared together with poles in ε . This was assured by taking D -dimensional phase space for contributions of both real and virtual gluons. Our final result is in perfect agreement with the formula derived by Jezabek and Kühn [2] and can be used as its independent check.

Chapter 4

Decay $t \rightarrow H^+ b$

4.1 Introduction

Many extensions of the Standard Model contain more than one Higgs doublet. The electroweak gauge bosons only absorb one of the charged Higgs fields, leaving the others as physical charged scalars, so that in a two-doublet model the top could decay to $H^+ b$ (if $m_t > m_{H^+} + m_b$). For certain choices of parameters, this process dominates over the expected $t \rightarrow W^+ b$ decay [5], so it is of interest to correctly calculate its QCD corrections.

It is well known that the QCD corrections to the decay rate of a heavy quark into a W are of order 10% in the Standard Model [1, 2]. Several groups have undertaken to calculate these corrections for the decay into a charged Higgs. The effect of the soft gluons has been calculated in ref. [52], and the decay $t \rightarrow H^+ b g$, with real gluons only, has been studied in ref. [53]. The full one-loop QCD corrections have been computed, at first by neglecting the mass of the b -quark in ref. [54], and then with a nonzero m_b in ref. [55] (in the framework of what is called the Model I - see discussion below). The claim of the latter paper is that the QCD correction for $m_t = 150$ GeV, $m_b = 4.5$ GeV and $\alpha_s = 0.1$ is as large as -15% in the (unphysical) limit of the massless Higgs. However, as will be argued in the following sections, according to the Equivalence Theorem (see [56, 57, 58] as well as [59] and references therein) the correction in this limit should be the same as the correction to the decay $t \rightarrow W^+ b$, which for the above values of parameters is -8.6% [1, 8]. The purpose of this Chapter is to reevaluate the first order QCD corrections

with non-zero b -quark mass. We use dimensional regularization for both the ultraviolet and the infrared divergences, which leads to simpler algebra than if one assigns a finite mass to the gluon, as was done in [54, 55, 59]. Our result is consistent with the Equivalence Theorem.

In a model with two Higgs doublets and generic couplings to all the quarks, it is difficult to avoid flavour-changing neutral currents. We therefore limit ourselves to models that naturally side-step these problems by restricting the Higgs couplings [5]. The first possibility is to have the doublet H_2 coupling to all the quarks, and the H_1 doublet interacting with none of them. The vacuum expectation value of $H_1 = v_1$ will nonetheless contribute to the W mass, leading to an $H^- t \bar{b}$ vertex of the form

$$\frac{gV_{tb}}{\sqrt{2}m_W} H^- \bar{b} \{m_t \cot \beta R - m_b \cot \beta L\} t \quad (\text{model I}) \quad (4.1)$$

where H^- is the physical charged Higgs, V_{tb} is the ‘33’ element of the CKM matrix, L and R are the chiral projection operators, and $\tan \beta = v_2/v_1$ is the ratio of the vacuum expectation values of the two Higgs. The second possibility is to have H_2 couple to the right-handed up-type quarks (u_R, c_R, t_R), and the H_1 couple to the right-handed down-type quarks. This is what happens in the Minimal Supersymmetric Standard Model. It is easy to show that the interaction Lagrangian

$$H_2 \bar{u}_R^i h_{ij}^{(u)} q_L^j + H_1 \bar{d}_R^i h_{ij}^{(d)} q_L^j + h.c. \quad (4.2)$$

leads to the vertex

$$\frac{gV_{tb}}{\sqrt{2}m_W} H^- \bar{b} \{m_t \cot \beta R - m_b \tan \beta L\} t \quad (\text{model II}) \quad (4.3)$$

where we have numbered the models in accordance with [5].

4.2 Limiting case of a very heavy top quark

The first order QCD corrections to this process have been calculated by two groups [54, 55, 59] who disagreed with each other. The work presented in this section was motivated by this disagreement. The question of the limiting case of a massless b quark was clarified when an erratum to the paper

[54] appeared. In this section we present a calculation of these corrections in the limit of a very heavy top quark, i.e., neglecting the masses of the bottom quark and the Higgs boson. The effect of finite m_H and m_b will be addressed in a following section. We use dimensional regularization to cope with both the ultraviolet and infrared divergences, which greatly simplifies the calculation, especially the real radiation part.

We take H_1 and H_2 to be the doublets whose vacuum expectation values respectively give masses to the down and up type quarks. The physical charged Higgs H^+ is a linear combination of the charged components of H_1 and H_2 , so if we neglect all the Yukawa couplings except that of H_2 to the third generation $= h_{tt}^{(2)}$, the top only couples to the H_2 component of H^+ . The interaction Lagrangian relevant to the decay $t \rightarrow H^+ b$ is then:

$$\begin{aligned}\mathcal{L} &= h_{tt}^{(2)} \cos \beta V_{tb} H^+ \bar{t} \left(\frac{1 - \gamma_5}{2} \right) b + h.c. \\ &= \frac{g}{2\sqrt{2}m_W} V_{tb} \cot \beta m_t H^+ \bar{t} (1 - \gamma_5) b + h.c.\end{aligned}\quad (4.4)$$

where $H^+ = \cos \beta H_2^+ - \sin \beta H_1^+$ and $\cot \beta = \langle H_1 \rangle / \langle H_2 \rangle$ is the ratio of vacuum expectation values of the two Higgs doublets.

In the following calculations we take the space-time dimension to be $D = 4 - 2\varepsilon$. The mass of the decaying quark is taken to be the renormalization mass scale, and we also use it as a unit of energy: $m_t = 1$. In the limit of a very heavy top quark the above interaction leads to the tree-level decay rate:

$$\begin{aligned}\Gamma^{(0)}(t \rightarrow H^+ b) &= \frac{G_F}{\sqrt{2}} \frac{\Gamma(1 - \varepsilon)}{2^{3-2\varepsilon} \pi^{1-\varepsilon} \Gamma(2 - 2\varepsilon)} \cot^2 \beta |V_{tb}|^2 \\ &\rightarrow \frac{G_F}{8\sqrt{2}\pi} \cot^2 \beta |V_{tb}|^2.\end{aligned}\quad (4.5)$$

The first order QCD corrections to this formula arise due to virtual gluon exchange and radiation of a real gluon. We first deal with the virtual gluon correction to the vertex tH^+b . In the limit $m_b = m_H = 0$ the spinor structure of this vertex remains unchanged and the unrenormalized correction amounts to the multiplication of the tree level rate by a factor:

$$\Lambda = C_F g_s^2 \frac{\Gamma(1 + \varepsilon)}{(4\pi)^{\frac{D}{2}}} \left(-\frac{1}{\varepsilon^2} + \frac{2}{\varepsilon} \right). \quad (4.6)$$

where the colour factor C_F is $4/3$ for $SU(3)$. The counterterm for this vertex involves the wave function and mass renormalization constants [60, 54]:

$$\Lambda_{c.t.} = \frac{1}{2} (Z_2^t - 1) + \frac{1}{2} (Z_2^b - 1) - \frac{\delta m_t}{m_t}. \quad (4.7)$$

If we use the same ε to regularize both UV and IR divergencies we obtain for the renormalization constants:

$$\begin{aligned} Z_2^t - 1 &= -\frac{\delta m_t}{m_t} = C_F g_s^2 \frac{\Gamma(1+\varepsilon)}{(4\pi)^{\frac{D}{2}}} \left(-\frac{3}{\varepsilon} - 4 \right), \\ Z_2^b - 1 &= 0. \end{aligned} \quad (4.8)$$

The contribution of the virtual correction to the decay rate is:

$$\begin{aligned} \Gamma_{virt}^{(1)}(t \rightarrow H^+ b) &= 2(\Lambda + \Lambda_{c.t.}) \Gamma^{(0)}(t \rightarrow H^+ b) \\ &= \frac{G_F}{\sqrt{2}} \cot^2 \beta |V_{tb}|^2 \alpha_s \frac{2^{-3+4\varepsilon} \pi^{-2+2\varepsilon}}{3\Gamma(2-2\varepsilon)} \left(-\frac{2}{\varepsilon^2} - \frac{5}{\varepsilon} - 12 - \frac{\pi^2}{3} \right). \end{aligned} \quad (4.9)$$

We now turn our attention to the effect of real gluon radiation from the initial or final quark. If we denote the amplitudes for these processes by \mathcal{A}_1 and \mathcal{A}_2 respectively, the contribution of the real radiation to the decay width is:

$$\Gamma_{real}^{(1)}(t \rightarrow H^+ b G) = \frac{1}{2} \frac{G_F}{\sqrt{2}} \cot^2 \beta |V_{tb}|^2 4\pi \alpha_s \int dR_3(t; b, H, G) |\mathcal{A}_1 + \mathcal{A}_2|^2 \quad (4.10)$$

where the coupling constants have been factored out and t, b, H and G denote the four-momenta of the initial and final quarks, charged Higgs boson and the gluon.

The advantage of using dimensional regularization for the infrared and collinear divergences is that we need not introduce a mass for the gluon and the integration over three body massless phase space is very simple [61]. We choose to parametrise it by the variables $x = 2t \cdot G$ and $z = 1 - 2t \cdot b$ in terms of which the three body phase space integration becomes:

$$\int dR_3(t; b, H, G) = \frac{2^{4\varepsilon-7} \pi^{2\varepsilon-3}}{\Gamma(2-2\varepsilon)} \int_0^1 \frac{dx}{(1-x)^\varepsilon} \int_0^x \frac{dz}{z^\varepsilon (x-z)^\varepsilon}. \quad (4.11)$$

After summing over the polarizations of the b quark and the gluon, and averaging over the polarizations of the t quark, the squares of the amplitudes become:

$$\begin{aligned} |\mathcal{A}_1|^2 &= -\frac{4}{x^2} [2(1-x) + x(1-\varepsilon)(z-x)] \\ |\mathcal{A}_2|^2 &= \frac{4x}{x-z}(1-\varepsilon) \\ \mathcal{A}_1\mathcal{A}_2^* + \mathcal{A}_2\mathcal{A}_1^* &= \frac{8}{x(x-z)} [1-x + x(1-\varepsilon)(z-x)] \end{aligned} \quad (4.12)$$

The integration over the phase space can be done exactly in any dimension. In the limit $\varepsilon \rightarrow 0$ the contribution of the real radiation becomes:

$$\Gamma_{real}^{(1)}(t \rightarrow H^+b) = \frac{G_F}{\sqrt{2}} \cot^2 \beta |V_{tb}|^2 \alpha_s \frac{2^{-3+4\varepsilon} \pi^{-2+2\varepsilon}}{3\Gamma(2-2\varepsilon)} \left(\frac{2}{\varepsilon^2} + \frac{5}{\varepsilon} + 17 - \pi^2 \right). \quad (4.13)$$

Although the respective phase space integrations of $|\mathcal{A}_1|^2$, $|\mathcal{A}_2|^2$ and $\mathcal{A}_1\mathcal{A}_2^* + \mathcal{A}_2\mathcal{A}_1^*$ give different results from the analogous amplitudes with a W^+ replacing the charged scalar, their sum nevertheless gives the same total contribution in both processes. This is in agreement with the general argument based on the equivalence theorem in ref. [59].

Finally we add the effects of the virtual and real gluons to obtain the first order QCD correction, so the decay rate (with m_t reinstated) becomes:

$$\Gamma(t \rightarrow H^+b) = \frac{G_F}{8\sqrt{2}\pi} m_t^3 \cot^2 \beta |V_{tb}|^2 \left[1 + \frac{\alpha_s}{3\pi} \left(5 - \frac{4\pi^2}{3} \right) \right]. \quad (4.14)$$

This is identical to the result obtained in ref. [59] and also to the analogous correction to the decay $t \rightarrow W^+b$ [1, 8, 62, 63]. If we take $\alpha_s = 0.1$ the first order correction in the limit $m_b = m_H = 0$ is approximately equal to -8.7% . This is in disagreement with the value reported in ref. [54, 55].

4.3 Effects of b and H^+ masses

In this and the following sections we discuss the effects of b quark and H^+ scalar masses in the QCD corrections to the decay $t \rightarrow H^+b$. In order to

simplify the following formulas we introduce dimensionless parameters for the scaled masses:

$$\epsilon = \frac{m_b}{m_t}, \quad \chi = \frac{m_H}{m_t}, \quad w = \frac{m_W}{m_t}, \quad (4.15)$$

and write the vertex $t \rightarrow H^+ b$ as

$$i \frac{g}{2\sqrt{2}w} V_{tb} \bar{b} (a + b\gamma_5) t. \quad (4.16)$$

where from (4.1) and (4.3)

$$\text{Model I: } \begin{cases} a = \cot \beta (1 - \epsilon) \\ b = \cot \beta (1 + \epsilon) \end{cases} \quad \text{Model II: } \begin{cases} a = \cot \beta + \epsilon \tan \beta \\ b = \cot \beta - \epsilon \tan \beta \end{cases}$$

The next section contains our result, which is examined in section 4.3.2. Section 4.3.4 contains some details of the calculation.

4.3.1 QCD Corrections

The notation we use is similar to that used in the analysis of semileptonic decays [1, 2]. In terms of the dimensionless parameters (4.15), we define the following kinematic variables:

$$\begin{aligned} \bar{P}_0 &\equiv \frac{1}{2}(1 - \chi^2 + \epsilon^2) \\ \bar{P}_3 &\equiv \frac{1}{2}\sqrt{1 + \chi^4 + \epsilon^4 - 2(\chi^2 + \epsilon^2 + \chi^2\epsilon^2)} \\ \bar{P}_\pm &\equiv \bar{P}_0 \pm \bar{P}_3 \\ \bar{Y}_p &\equiv \frac{1}{2} \ln \frac{\bar{P}_+}{\bar{P}_-} \\ \bar{W}_3 &\equiv \frac{1}{2}(1 + \chi^2 - \epsilon^2) \\ \bar{W}_\pm &\equiv \bar{W}_0 \pm \bar{P}_3 \\ \bar{Y}_w &\equiv \frac{1}{2} \ln \frac{\bar{W}_+}{\bar{W}_-} \end{aligned} \quad (4.17)$$

The tree level decay rate is

$$\Gamma^0(t \rightarrow H^+ b) = \frac{G_F m_t^3}{4\sqrt{2}\pi} |V_{tb}|^2 [\bar{P}_0(a^2 + b^2) + \epsilon(a^2 - b^2)] \bar{P}_3 \quad (4.18)$$

and the $O(\alpha_s)$ correction is

$$\Gamma^{(1)} = \frac{\alpha_s}{6\pi^2} \frac{G_F m_t^3 |V_{tb}|^2}{\sqrt{2}} \left[(a^2 + b^2) G_+ + (a^2 - b^2) \epsilon G_- + ab G_0 \right] \quad (4.19)$$

with

$$\begin{aligned} G_+ &= \bar{P}_0 \mathcal{H} + \bar{P}_0 \bar{P}_3 \left[\frac{9}{2} - 4 \ln \left(\frac{4\bar{P}_3^2}{\epsilon \chi} \right) \right] \\ &\quad + \frac{1}{4\chi^2} \bar{Y}_p \left(2 - \chi^2 - 4\chi^4 + 3\chi^6 - 2\epsilon^2 - 2\epsilon^4 + 2\epsilon^6 - 4\chi^2 \epsilon^2 - 5\chi^2 \epsilon^4 \right), \\ G_- &= \mathcal{H} + \bar{P}_3 \left[6 - 4 \ln \left(\frac{4\bar{P}_3^2}{\epsilon \chi} \right) \right] + \frac{1}{\chi^2} \bar{Y}_p \left(1 - \chi^2 - 2\epsilon^2 + \epsilon^4 - 3\chi^2 \epsilon^2 \right), \\ G_0 &= -6\bar{P}_0 \bar{P}_3 \ln \epsilon, \end{aligned} \quad (4.20)$$

and

$$\begin{aligned} \mathcal{H} &= 4\bar{P}_0 \left[\text{Li}_2(\bar{P}_+) - \text{Li}_2(P_-) - 2\text{Li}_2 \left(1 - \frac{\bar{P}_-}{\bar{P}_+} \right) \right. \\ &\quad \left. + \bar{Y}_p \ln \left(\frac{4\bar{P}_3^2 \chi}{\bar{P}_+^2} \right) - \bar{Y}_w \ln \epsilon \right] + 2\bar{Y}_w (1 - \epsilon^2) + \frac{2}{\chi^2} \bar{P}_3 \ln \epsilon (1 + \chi^2 - \epsilon^2). \end{aligned}$$

In the limit of the zero mass of the b quark the QCD correction becomes

$$\lim_{\epsilon \rightarrow 0} \Gamma^{(1)} = \frac{\alpha_s}{6\pi^2} \frac{G_F m_t^3 |V_{tb}|^2}{\sqrt{2}} \cot^2 \beta (2\tilde{G}_+ + \tilde{G}_0), \quad (4.21)$$

where

$$\begin{aligned} \tilde{G}_+ &= (1 - \chi^2)^2 \left[\text{Li}_2(1 - \chi^2) - \frac{\chi^2}{1 - \chi^2} \ln \chi \right. \\ &\quad \left. + \ln \chi \ln(1 - \chi^2) + \frac{1}{2\chi^2} \left(1 - \frac{5}{2}\chi^2 \right) \ln(1 - \chi^2) - \frac{\pi^2}{3} + \frac{9}{8} + \frac{3}{4} \ln \epsilon \right], \\ \tilde{G}_0 &= -\frac{3}{2} (1 - \chi^2)^2 \ln \epsilon, \end{aligned} \quad (4.22)$$

and we see that the mass singularities $\sim \ln \epsilon$ cancel in the expression for the total rate (4.21). Our result in this limit is identical to the one obtained by Liu and Yao [59] and is in agreement with the corrected version of ref. [54].

If we further take the limit $m_H \rightarrow 0$ the rate becomes:

$$\lim_{\epsilon, \lambda \rightarrow 0} \Gamma^{(1)} = \frac{\alpha_s}{6\pi^2} \frac{G_F m_t^3 |V_{tb}|^2}{\sqrt{2}} \cot^2 \beta \left(\frac{5}{4} - \frac{\pi^2}{3} \right), \quad (4.23)$$

which is in agreement with the conclusion of the ref. [59] as well as with our previous result [9].

Now we would like to compare the corrections to the decay width $\Gamma(t \rightarrow H^+ b)$ with those to $\Gamma(t \rightarrow W^+ b)$. For simplicity we now take $m_b = 0$ and $\cot \beta = 1$, and examine the ratio of the first order correction to the Born rate:

$$\begin{aligned} f_H(\lambda) &= \frac{\Gamma^{(1)}(t \rightarrow H^+ b)}{\Gamma^{(0)}(t \rightarrow H^+ b)}, \\ f_W(w) &= \frac{\Gamma^{(1)}(t \rightarrow W^+ b)}{\Gamma^{(0)}(t \rightarrow W^+ b)}. \end{aligned} \quad (4.24)$$

It has been noted in [59] that in the limit of the infinite top mass these ratios are equal: $f_H(0) = f_W(0)$. On the other hand, when m_H approaches m_t , we have:

$$f_H(\lambda) \xrightarrow{\lambda \rightarrow 1} \frac{\alpha_s}{3\pi} \left[-6 \ln(1 - \lambda^2) - \frac{8}{3} \pi^2 + 13 \right]. \quad (4.25)$$

By comparison with [1] we see that:

$$\lim_{x \rightarrow 1} \frac{f_H(x)}{f_W(x)} = 1. \quad (4.26)$$

Finally, we examine the corrections in the limiting case where the mass of the charged Higgs is zero but the b quark mass is finite. This is of course unphysical, but serves as a useful check on our equations. If we choose the parameters a and b from (4.16) to correspond to the couplings of the single Standard Model Higgs, then the Equivalence Theorem implies that the corrections are the same as in the process $t \rightarrow bW$ in the limit of massless W boson and nonzero m_b . The latter can be obtained by taking the limit of the relevant formula [1, 8]:

$$\lim_{m_W \rightarrow 0} \Gamma^{(1)}(t \rightarrow bW) = \frac{\alpha_s}{24\pi^2} \frac{G_F m_t^3 |V_{tb}|^2}{\sqrt{2}}$$

$$\begin{aligned}
& \left\{ 8(1 - \epsilon^2)^2(1 + \epsilon^2) \left[\text{Li}_2(\epsilon^2) - \frac{\pi^2}{6} + \ln(\epsilon) \ln(1 - \epsilon^2) \right] \right. \\
& - 4\epsilon^2 (7 - 5\epsilon^2 + 4\epsilon^4) \ln(\epsilon) - 8(1 - \epsilon^2)^3 \ln(1 - \epsilon^2) \\
& \left. - (1 - \epsilon^2)(-5 + 22\epsilon^2 - 5\epsilon^4) \right\} \quad (4.27)
\end{aligned}$$

The couplings of the Goldstone boson charged Higgs of the Standard Model (longitudinal W) to t and b can easily be calculated to be those of Model I, with $\cot \beta = 1$. In this case, the corrections to the decay $t \rightarrow bH^+$ are, in the limit $m_H \rightarrow 0$:

$$\lim_{m_H \rightarrow 0} \Gamma^{(1)}(t \rightarrow bH^+) = \frac{\alpha_s}{6\pi^2} \frac{G_F m_t^3 |V_{tb}|^2}{\sqrt{2}} \left[2(1 + \epsilon^2)G_+^0 - 4\epsilon^2 G_-^0 + (1 - \epsilon^2)G_0^0 \right] \quad (4.28)$$

where G_i^0 are limits of corresponding functions G_i for $m_H = 0$:

$$\begin{aligned}
G_+^0 &= (1 + \epsilon^2)^2 \left[\text{Li}_2(\epsilon^2) - \frac{\pi^2}{6} + \ln(\epsilon) \ln(1 - \epsilon^2) \right] \\
&\quad + \left(\frac{3}{4} + \epsilon^2 - \frac{5}{4}\epsilon^4 \right) \ln(\epsilon) - (1 - \epsilon^4) \ln(1 - \epsilon^2) + \frac{5}{8}(1 - \epsilon^4) \\
G_-^0 &= 2(1 + \epsilon^2) \left[\text{Li}_2(\epsilon^2) - \frac{\pi^2}{6} + \ln(\epsilon) \ln(1 - \epsilon^2) \right] \\
&\quad + (3 - \epsilon^2) \ln(\epsilon) - 2(1 - \epsilon^2) \ln(1 - \epsilon^2) + 2(1 - \epsilon^2) \\
G_0^0 &= -\frac{3}{2}(1 - \epsilon^4) \ln(\epsilon) \quad (4.29)
\end{aligned}$$

Inserting these expressions into equation (4.28) we obtain the same formula as (4.17).

4.3.2 Discussion

In Figure (4.1) the ratio of the first order QCD correction to the Born rate for the decay $t \rightarrow H^+ b$ is plotted as the function of the ratio of masses $\chi = m_H/m_t$. We have chosen the set of parameters $\cot \beta = 1$, $m_t = 150$ GeV

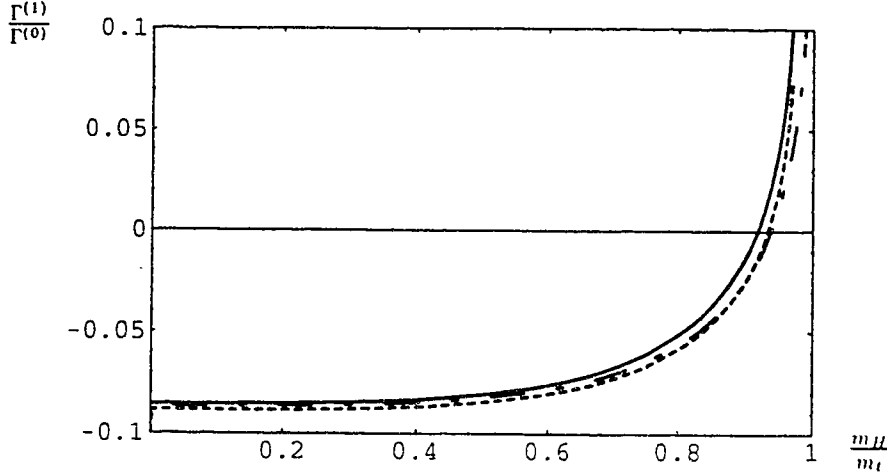


Figure 4.1: Ratio of the first order correction to the Born rate for $\tan \beta = 1$ and $m_t = 150$ GeV: $m_b = 4.5$ GeV (Model I - solid, Model II - dotted), $m_b = 0$ (dash-dotted line).

for an easy comparison with the analogous diagram in ref. [55]. It can be seen that the effect of the mass of the b -quark is negligible, except in the case of $m_t - m_H \sim m_b$.

There are also logarithmic corrections ($\sim \epsilon^2 \ln \epsilon$) to the decay rate in model II, as can be seen from Figure (4.2). Here we compare the branching ratios of the decays $t \rightarrow H^+ b$ and $t \rightarrow W^+ b$, taking $m_t = 100$ GeV so that this plot can be easily compared with a similar one published in ref. [5]. Our graph is different from theirs in that we now include QCD corrections to both decay rates. These corrections modify the diagram significantly only in the case of large values of $\tan \beta$ in Model II. It must be noted however, that although the corrections are relatively large, the top decays principally to $W^+ b$ in this region of $\tan \beta$. In model I, both a and b are proportional to $\cot \beta$, so the log of the branching ratio as a function of $\tan \beta$ decreases with a slope of -2. As can be seen from figure (4.2), the $\ln \epsilon$ corrections cancel to order ϵ^2 among G_+ , G_- and G_0 . However in model II, the decay rate is a polynomial in $\tan \beta$ with exponents -2, 0 and 2, and the $\ln \epsilon$ does not cancel in the “0” and “2” terms.

The logarithmic corrections in Model II can be interpreted in terms of running mass of the b quark [60]. To this end we rewrite the formulas for the

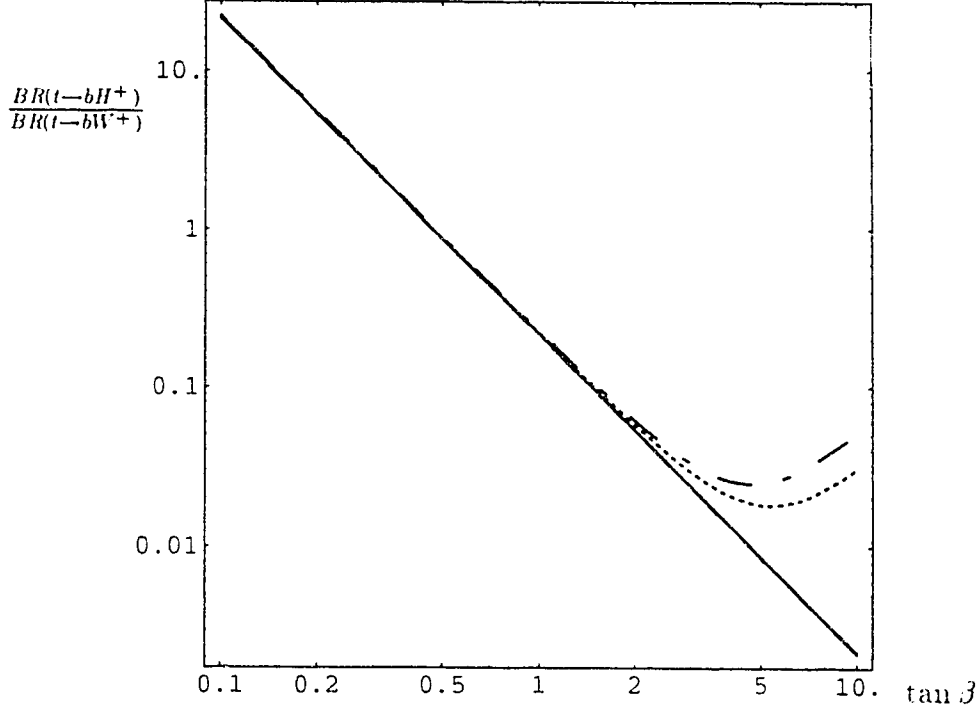


Figure 4.2: Ratio of the branching ratios of $t \rightarrow bH^+$ and $t \rightarrow bW^+$ for $m_b = 4.5$ GeV: in the Model I with and without QCD corrections (solid and dashed lines, indistinguishable) and in the Model II (dotted and dash-dotted lines, respectively).

tree level decay rate and for the first order corrections in the limit of very large $\tan \beta$ and mass of the top quark:

$$\begin{aligned}\Gamma^{(0)}(t \rightarrow H^+ b) &= \frac{G_F m_t^3}{8\sqrt{2}\pi} |V_{tb}|^2 (1 - \chi^2) [4 + (1 - \chi^2) \tan \beta] \epsilon^2, \\ \Gamma^{(1)}(t \rightarrow H^+ b) &= \frac{\alpha_s}{6\pi} \frac{G_F m_t^3 |V_{tb}|^2}{\sqrt{2}\pi} [(2G_+ - G_0) \tan^2 \beta + 4G_-] \epsilon^2.\end{aligned}\tag{4.30}$$

If we retain only terms $\sim \ln \epsilon$, the coefficient functions G_i become:

$$\begin{aligned}G_+ &\rightarrow \frac{3}{4}(1 - \chi^2)^2 \ln \epsilon, \\ G_- &\rightarrow 3(1 - \chi^2) \ln \epsilon, \\ G_0 &\rightarrow -\frac{3}{2}(1 - \chi^2)^2 \ln \epsilon.\end{aligned}\tag{4.31}$$

Using these expressions we can calculate the asymptotic value of first order corrections for large values of $\tan \beta$ and m_t :

$$\Gamma^{(1)} = \frac{4\alpha_s}{\pi} \ln \left(\frac{m_b}{m_t} \right) \Gamma^{(0)}.\tag{4.32}$$

We see that for $\alpha_s \sim 0.1$, $m_b = 4.5$ GeV and $m_t = 100$ GeV this correction is of the order of -40% , in agreement with Figure (4.2). The size of corrections becomes even larger as the mass of the top quark increases, and eventually the one loop corrected rate of decay becomes negative; such large corrections are a sign of a breakdown of the perturbation theory. However, it is possible to avoid the large corrections by renormalizing mass of the b quark not on mass shell but at the energy scale characteristic to the process, which is mass of the top quark. The running mass of the bottom quark at this energy is:

$$\widetilde{m}_b(m_t) = m_b \left(1 + \frac{2\alpha_s}{\pi} \ln \frac{m_b}{m_t} \right),\tag{4.33}$$

and we see from the formula (4.32) that for large $\tan \beta$ and m_t the one loop corrected decay rate approaches the Born rate expressed in terms of the running b quark mass.

4.3.3 Summary

We have calculated an analytic expression for the $O(\alpha_s)$ corrections to the decay $t \rightarrow H^+ b$ for non-zero m_H and m_b . The $m_b = 0$ limit of our result is the same as in [59] and the corrected version of [54]; however, our full expression disagrees with the $m_b \neq 0$ result presented in [55]. To check the m_b dependence of our results we have compared it with the corresponding formula for the decay $t \rightarrow W^+ b$.

4.3.4 Details of the calculation

Throughout this calculation we have used dimensional regularization, working in $d = 4 - 2\varepsilon$ dimensions. The counterterm for the vertex function has been calculated according to ref. [54, 60]:

$$\begin{aligned} \delta\Lambda = & a \left\{ \frac{1}{2}(Z_t - 1) + \frac{1}{2}(Z_b - 1) \right\} - \frac{a + b}{2} \frac{\delta m_t}{m_t} - \frac{a - b}{2} \frac{\delta m_b}{m_b} \\ & + \left[b \left\{ \frac{1}{2}(Z_t - 1) + \frac{1}{2}(Z_b - 1) \right\} - \frac{a + b}{2} \frac{\delta m_t}{m_t} + \frac{a - b}{2} \frac{\delta m_b}{m_b} \right] \gamma_5 \end{aligned}$$

and the renormalization constants are (we take the renormalization scale equal to the mass of the decaying quark):

$$\begin{aligned} Z_t - 1 &= -\frac{\delta m_t}{m_t} = \frac{\alpha_s}{3\pi} \left(-\frac{3}{\varepsilon} + 3\gamma - 3 \ln 4\pi - 4 \right), \\ Z_b - 1 &= -\frac{\delta m_b}{m_b} = \frac{\alpha_s}{3\pi} \left(-\frac{3}{\varepsilon} + 3\gamma - 3 \ln \frac{4\pi}{\epsilon^2} - 4 \right). \end{aligned} \quad (4.34)$$

The contribution of the virtual corrections to the total decay rate is:

$$\Gamma_{virt}^{(1)} = \frac{\alpha_s}{6\pi^2} \frac{G_F m_t^3 |V_{tb}|^2}{\sqrt{2}} \left[(a^2 + b^2) V_+ + (a^2 - b^2) \epsilon V_- + ab G_0 \right], \quad (4.35)$$

where

$$\begin{aligned} V_+ &= \bar{P}_0 \mathcal{V} + \frac{\bar{Y}_p}{2\lambda^2} \left[(1 - \epsilon^2)^2 (1 + \epsilon^2) - \lambda^4 (3 + 3\epsilon^2 - 2\lambda^2) \right], \\ V_- &= \mathcal{V} + \bar{Y}_p \frac{(1 - \epsilon^2)^2 - \lambda^4}{\lambda^2}, \end{aligned} \quad (4.36)$$

with

$$\begin{aligned} \mathcal{V} = & 2\bar{P}_3 \left[-\frac{1}{\varepsilon} + 2\gamma + 2\ln \frac{\bar{P}_3}{2\pi} - 3 + \frac{1}{\chi^2}(1 - \epsilon^2 + \chi^2) \ln \epsilon \right] \\ & + 2\bar{P}_0 \left[\text{Li}_2(\bar{P}_+) - \text{Li}_2(\bar{P}_-) - \text{Li}_2\left(1 - \frac{\bar{P}_-}{\bar{P}_+}\right) - \bar{Y}_p^2 - 2\ln \epsilon \bar{Y}_w \right. \\ & \left. - 2\bar{Y}_p \left(-\frac{1}{2\varepsilon} + \gamma + \ln \frac{\bar{P}_3 \epsilon}{2\pi\chi} \right) \right]. \end{aligned}$$

The real gluon radiation calculation requires an integration over three body phase space $\Phi(t; H, b, g)$. This leads to divergences due to the emission of soft and collinear gluons, for which we use dimensional regularization (see ref. [44] and references quoted therein). The phase space integration we are considering now is analogous to the decay $t \rightarrow Wbg$, for which the relevant integrals have been listed in [8]. Adding the result to the virtual gluon contribution (4.35) yields the final formula (4.19).

It should be added that this calculation was greatly facilitated by the use of algebraic manipulation programs FORM [32] and Mathematica [64].

4.4 QCD corrections to two body decays of the top

The purpose of this section is to discuss QCD corrections to the decay $t \rightarrow H^+b$ with all mass effects taken into account and to compare them with the analogous corrections to $t \rightarrow W^+b$. The main difference lies of course in the structure of the vertices responsible for these decays, and in the resulting renormalization procedure. This will be discussed first. Second, we observe that despite this difference the resulting formulae are equal (up to corrections of order m_W/E) in the limit where m_W and m_H are small, and when the Higgs coupling is taken to correspond to that of the Goldstone boson eaten by the W . This striking feature is due to the Equivalence Theorem¹. It is useful as a check on the full calculations, but one must note that for physical values of the W and top masses, the order m_W/E_W corrections are quite large.

¹We are indebted to Professor M.K. Gaillard for a comment which led us to this observation.

4.4.1 Structure of counterterms

For simplicity we take the CKM matrix element V_{tb} , as well as the ratio of the Higgs vacuum expectation values, to be one (the physical charged Higgs in the two doublet model then has the same coupling as the Goldstone boson of the Standard Model). The term in the lagrangian responsible for the decay $t \rightarrow H^+ b$ is then:

$$\frac{g}{\sqrt{2}m_W} H^- \bar{b} \{m_t R - m_b L\} t \quad (4.37)$$

where we denoted the chiral projection operators $(1 \pm \gamma_5)/2$ by R and L. On the other hand the standard decay $t \rightarrow W^+ b$ is due to the term:

$$\frac{g}{\sqrt{2}} W_\mu^- \bar{b} \gamma^\mu L t. \quad (4.38)$$

In order to incorporate QCD corrections to these decays we introduce renormalized quark fields and masses (the Higgs and W fields are not renormalized at first order in α_s):

$$\begin{aligned} m_t &= m_t^R - \delta m_t, \\ m_b &= m_b^R - \delta m_b, \\ t &= \sqrt{Z_2^t} t^R, \\ b &= \sqrt{Z_2^b} b^R. \end{aligned} \quad (4.39)$$

Because of the presence of quark masses in the Higgs coupling in (4.37) the counterterm for that vertex is:

$$\begin{aligned} \frac{g}{\sqrt{2}m_W} H^- \bar{b} \left\{ \left(\frac{Z_2^t - 1}{2} + \frac{Z_2^b - 1}{2} - \frac{\delta m_t}{m_t} \right) m_t R \right. \\ \left. - \left(\frac{Z_2^t - 1}{2} + \frac{Z_2^b - 1}{2} - \frac{\delta m_b}{m_b} \right) m_b L \right\} t. \end{aligned} \quad (4.40)$$

whereas the counterterm for the decay $t \rightarrow W^+ b$ is simply:

$$\frac{g}{\sqrt{2}} W_\mu^- \bar{b} \left\{ \frac{Z_2^t - 1}{2} + \frac{Z_2^b - 1}{2} \right\} \gamma^\mu L t. \quad (4.41)$$

The form of these counterterms suggests that the virtual corrections to these decays should be quite different. In the following we shall see that if the emitted W boson is longitudinal, then in the limit of a very heavy top quark the corrections to both processes become equal.

4.4.2 Equivalence Theorem

The three polarization vectors of a massive gauge boson with momentum \vec{W} along the \hat{z} axis are:

$$\begin{aligned}\epsilon_T^1 &= \frac{1}{\sqrt{2}}(0, 1, i, 0) \\ \epsilon_T^2 &= \frac{1}{\sqrt{2}}(0, 1, -i, 0) \\ \epsilon_L &= \frac{1}{m_W}(|\vec{W}|, 0, 0, E_W)\end{aligned}\tag{4.42}$$

where the longitudinal polarizarization vector is the four-momentum W^μ , up to corrections of order m_W/E_W . If we examine the situation where the top quark is very massive, then the longitudinal polarization vector dominates over the transverse, and to order m_W/E_W , the sum over W polarizations can be taken to be $W^\mu W^\nu/m_W^2$. The equivalence theorem then states that amplitudes involving external longitudinal W 's are equal, up to corrections of order m_W/E_W , to the same amplitudes with the W_L s replaced by (unphysical) Goldstone bosons.

Let us now compare the tree level amplitudes. For $t \rightarrow W^+ b$ we have

$$\begin{aligned}\epsilon_L^\mu \frac{g}{\sqrt{2}} \bar{u}_b \gamma_\mu L u_t &= \frac{g}{\sqrt{2} m_W} \bar{u}_b (\not{f} - \not{b}) L u_t + O(m_W/E_W) \\ &= \frac{g}{\sqrt{2} m_W} \bar{u}_b \{m_t R - m_b L\} u_t + O(m_W/E_W)\end{aligned}\tag{4.43}$$

where we made use of the Dirac equation (\not{f} and \not{b} are t and b quark four-momenta contracted with Dirac matrices). To leading order, this is the amplitude for $t \rightarrow H^+ b$. Let us now consider the decay process with radiation of a gluon (see Figure 4.3). There are two amplitudes contributing to this process and we examine their sum (we now neglect all corrections of order m/E):

$$\begin{aligned}&\bar{u}_b (\not{f} - \not{b} - \not{G}) L \mathcal{P}_{tG} \not{f} u_t + \bar{u}_b \not{f} \mathcal{P}_{bG} (\not{f} - \not{b} - \not{G}) L u_t \\ &= \bar{u}_b \{(m_t R - m_b L) \mathcal{P}_{tG} \not{f} + \not{f} \mathcal{P}_{bG} (m_t R - m_b L)\} u_t,\end{aligned}\tag{4.44}$$

where \not{G} is the gluon polarization, and we have introduced the following notation for the propagators:

$$\mathcal{P}_{tG} = \frac{1}{\not{f} - \not{G} - m_t},$$

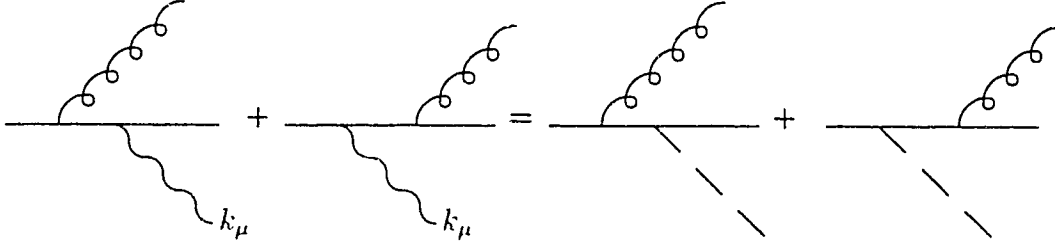


Figure 4.3: Real gluon radiation amplitudes

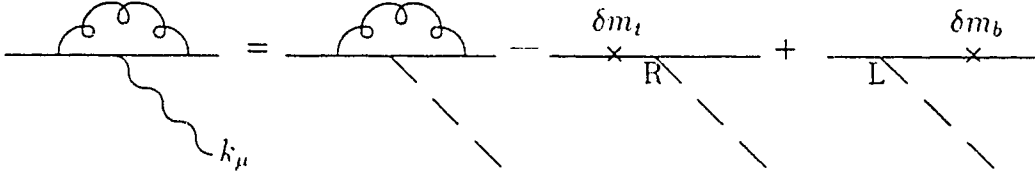


Figure 4.4: Virtual one loop amplitudes

$$\mathcal{P}_{bG} = \frac{1}{\not{p} + \not{G} - m_b}, \quad (4.45)$$

and we used:

$$\begin{aligned} (\not{t} - \not{G})\mathcal{P}_{tG} &= 1 + m_t\mathcal{P}_{tG}, \\ (\not{p} + \not{G})\mathcal{P}_{bG} &= 1 + m_b\mathcal{P}_{bG}. \end{aligned} \quad (4.46)$$

As the last example we take the virtual gluon correction to the vertex (see Figure 4.4). As the result does not depend on QCD gauge, we take a generic gluon propagator, denoted by $D_{\mu\nu}$. We then have for $t \rightarrow W^+b$:

$$\begin{aligned} &\bar{u}_b \gamma^\mu P_{b\bar{G}} (\not{t} - \not{p}) L \mathcal{P}_{tG} \gamma^\nu u_t D_{\mu\nu} \\ &= \bar{u}_b \gamma^\mu P_{b\bar{G}} [m_t R - m_b L] \mathcal{P}_{tG} \gamma^\nu u_t D_{\mu\nu} + \bar{u}_b \gamma^\mu [P_{b\bar{G}} R - L \mathcal{P}_{tG}] \gamma^\nu u_t D_{\mu\nu}. \end{aligned} \quad (4.47)$$

where $P_{b\bar{G}}$ is now

$$P_{b\bar{G}} = \frac{1}{\not{p} - \not{G} - m_b}. \quad (4.48)$$

The second term of the RHS can be written as:

$$\bar{u}_b(\delta m_b L - \delta m_t R) u_t, \quad (4.49)$$

and thus the difference between vertex loop amplitudes of $t \rightarrow W^+ b$ and $t \rightarrow H^+ b$ is exactly cancelled by the counterterms calculated in formulas (4.40) and (4.41).

We have shown that to first order in the QCD coupling, the amplitude for $t \rightarrow W^+ b$ differs from the amplitude for $t \rightarrow H^+ b$ by terms of order m_W/E_W . In this context, H^+ was a physical particle whose interactions with the Standard Model fermions were chosen to match the coupling of the Goldstone boson eaten by the W^+ . We could therefore use the Equivalence Theorem, which relates longitudinal W to Goldstone boson amplitudes, to relate $t \rightarrow W^+ b$ to $t \rightarrow H^+ b$.

We now wish to discuss the Equivalence Theorem [56, 57, 58] in more detail. Since the W boson has been detected, its three polarization states are physical degrees of freedom: on the other hand, the Goldstone boson is gauge-dependent. The Equivalence Theorem therefore relates physical and unphysical amplitudes, and is only true for an appropriate choice of gauge (and renormalization scheme). We work in the Feynman 't Hooft gauge, and neglect all higher order effects in the electroweak and scalar couplings. We will therefore show (following [65]) the Equivalence Theorem as it applies to our amplitudes to all orders in QCD, but at tree level in the other couplings. This restriction is not necessary [58, 66], but makes the discussion much simpler; a renormalized version of the following can be found in ref. [67].

We take as a gauge fixing condition for the W^+

$$G = \partial^\mu W_\mu^+ - \frac{gv}{2} \phi^+ \quad (4.50)$$

where ϕ is the Goldstone boson, v the Higgs vacuum expectation value and g the weak coupling constant. The equations of motion give $G = 0$. The physical states, and the gauge-fixed Lagrangian are invariant under BRS transformations [68], which correspond in some sense to a residual global version of the gauged symmetry. One can therefore show that Greens functions are BRS invariant, so that

$$S < f | \bar{c}(x) | i > = 0 \quad (4.51)$$

where G is the BRST generator, i is the initial top quark, f is the final state consisting of a b quark and some number of gluons, and \bar{c} is an anti-ghost. From the definition of the BRST transformation, we have

$$S\bar{c} = -G \quad (4.52)$$

so that

$$\partial^\mu \langle f | W_\mu^+ | i \rangle = m_W \langle f | \phi^+ | i \rangle . \quad (4.53)$$

We can obtain the Equivalence Theorem, which relates S-matrix elements, from this statement about Greens functions via LSZ reduction. This is simple at tree level in this gauge because the Goldstone and gauge bosons have the same propagator; at higher order in the scalar and electroweak gauge coupling, this step is no longer obvious. So to all orders in QCD, but at tree level for everything else, we have

$$\partial^\mu \langle b, G^n, W_\mu^+ | t \rangle = m_W \langle b, G^n, \phi^+ | t \rangle \quad (4.54)$$

where G^n are n final-state gluons. If this expression is written in momentum space, it is the Equivalence Theorem for the processes of interest to us, because the longitudinal polarization vector of the W is the momentum vector up to corrections of order m/E .

4.4.3 Summary

The connection between the top quark decay rates $t \rightarrow W^+ b$ and $t \rightarrow H^+ b$ could be very useful in future calculations. First, if we want to estimate the size of the two-loop QCD corrections, it is sufficient to calculate them in the limit of a very heavy top quark; at least at the one-loop level, the corrections in this limit have correct size for a large range m_t/m_W . This limit can now be calculated by considering the Higgs ghost instead of the W boson, which is much simpler. A second useful application is as a non-trivial check on electroweak corrections which have been calculated numerically. If the mass of the W in the final state is set equal to zero, the results should be the same as for a massless Higgs ghost, irrespective of the other quark masses in the problem. This should provide a useful check for the numerical program.

Chapter 5

Electroweak corrections to decays involving a charged Higgs boson

5.1 Introduction

Due to the expected large mass of the top quark and its possible large Yukawa coupling to Higgs bosons, decays of this particle (once it is observed, presumably at the Tevatron) can give us an insight into the Higgs sector and the mechanism of mass generation. A topic of particular importance is the number of Higgs doublets. The supersymmetric extensions of the Standard Model, for example, predicts existence of at least two Higgs doublets. In such scenarios, in addition to the charged Goldstone boson of the standard electroweak theory, there would be a physical charged scalar particle H^\pm . Its presence could influence the rate of top quark decay and even open up a new decay channel.

If the charged Higgs boson is heavier than the top quark, its effect on the decay rate of the top will only be in the virtual corrections to the standard process $t \rightarrow W^+ b$. This has been examined in ref. [3, 4], and in some models the effect was found to be large, of the order of several percent. On the other hand, if the decay of the top into the charged Higgs and a bottom quark is kinematically allowed, it can become the dominant decay channel, especially if the ratio of vacuum expectation values of the two doublets is such

that the Yukawa coupling to the top is not suppressed. It is this scenario that is the topic of the present chapter. We examine the effects of first order electroweak corrections on the width of the decay $t \rightarrow H^+ b$ in the two Higgs doublet extension of the Standard Model suggested by supersymmetry [69, 5]. In this model one of the Higgs fields, H_1 , is responsible for giving masses to down-quarks, and the other one, H_2 - to up-quarks. The ratio of the expectation values of these two fields is denoted by $\tan \beta = v_2/v_1$. In the present work we consider the range of small values of $\tan \beta$, in which the mass of the bottom quark can be safely neglected, which considerably simplifies the calculations.

Radiative corrections to the decay $t \rightarrow H^+ b$ have been subject of several recent publications. The QCD corrections were summarized in the previous chapter. In the electroweak sector the corrections were studied only to the order $O(\alpha m_t^2/m_W^2)$. They have been calculated in ref. [70] and further analyzed in [71]. Such corrections would be dominant if the top quark was much heavier than the W boson. However in view of the expected mass of the top quark of the order of $(1.5 - 2)m_W$ it is important to compute also the remaining corrections not involving the top quark mass, as well as the effect of real photon radiation.

This chapter is organized as follows: the next section explains the renormalization scheme and various kinds of corrections. Section 5.3 discusses cancellation of infrared and ultraviolet divergences, especially the quadratic ones. Calculation of virtual corrections to vertices and evaluation of the bremsstrahlung are explained in sections 5.4 and 5.5. Section 5.6 presents final results; previously unpublished formulas for renormalization constants are collected in the last section.

5.2 Renormalization scheme

At the tree level the decay rate for $t \rightarrow H^+ b$ is obtained from the Feynman rule for the tbH^+ vertex:

$$i \frac{em_t}{\sqrt{2}m_W s_W} \cot \beta \bar{b} R t, \quad (5.1)$$

where we have taken the relevant element of the Kobayashi-Maskawa matrix to be equal 1 (and neglected the effect of the b quark mass). R denotes the

right chiral projection operator $(1 + \gamma_5)/2$. We use m_W and m_Z as input parameters and define $c_W^2 = 1 - s_W^2 = m_W^2/m_Z^2$. The resulting rate of the decay is:

$$\Gamma^{(0)}(t \rightarrow H^+ b) = \frac{\alpha m_t^3}{16 m_W^2 s_W^2} \cot^2 \beta \left(1 - \frac{m_{H^+}^2}{m_t^2}\right)^2. \quad (5.2)$$

Electroweak corrections modify the values of parameters in the vertex: the coupling constant e , masses m_W , m_Z and m_t , and the angle β . It is also necessary to calculate effects of the real photon radiation, virtual corrections to the vertex (triangle diagrams) and the renormalization of wave functions of the charged Higgs and of the quarks t and b . On the one loop level there are also contributions from the mixing of the charged Higgs with the W boson. Finally, since we are going to work in the 't Hooft-Feynman gauge, we have to include the mixing between H^+ and the charged Goldstone boson G^+ . The one loop correction to the decay rate can be written in the following form:

$$\Gamma^{(1)}(t \rightarrow H^+ b) = 2\Gamma^{(0)}(t \rightarrow H^+ b) \left(\frac{\delta e}{e} - \frac{\delta s_W}{s_W} + \frac{\delta m_t}{m_t} - \frac{\delta m_W}{m_W} + \frac{\delta \cot \beta}{\cot \beta} \right. \\ \left. + \frac{1}{2} \delta_{REAL}' + \delta_{\Delta}' + \frac{1}{2} \delta Z_b^L + \frac{1}{2} \delta Z_t^R + \frac{1}{2} \delta Z_H + \delta_{MIX}' \right) \quad (5.3)$$

δ_{REAL}' , δ_{Δ}' and δ_{MIX}' denote contributions of the real photon radiation, triangle diagrams and mixing of H^+ with W^+ and with G^+ respectively. For the renormalization of the angle β we employ the prescription introduced by Méndez and Pomarol [72, 73], with a small modification. It is assumed that the value of β will be extracted from the leptonic decay channel of the charged Higgs boson. Since the coupling is proportional to the mass, the dominant decay will be into a τ lepton and its neutrino. The renormalization of the angle β is fixed by the condition that radiative corrections to the vertex $\tau \nu_\tau H$ vanish. However, the renormalization constant for β defined in this way is infrared divergent; this problem was not addressed in the original papers [72, 73], because only the fermionic loop corrections were discussed there. The infrared divergence could also be removed in the suitable process of extracting the value of the β angle from the experimental measurement of the decay width of the charged Higgs boson. For the purpose of the current calculation it is convenient to include the effect of the real photon radiation

in the definition of $\delta\beta$. The one loop correction to the decay rate of the charged Higgs into tau and the neutrino can be written in analogy to the top decay:

$$\Gamma^{(1)}(H^- \rightarrow \tau \bar{\nu}_\tau) = 2\Gamma^{(0)}(H^- \rightarrow \tau \bar{\nu}_\tau) \left(\frac{\delta e}{e} - \frac{\delta s_W}{s_W} + \frac{\delta m_\tau}{m_\tau} - \frac{\delta m_W}{m_W} - \frac{\delta \cot \beta}{\cot \beta} + \frac{1}{2}\delta_{REAL}^\tau + \delta_\Delta^\tau + \frac{1}{2}\delta Z_\nu^L + \frac{1}{2}\delta Z_\tau^R + \frac{1}{2}\delta Z_H + \delta_{MIX}^\tau \right). \quad (5.4)$$

The notation here is analogous to the formula (5.3). Since the coupling of the charged Higgs to leptons is proportional to $\tan \beta$, the effect of renormalization of β has an opposite sign in the two decays under consideration. The reason for this is that in both cases we have only one fermion with non-negligible mass, but they have opposite values of the weak isospin.

The condition of vanishing of radiative corrections to the tau channel of the decay of the charged Higgs allows us to express the renormalization constant of the β angle in terms of corrections to the $H\tau\nu_\tau$ vertex. This leads to the following formula for the relative correction to the rate $t \rightarrow H^+b$:

$$\begin{aligned} \Delta\Gamma &\equiv \frac{\Gamma^{(1)}(t \rightarrow H^+b)}{\Gamma^{(0)}(t \rightarrow H^+b)} \\ &= 2 \left(2\frac{\delta e}{e} - 2\frac{\delta s_W}{s_W} + \frac{\delta m_\tau}{m_\tau} + \frac{\delta m_t}{m_t} - \frac{\delta m_W^2}{m_W^2} \right. \\ &\quad + \frac{1}{2}\delta_{REAL}^\tau + \frac{1}{2}\delta_{REAL}^t + \delta_\Delta^\tau + \delta_\Delta^t + \frac{1}{2}\delta Z_\nu^L + \frac{1}{2}\delta Z_\tau^R \\ &\quad \left. + \frac{1}{2}\delta Z_b^L + \frac{1}{2}\delta Z_t^R + \delta Z_H + \delta_{MIX}^\tau + \delta_{MIX}^t \right). \end{aligned} \quad (5.5)$$

As will be seen later, the mixing can be described by one constant δ_{MIX} defined so that

$$\delta_{MIX}^\tau + \delta_{MIX}^t = \frac{\cot \beta - \tan \beta}{m_{H^+}^2 - m_W^2} \delta_{MIX}. \quad (5.6)$$

The renormalization of the electroweak parameters is done in the on-shell scheme of ref. [74, 4, 75]. In particular, for the weak coupling constant e/s_W we have:

$$\frac{\delta e}{e} - \frac{\delta s_W}{s_W} \equiv \delta Z_e + \frac{\delta m_Z^2}{2m_Z^2} - \frac{\delta m_Z^2 - \delta m_W^2}{2(m_Z^2 - m_W^2)} \quad (5.7)$$

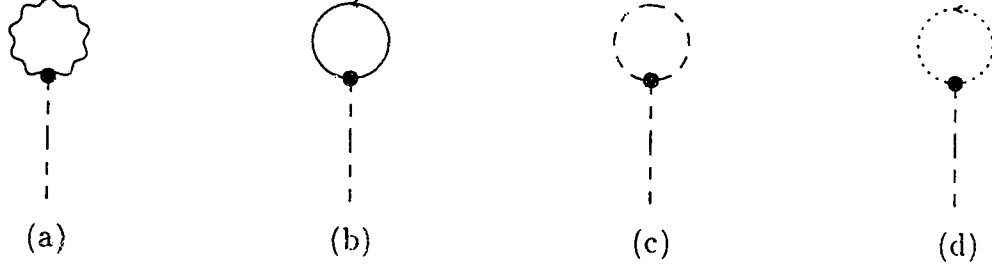


Figure 5.1: Types of tadpole diagrams in 2HDM

$$= \frac{1}{2} \frac{\partial \Sigma_T^{AA}(s)}{\partial s} \Big|_{s=0} - \frac{s_W}{c_W} \frac{\Sigma_T^{AZ}(0)}{m_Z^2} + \frac{\delta m_Z^2}{2m_Z^2} - \frac{\delta m_Z^2 - \delta m_W^2}{2(m_Z^2 - m_W^2)}.$$

This leads to the final formula from which we are going to calculate the one loop corrections:

$$\begin{aligned} \Delta\Gamma = 2 \left(2\delta Z_\epsilon + \frac{\delta m_\tau}{m_\tau} + \frac{\delta m_t}{m_t} - \frac{\delta m_W^2}{m_W^2} + \frac{\delta m_Z^2}{m_Z^2} - \frac{\delta m_Z^2 - \delta m_W^2}{(m_Z^2 - m_W^2)} \right. \\ \left. + \frac{1}{2}\delta_{REAL}^\tau + \frac{1}{2}\delta_{REAL}^t + \delta_\Delta^\tau + \delta_\Delta^t + \frac{1}{2}\delta Z_\nu^L + \frac{1}{2}\delta Z_\tau^R \right. \\ \left. + \frac{1}{2}\delta Z_b^L + \frac{1}{2}\delta Z_t^R + \delta Z_H + \frac{\cot\beta - \tan\beta}{m_{H^\pm}^2 - m_W^2} \delta_{MIX} \right). \end{aligned} \quad (5.8)$$

Many details and explicit formulas for some of the renormalization constants can be found in ref. [76]. There are no external Higgs particles in processes described in that reference, so the wave function renormalization of the charged Higgs boson and mixing with W^+ and Goldstone boson was not included. The relevant formulas can be found in section 5.7 of the present work.

5.3 Remarks on cancellation of divergences

In the calculation of electroweak corrections to decays $t \rightarrow H^+ b$ and $H^- \rightarrow \tau \bar{\nu}_\tau$ one encounters three kinds of infinite quantities: infrared divergences, and logarithmic and quadratic ultraviolet divergences.

The infrared divergent integrals result from the radiation of soft and collinear photons from external charged particles. They are cancelled in

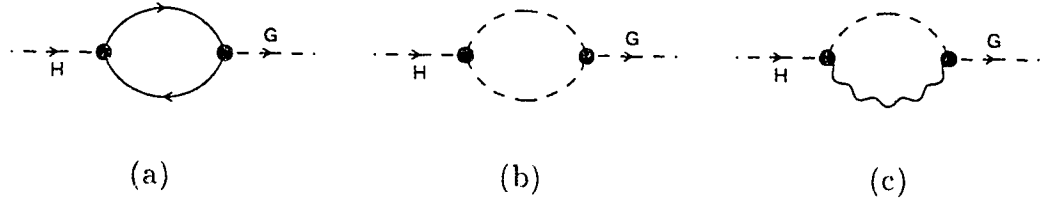


Figure 5.2: Mixing between the charged Higgs and the Goldstone boson

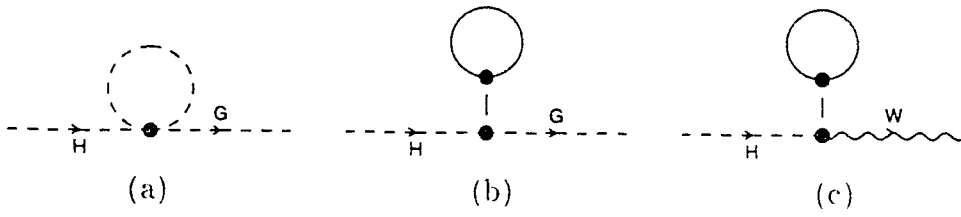


Figure 5.3: Momentum independent contributions to mixing

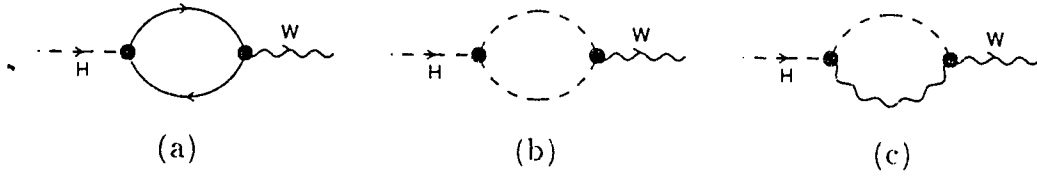


Figure 5.4: Mixing between the charged Higgs and the W boson

the calculation of the total decay rate by wave function renormalization constants of the Higgs boson and of fermions, as well as by corrections to the Higgs-fermion vertex. For the purpose of the present calculation the infrared divergence was regularized by introducing a small mass λ of the photon. All phase space integrals relevant to this problem have been listed in ref. [75].

The ultraviolet divergent integrals are regularized dimensionally. In this scheme, the quadratic divergences show up as poles at number of dimensions $n = 2$. They originate from tadpole diagrams and from the fermionic loop contribution to charged Higgs - Goldstone boson mixing. Some individual non-tadpole diagrams in boson self energies also contain quadratic divergences, but the relevant sums of diagrams are free from them (in the 't Hooft-Feynman gauge), as in the Standard Model [77]. Goldstone bosons are absent in the unitary gauge and there all the tadpole contributions cancel out. The problem is more delicate in the 't Hooft-Feynman gauge, in which the present calculation is done¹.

The different types of tadpole diagrams in the two Higgs doublet model are shown in figure (5.1). The external particle can be one of the CP-even neutral Higgs bosons, H^0 or h^0 . These diagrams contribute to mass renormalization of external fermions, to δm_W and δm_Z , and to the mixing between the Higgs boson and Goldstone and W bosons. The quadratic divergence from the fermionic loop in figure (5.1b) cancels the one from the fermionic contribution to the Higgs-Goldstone mixing shown in figure (5.2a). The sum of contributions of the remaining, bosonic tadpole diagrams, is free from quadratic divergences. The logarithmic divergences of tadpole diagrams are cancelled by loop diagrams of Higgs-Goldstone boson mixing depicted in figures (5.3a) and (5.2b,c). The sum of bosonic loops of Higgs- W boson mixing, shown in figures (5.3c) and (5.4) is finite.

5.4 Vertex corrections

Electroweak corrections to vertices are of two kinds: there are modifications of the values of parameters determining the strength of the coupling and relations among them, and triangle diagrams. It is this second type which will be considered in this section. The basic types of triangle diagrams con-

¹A discussion of tadpole diagrams with a fermion loop can be found in ref. [78] which also contains further references.

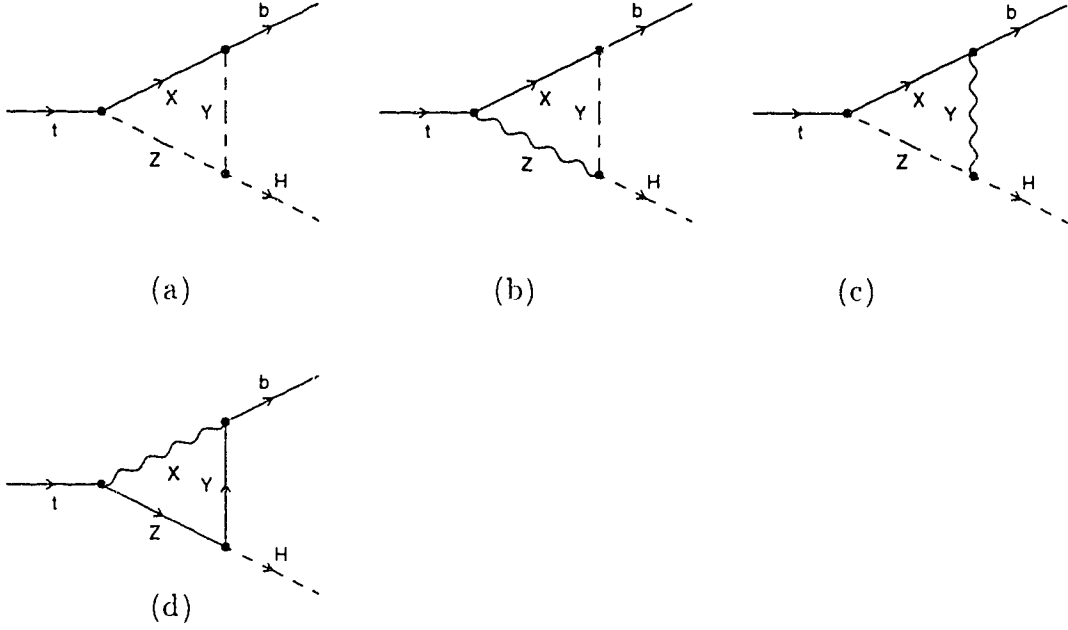


Figure 5.5: Vertex corrections to the decay of t quark

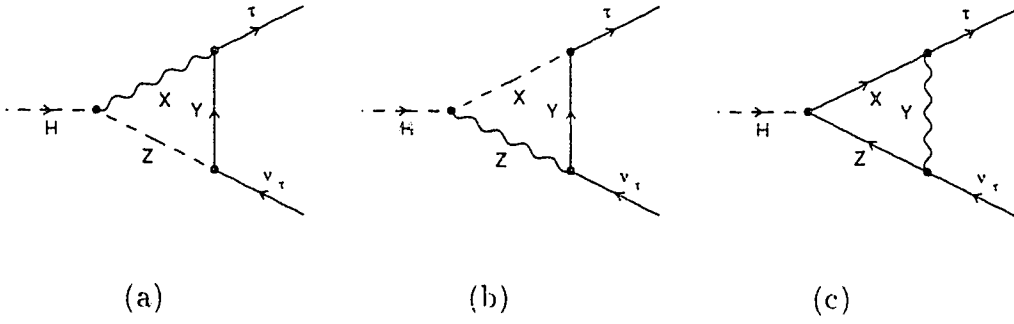


Figure 5.6: Vertex corrections to the charged Higgs boson decay

tributing to decays of the t quark and the charged Higgs boson are depicted in figures (5.5) and (5.6). Since the number of diagrams of is fairly large it is most convenient to employ the method of standard matrix elements (see ref. [75] for a review and further references). The principle of this method is to calculate coefficients in a representation of an invariant matrix element in the form of a sum over certain standard tensors, which depend only on the Lorentz structure of the process. In particular, in the case of scalar-fermion interaction, there are only two standard matrix elements:

$$\begin{aligned}\mathcal{M}^L &= \bar{u}(p)Lu(q), \\ \mathcal{M}^R &= \bar{u}(p)Ru(q),\end{aligned}\tag{5.9}$$

where $L = (1 - \gamma_5)/2$. The Born amplitude of the decay of the Higgs boson into leptons is proportional to \mathcal{M}^L , and since on the level of one-loop corrections we need to compute only the interference of triangle and tree diagrams, it is sufficient to evaluate only the \mathcal{M}^L component of the triangle diagrams. Analogously, in the case of the top quark decay, we need the \mathcal{M}^R part only. The resulting formulas are quite large and will not be shown here. In contrast to the two point functions their applicability in other contexts is rather limited. However, in Table 5.1 we list concrete particle assignments to the general diagrams of figures (5.5) and (5.6) together with explicit expressions of their ultraviolet divergent parts.

Complete analytic formulas are obtained using *Feyn Arts* [79] (also used to illustrate this thesis) and *Feyn Calc* [80]. Fortran output of these programs is evaluated using the library *FF* [81].

5.5 Real photon radiation

Triangle diagrams discussed in the previous section are infrared divergent due to exchange of soft photons. These divergences are cancelled by bremsstrahlung processes depicted in figures (5.7) and (5.8). These diagrams can be easily evaluated in terms of phase space integrals listed in ref. [75]. We give here as an example an explicit formula for the width of the process $H^- \rightarrow \tau \bar{\nu}_\tau \gamma$:

$$\Gamma(H^- \rightarrow \tau \bar{\nu}_\tau \gamma) = \frac{e^4 m_\tau^2 \tan^2 \beta}{27 \pi^3 s_W^2 m_{H^-} m_{A^\pm}^2} (|A|^2 + |B|^2 + A^* B + B^* A), \tag{5.10}$$

Diagram (Figure No.)	Particle assignments			Residuum
	X	Y	Z	
5.5(a)	t	H^+	H^0	0
5.5(a)	t	H^+	h^0	0
5.5(a)	t	G^+	A^0	0
5.5(b)	t	H^+	γ	2/3
5.5(b)	t	H^+	Z	$-1/3 + s_{W'}^2/(3c_{W'}^2)$
5.5(c)	t	W^+	H^0	$-\sin\alpha \sin(\beta - \alpha)/(4s_{W'}^2 \cos\beta)$
5.5(c)	t	W^+	h^0	$\cos\alpha \cos(\beta - \alpha)/(4s_{W'}^2 \cos\beta)$
5.5(c)	t	W^+	A^0	$1/(4s_{W'}^2)$
5.5(c)	b	γ	H^+	1/3
5.5(c)	b	Z	H^+	$(2s_{W'}^2 - 3)(s_{W'}^2 - c_{W'}^2)/(12s_{W'}^2 c_{W'}^2)$
5.5(d)	γ	b	t	-8/9
5.5(d)	Z	b	t	$(12 - 8s_{W'}^2)/(9c_{W'}^2)$
5.6(a)	γ	τ	H^-	1
5.6(a)	Z	τ	H^-	$(s_{W'}^2 - c_{W'}^2)/(2c_{W'}^2)$
5.6(b)	W	τ	H^0	$\cos\alpha \sin(\beta - \alpha)/(4s_{W'}^2 \sin\beta)$
5.6(b)	W	τ	h^0	$\sin\alpha \cos(\beta - \alpha)/(4s_{W'}^2 \sin\beta)$
5.6(b)	W	τ	A^0	$1/(4s_{W'}^2)$
5.6(b)	Z	ν_τ	H^-	$(c_{W'}^2 - s_{W'}^2)/(2s_{W'} c_{W'})^2$
5.6(c)	Z	ν_τ	τ	$2/c_{W'}^2$

Table 5.1: Particle contents of triangle diagrams. The last column shows the coefficient of $\frac{\alpha}{4\pi} \frac{2}{4-n}$ in δ_Δ^t and δ_Δ^τ .

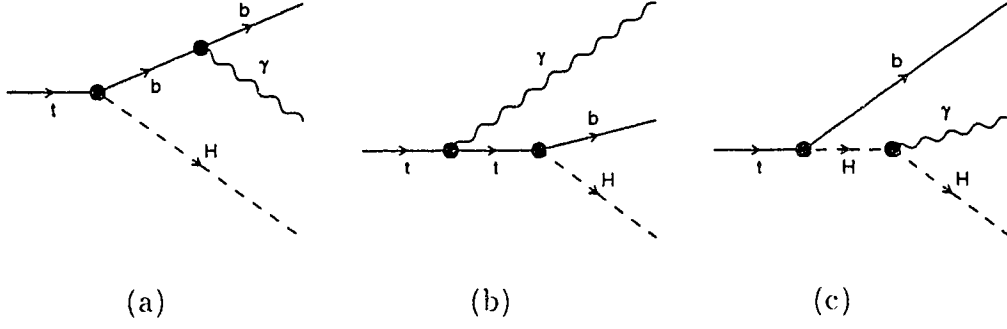


Figure 5.7: Real photon corrections to the decay of t quark

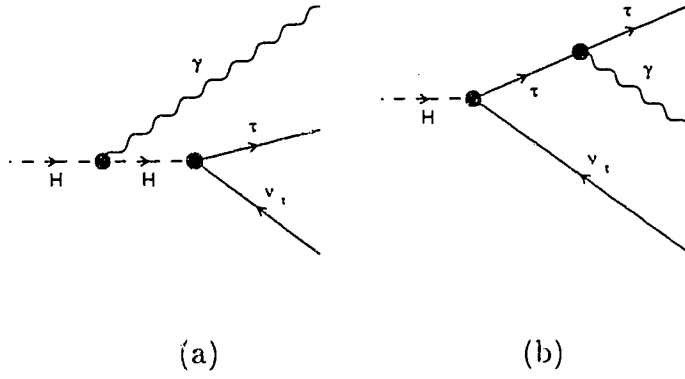


Figure 5.8: Real photon corrections to the charged Higgs boson decay

where \mathcal{A} and \mathcal{B} denote the amplitudes corresponding to diagrams in figure (5.8), for which we have:

$$\begin{aligned} |\mathcal{A}|^2 &= 4m_{H^-}^2(m_\tau^2 - m_{H^-}^2)I_{00} + 2(m_\tau^2 - 3m_{H^-}^2)I_0 - 2I, \\ |\mathcal{B}|^2 &= 4m_\tau^2(m_\tau^2 - m_{H^-}^2)I_{11} + 4m_\tau^2I_1 - 2I - 2I_1^0, \\ \mathcal{A}^*\mathcal{B} + \mathcal{B}^*\mathcal{A} &= 4(m_\tau^4 - m_{H^-}^4)I_{01} + 2(m_\tau^2 + m_{H^-}^2)I_0 - 4m_{H^-}^2I_1 + 2I. \end{aligned} \quad (5.11)$$

Integrals I are taken from ref. [75], where explicit expressions can be found. Here we only quote the definition:

$$I_{i_1, \dots, i_n}^{j_1, \dots, j_m} = \frac{1}{\pi^2} \int \frac{d^3p_1}{2p_{10}} \frac{d^3p_2}{2p_{20}} \frac{d^3q}{2q_0} \delta^{(4)}(p_0 - p_1 - p_2 - q) \frac{(\pm 2qp_{j_1}) \dots (\pm 2qp_{j_m})}{(\pm 2qp_{i_1}) \dots (\pm 2qp_{i_n})}, \quad (5.12)$$

where we q , p_0 , p_1 and p_2 denote momenta of the photon, Higgs boson, tau and neutrino respectively, and the signs should be chosen in the following way: minus sign if i_k or j_k is zero, plus in all other cases. Functions I_{00} , I_{01} and I_{11} contain infrared divergences, regularized by introducing a small mass of the photon λ . If the mass of neutral particle in the final state is small, the representation of these functions given in [75] becomes numerically unstable and it is more convenient to use the corresponding formulas from ref. [8].

5.6 Results and discussion

Following ref. [4, 76], the electroweak correction can be expressed by comparing the one-loop decay width to the Born rate parameterized by Fermi coupling constant G_F instead of the fine structure constant α :

$$\Gamma^{(0)}(G_F) = \frac{\Gamma^{(0)}(\alpha)}{1 - \Delta r}, \quad (5.13)$$

where Δr denotes radiative corrections to the muon decay, from which Fermi constant is determined. Such representation has the advantage of including large corrections due to fermion loops in the Born rate. In the present renormalization scheme, based on the condition of vanishing of radiative corrections to the $H^+ \tau \nu_\tau$ vertex, the effect of coupling constant renormalization

is doubled (see equation 5.8), and one ought to subtract $2\Delta r$ in order to cancel the fermion loop contribution from universal corrections. This is due to the fact that in order to avoid the artificially large corrections one has to parameterize *both* decay rates $\Gamma^0(H^\pm \rightarrow \tau\nu_\tau)$ and $\Gamma^0(t \rightarrow H^+b)$ by G_F . At this point our analysis differs from ref. [70]. For moderate values of $\tan\beta > 1$ the corrections consist typically of -4% bosonic contributions and +7% from fermion loops. This last part is cancelled by subtraction of Δr , so that the fermionic contribution to the corrections becomes slightly negative. This can be seen in figure (5.9).

Numerical evaluation of corrections to the decay width $\Gamma^{(0)}(G_F)$ proceeds in the following way. The set of input parameters consists of m_Z , G_F , α , masses of fermions and CKM matrix elements; values of them are taken from a recent review [75]. All the numerical results are presented for mass of the top quark equal 140 GeV. In addition we need two parameters of the Higgs sector: we choose angle β and mass of the charged Higgs boson. Masses of the remaining Higgs particles and angle α are found using the formulas of ref. [5]. Mass of the W boson is found by solving a nonlinear equation [4]:

$$m_W^2 \left(1 - \frac{m_W^2}{m_Z^2}\right) = \frac{\pi\alpha}{\sqrt{2}G_F} \frac{1}{1 - \Delta r}. \quad (5.14)$$

Finally, using this value of m_W , we find Δr and $\Delta\Gamma$. The resulting corrections $\overline{\Delta\Gamma} = \Delta\Gamma - 2\Delta r$ are plotted as a function of mass of the charged Higgs boson in figure (5.10) and as function of $\tan\beta$ in (5.11).

Similarly to the case of the decay $t \rightarrow W^+b$ [4], the corrections become large when mass of the lighter CP-even neutral Higgs boson h^0 is small. In particular, they diverge at the point $\tan\beta = 1$ where $m_{h^0} = 0$. This divergence should be cancelled by adding width of the decay $t \rightarrow H^+bh^0$, just like the infrared divergence due to virtual photon exchange is cancelled by the real photon radiation. As $\tan\beta$ becomes larger (or smaller) than 1, mass of h^0 increases, and at the point where it reaches $m_{H^+} - m_{W^+}$, amplitudes of both decays $H^\pm \rightarrow \tau\nu_\tau$ and $t \rightarrow H^+b$ have singularities which show up as discontinuities of the derivative of the one-loop decay rate and can be noticed on the diagrams; the value of $\tan\beta$ where this happens is close to 1 for light H^+ , and gets further away as H^+ becomes heavier. The corresponding cusps on the diagrams are easier to recognize for $\tan\beta > 1$, but they are present also in the region of $\tan\beta < 1$.

5.7 Renormalization constants

In this section we list those of renormalization constants of the 2 Higgs doublet model which have not been published so far. We first give expressions for the wave function renormalization of the charged Higgs boson and then analyze various contributions to the mixing of Higgs boson with W and Goldstone boson δ_{MX} . The results are given in terms of standard Passarino-Veltman integrals [82], using the conventions of ref. [75, 76], where many useful properties of these functions have been collected. Below the definitions of the one- and two-point functions are listed according to ref. [75]:

$$\begin{aligned} A(m^2) &= \frac{(2\pi\mu)^{4-D}}{i\pi^2} \int d^D q \frac{1}{q^2 - m^2}, \\ B_0(p^2, m_1^2, m_2^2) &= \frac{(2\pi\mu)^{4-D}}{i\pi^2} \int d^D q \frac{1}{[(q+p)^2 - m_1^2](q^2 - m_2^2)}, \\ p^\nu B_1(p^2, m_1^2, m_2^2) &= \frac{(2\pi\mu)^{4-D}}{i\pi^2} \int d^D q \frac{q^\nu}{[(q+p)^2 - m_1^2](q^2 - m_2^2)}, \end{aligned}$$

where ν is an arbitrary mass scale; the final result is independent of it. It is understood that the masses are assigned small negative imaginary parts.

The wave function renormalization constant of the charged Higgs boson gets contributions from diagrams with fermion, scalar and vector-scalar loops. To make the formula more compact it is convenient to introduce the notation:

$$\lambda(m_i, m_j, m_k) \equiv m_i^4 + m_j^4 + m_k^4 - 2m_i^2 m_j^2 - 2m_i^2 m_k^2 - 2m_j^2 m_k^2. \quad (5.15)$$

The bosonic contribution to the renormalization constant δZ_H is (α in the argument of trigonometric functions denotes the mixing angle in the neutral Higgs sector, as defined in [5]):

$$\begin{aligned} \delta Z_H^{\text{bos}} &= \frac{\alpha}{4\pi} \left\{ \sum_{H=H^0, h^0, A^0} \left\{ \frac{1}{4m_W^2 s_W^2} \right. \right. \\ &\quad \left. \left(\delta_{HH^0} \sin^2(\beta - \alpha) + \delta_{Hh^0} \cos^2(\beta - \alpha) + \delta_{HA^0} \right) \right. \\ &\quad \left. \left[2m_W^2 B_0(m_{H^+}^2, m_H, m_W) - \lambda(m_{H^+}, m_H, m_W) B'_0(m_{H^+}^2, m_H, m_W) \right] \right\} \\ &\quad + \frac{(s_W^2 - c_W^2)^2}{4s_W^2 c_W^2} \left[2B_0(m_{H^+}^2, m_{H^+}, m_Z) \right. \end{aligned}$$

$$\begin{aligned}
& + (4m_{H^+}^2 - m_Z^2) B'_0(m_{H^+}^2, m_{H^+}, m_Z) \\
& + 2B_0(m_{H^+}^2, m_{H^+}, \lambda) + 4m_{H^+}^2 B'_0(m_{H^+}^2, m_{H^+}, \lambda) \\
& - \frac{m_W^2}{s_W^2} \left\{ \left[\cos(\beta - \alpha) - \frac{\cos 2\beta \cos(\beta + \alpha)}{2c_W^2} \right]^2 B'_0(m_{H^+}^2, m_{H^+}, m_{H^0}) \right. \\
& \left. + \left[\sin(\beta - \alpha) + \frac{\cos 2\beta \sin(\beta + \alpha)}{2c_W^2} \right]^2 B'_0(m_{H^+}^2, m_{H^+}, m_{h^0}) \right\} \quad (5.16)
\end{aligned}$$

The contribution of one generation of quarks is:

$$\begin{aligned}
\delta Z_H^q &= \frac{\alpha}{4\pi} \frac{N_C}{2s_W^2 m_W^2} \left\{ - (m_d^2 \tan^2 \beta + m_u^2 \cot^2 \beta) B_0(m_{H^+}^2, m_d, m_u) \right. \\
& \quad \left. + \left[(m_d^2 \tan^2 \beta + m_u^2 \cot^2 \beta) (m_d^2 + m_u^2 - m_{H^+}^2) + 4m_d^2 m_u^2 \right] \right. \\
& \quad \left. B'_0(m_{H^+}^2, m_d, m_u) \right\}. \quad (5.17)
\end{aligned}$$

In the above formulas N_C denotes the number of colours ($=3$), and B'_0 is the derivative of B_0 with respect to its first argument.

Finally, the contribution of a lepton-neutrino pair is obtained from the formula (5.17) by taking $N_C = 1$, $m_u = 0$ and using:

$$\frac{d}{ds} B_0(s, 0, m) = \frac{1}{m^2 - s} \left\{ -\frac{m^2}{s} [B_0(s, 0, m) - B_0(0, 0, m)] + 1 \right\}. \quad (5.18)$$

The result is:

$$\begin{aligned}
\delta Z_H^l &= \frac{\alpha}{4\pi} \frac{m^2 \tan^2 \beta}{2s_W^2 m_W^2} \left\{ -\frac{m^2}{m_{H^+}^2} [B_0(m_{H^+}^2, 0, m) - B_0(0, 0, m)] \right. \\
& \quad \left. + 1 - B_0(m_{H^+}^2, 0, m) \right\}. \quad (5.19)
\end{aligned}$$

The contribution of bosons to mixing can be represented by the following formula:

$$\begin{aligned}
\delta_{MIX}^{\text{bos}} &= \frac{\alpha}{4\pi s_W^2} \sum_{H=H^0, h^0} \left[\frac{\sin(\beta - \alpha) \cos(\beta - \alpha)}{4} (\delta_{H, H^0} - \delta_{H, h^0}) \right. \\
& \quad \left. \cdot \left\{ \frac{(m_H^2 - m_W^2)^2}{m_{H^+}^2} (B_0(m_{H^+}^2, m_H, m_W) - B_0(0, m_H, m_W)) \right\} \right]
\end{aligned}$$

$$\begin{aligned}
& + \left(2m_{H^+}^2 + m_H^2 - 3m_W^2 \right) B_0 \left(m_{H^+}^2, m_H, m_W \right) \Big\} \\
& + \frac{m_W^2}{2m_{H^+}^2} \left\{ \delta_{H,H^0} \sin(\beta - \alpha) \left(\cos(\beta - \alpha) - \frac{\cos 2\beta \cos(\beta + \alpha)}{2c_W^2} \right) \right. \\
& \quad \left. - \delta_{H,h^0} \cos(\beta - \alpha) \left(\sin(\beta - \alpha) + \frac{\cos 2\beta \sin(\beta + \alpha)}{2c_W^2} \right) \right\} \\
& \cdot \left(m_H^2 - m_{H^+}^2 \right) \left[\left(1 - \frac{m_{H^+}^2}{m_W^2} \right) B_0 \left(m_{H^+}^2, m_{H^+}, m_H \right) - B_0 \left(0, m_{H^+}, m_H \right) \right] \\
& + \frac{\cos 2\beta}{4c_W^2} \left(\sin(\beta - \alpha) \cos(\beta + \alpha) \delta_{H,H^0} + \sin(\beta + \alpha) \cos(\beta - \alpha) \delta_{H,h^0} \right) \\
& \quad \cdot \left(m_{H^+}^2 - m_H^2 \right) B_0 \left(m_{H^+}^2, m_H, m_W \right) \Big] \\
& - \frac{\alpha}{4\pi} \frac{1}{8s_W^2 c_W^2} \left\{ \sin 2\beta \cos 2\beta [4A(m_W) - 4A(m_{H^+}) + A(m_Z) - A(m_{A^0})] \right. \\
& \quad \left. + \left(c_W^2 \sin 2\alpha \cos 2\beta + s_W^2 \cos 2\alpha \sin 2\beta \right) [A(m_{H^0}) - A(m_{h^0})] \right\} \\
& + \frac{g}{2m_W} \left[\left(m_W^2 - m_{H^+}^2 + m_{H^0}^2 \right) \sin(\beta - \alpha) t_1 \right. \\
& \quad \left. - \left(m_W^2 - m_{H^+}^2 + m_{h^0}^2 \right) \cos(\beta - \alpha) t_2 \right]. \tag{5.20}
\end{aligned}$$

The last two lines in the above formula represent contributions of tadpole diagrams. Formulas for fermion loops are given below for $H - G$ and $H - W$ mixing separately:

$$\begin{aligned}
\delta_{MX}^{HG} &= -\frac{\alpha}{4\pi} \frac{N_C}{2s_W^2 m_W^2} \left\{ \left(-m_d^2 \tan \beta + m_u^2 \cot \beta \right) \right. \\
& \quad \cdot \left[\left(m_d^2 + m_u^2 - m_{H^+}^2 \right) B_0 \left(m_{H^+}^2, m_u, m_d \right) + A(m_u) + A(m_d) \right] \\
& \quad \left. + 2m_u^2 m_d^2 (\tan \beta - \cot \beta) B_0 \left(m_{H^+}^2, m_u, m_d \right) \right\}, \\
\delta_{MX}^{HW} &= -\frac{\alpha}{4\pi} \frac{N_C}{s_W^2} \left[\left(m_d^2 \tan \beta + m_u^2 \cot \beta \right) B_1 \left(m_{H^+}^2, m_u, m_d \right) \right. \\
& \quad \left. + m_u^2 \cot \beta B_0 \left(m_{H^+}^2, m_u, m_d \right) \right]. \tag{5.21}
\end{aligned}$$

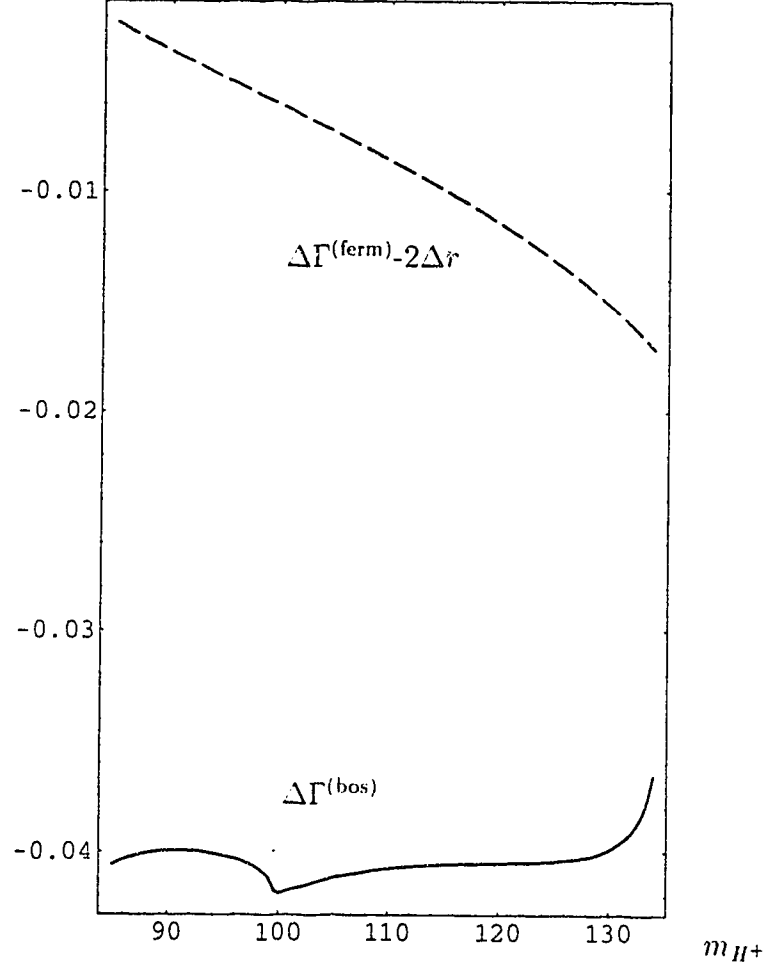


Figure 5.9: Bosonic contributions to corrections $\Delta\Gamma$ (solid line) and the fermionic contributions from which twice the value of universal corrections Δr was subtracted (dashed). Plotted as a function of m_{H+} for $\tan\beta = 1.5$

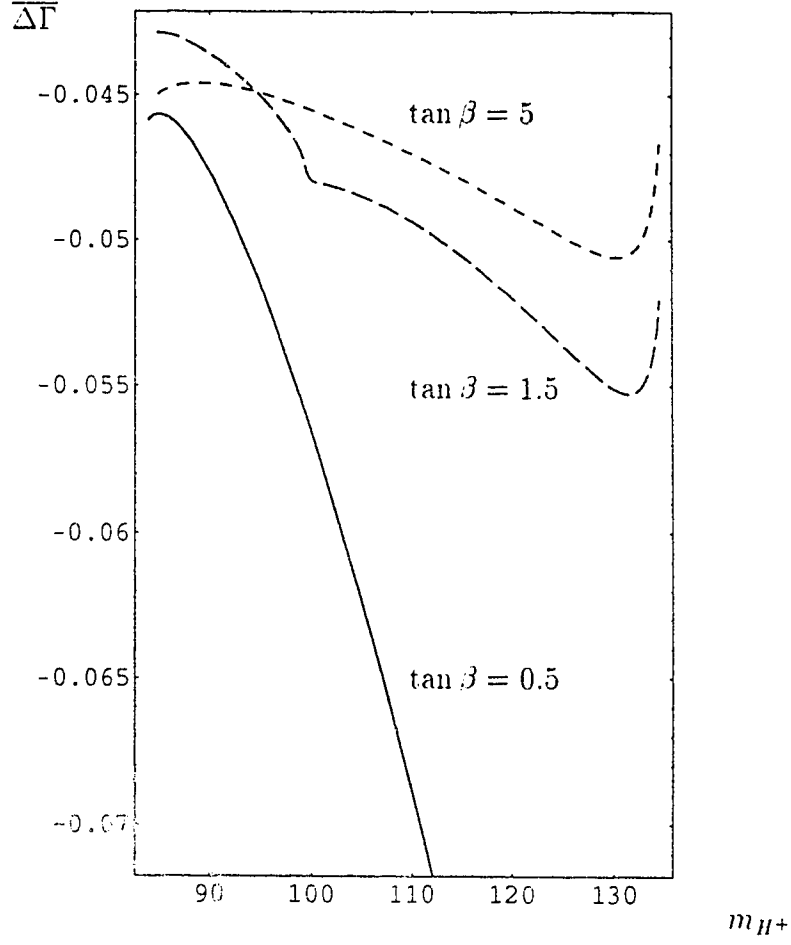


Figure 5.10: Corrections $\overline{\Delta\Gamma}$ plotted as a function of m_{H+} for various values of $\tan\beta$: $\tan\beta = 0.5$ (solid line), $\tan\beta = 1.5$ (long dash) and $\tan\beta = 5$ (short dash)

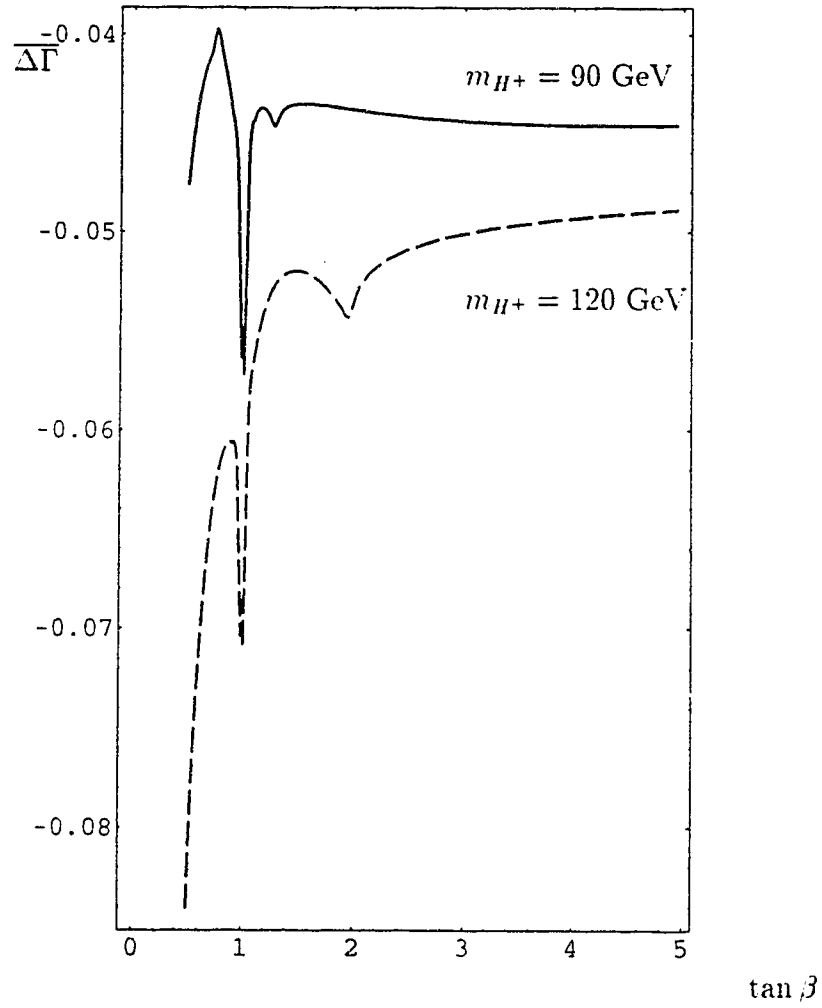


Figure 5.11: Corrections $\overline{\Delta\Gamma}$ plotted as a function of $\tan\beta$ for two different values of m_{H^+} : $m_{H^+} = 90$ GeV (solid line) and $m_{H^+} = 120$ GeV (dashed)

Chapter 6

On the calculation of the anomalous magnetic moment of the electron

6.1 Introduction

Theory and experiment are in excellent agreement as to the value of the electron magnetic moment [83]. This has been achieved on the theory side by computing radiative corrections to the interaction of an electron with a constant magnetic field up to the eighth order in the electromagnetic coupling constant e . These corrections can be expressed as a power series in $\frac{\alpha}{\pi} = \frac{e^2}{4\pi^2}$:

$$\frac{g-2}{2} = C_1 \left(\frac{\alpha}{\pi}\right) + C_2 \left(\frac{\alpha}{\pi}\right)^2 + C_3 \left(\frac{\alpha}{\pi}\right)^3 + C_4 \left(\frac{\alpha}{\pi}\right)^4 + \dots \quad (6.1)$$

The first correction, $C_1 = \frac{1}{2}$, has been computed by Schwinger [84] and the second, C_2 , by Sommerfield [85, 86] and Petermann [87, 88]. Ref. [89] contains a detailed description of a calculation of C_2 from which one can get an idea of the enormous effort one has to make in calculating C_2 using traditional methods. Matters get even worse when one proceeds to C_3 [90]. A large part of the diagrams in this order has been calculated analytically but there are still 8 which have to be integrated numerically. This is also the only known method to obtain C_4 [83]. Error in the numerical calculation is one of the sources of uncertainty in the theoretical prediction for $g-2$.

It is therefore important to look for new algorithms which will enable us to calculate multi-loop corrections analytically.

One such method has been proposed recently by Gray, Broadhurst, Grafe and Schilcher (GBGS) [91]. It is based on the idea of the integration by parts pioneered by Chetyrkin and Tkachov [92] in the context of massless Feynman integrals. The GBGS method can be applied to massive propagator-type integrals.

The purpose of this Chapter is threefold. First, a practical summary of the GBGS method is given in order to facilitate its applications. Second, it is discussed how this method can be extended to the calculation of the anomalous magnetic moment where we have to deal with vertex diagrams at zero momentum transfer. The example of two-loop calculation of the anomalous magnetic moment is worked out in detail, with special attention paid to the treatment of counterterms within the framework of the GBGS method. Finally one diagram contributing to two-loop virtual correction to the top quark decay is computed in order to show that an extension of the method to vertex diagrams might be applied in this case.

We now concentrate on two-loop on-shell fermion propagator diagrams of types encountered in QED and QCD. The essence of the GBGS method is the observation that in the framework of dimensional regularization all integrals needed to compute these propagator diagrams are of two types: $M(\alpha_1, \alpha_2, \alpha_3, \alpha_4, \alpha_5)$ and $N(\alpha_1, \alpha_2, \alpha_3, \alpha_4, \alpha_5)$. The external fermion momentum p is taken on-shell ($p^2 = m^2$) and the two relevant types of integrals are defined as follows (space-time dimension will be denoted by $D \equiv 4 - 2\varepsilon$):

$$\begin{aligned}
M(\alpha_1, \alpha_2, \alpha_3, \alpha_4, \alpha_5) &= \pi^{-D} (p^2)^{-D+\sum \alpha_i} \cdot \\
&\cdot \iint \frac{d^D k_1 d^D k_2}{k_1^{2\alpha_1} (k_1 - k_2)^{2\alpha_2} k_2^{2\alpha_3} (k_1^2 + 2p \cdot k_1)^{\alpha_4} (k_2^2 + 2p \cdot k_2)^{\alpha_5}}, \\
N(\alpha_1, \alpha_2, \alpha_3, \alpha_4, \alpha_5) &= \pi^{-D} (p^2)^{-D+\sum \alpha_i} \cdot \\
&\cdot \iint \frac{d^D k_1 d^D k_2}{k_1^{2\alpha_1} k_2^{2\alpha_2} (k_1^2 + 2p \cdot k_1)^{\alpha_3} (k_2^2 + 2p \cdot k_2)^{\alpha_4} ((k_1 + k_2)^2 + 2p \cdot (k_1 + k_2))^{\alpha_5}}.
\end{aligned} \tag{6.2}$$

The GBGS method of doing such integrals consists in making use of recurrence relations derived from the identities:

$$\iint d^D k_1 d^D k_2 \frac{\partial}{\partial k^\mu} [q^\mu f(k_1, k_2, p, \{\alpha_i\})] = 0 \tag{6.3}$$

for $k \in \{k_1, k_2\}$, $q \in \{k_1, k_2, p\}$ and f being an integrand in (6.2). Two more relations can be obtained by expressing integrals:

$$\iint d^D k_1 d^D k_2 k_j^\mu f(k_1, k_2, p, \{\alpha_i\}), \quad j = 1, 2 \quad (6.4)$$

in terms of $M(\alpha_1, \alpha_2, \alpha_3, \alpha_4, \alpha_5)$ and $N(\alpha_1, \alpha_2, \alpha_3, \alpha_4, \alpha_5)$ and then differentiating such formulas with respect to p^μ . These 16 recurrence relations are sufficient to express any two-loop fermion propagator diagram in terms of one-loop integrals and three structures R_i :

$$\begin{aligned} R_1 &= \Gamma^2(\varepsilon), \\ R_2 &= \frac{\varepsilon \Gamma^2(-\varepsilon) \Gamma(-4\varepsilon) \Gamma(2\varepsilon) \Gamma(\varepsilon)}{\Gamma(-2\varepsilon) \Gamma(-3\varepsilon)}, \\ R_3 &= N(1, 1, 1, 1, 1) \equiv I(\varepsilon), \end{aligned} \quad (6.5)$$

where $I(\varepsilon)$ is known exactly in 4 dimensions: $I(0) = \pi^2 \log 2 - \frac{3}{2} \zeta(3)$ [93].

In sections 6.2, 6.3 and 6.4 we discuss these two classes of integrals, show how the recurrence relations are derived, and present formulas for the three basic integral structures. In section 6.5 it is shown how this apparatus can be applied to the calculation of two-loop corrections to the electron magnetic moment.

6.2 Integrals $M(\alpha_1, \alpha_2, \alpha_3, \alpha_4, \alpha_5)$

There are 6 recurrence relations for the integrals M (defined in eq. (6.2)) which can be derived from the identity:

$$\iint d^D k_1 d^D k_2 \frac{\partial}{\partial k^\mu} [q^\mu f(k_1, k_2, p, \{\alpha_i\})] = 0 \quad (6.6)$$

where f is the integrand on the RHS of (6.2), $k \in \{k_1, k_2\}$ and $q \in \{k_1, k_2, p\}$. These relations will be labeled according to Table 6.1. Two more relations can be obtained by expressing integrals:

$$\iint d^D k_1 d^D k_2 k_j^\mu f(k_1, k_2, p, \{\alpha_i\}), \quad j = 1, 2 \quad (6.7)$$

in terms of $M(\alpha_1, \alpha_2, \alpha_3, \alpha_4, \alpha_5)$ and then differentiating such expressions with respect to p^μ . We will label these relations M_7 and M_8 for j in equation (6.7) equal to 1 and 2 respectively.

Table 6.1: Notation used for labeling the recurrence relations.

k	q		
	k_1	k_2	p
k_1	M_1	M_2	M_3
k_2	M_4	M_5	M_6

Before we derive the recurrence relations, we write down formulas for the derivatives needed in the identity (6.6). We adopt the operator notation [92, 91]: $\mathbf{1}^\pm f(\alpha_1, \alpha_2, \dots) \equiv f(\alpha_1 \pm 1, \alpha_2, \dots)$. Using this notation the action of the derivative operators can be expressed as follows:

$$\begin{aligned}
\frac{\partial}{\partial k_1^\mu} \frac{1}{k_1^{2\alpha_1}} &= -2\alpha_1 k_{1\mu} \frac{1}{k_1^{2(\alpha_1+1)}} \equiv -2\alpha_1 k_{1\mu} \mathbf{1}^+ \frac{1}{k_1^{2\alpha_1}}. \\
\frac{\partial}{\partial k_1^\mu} \frac{1}{(k_1 - k_2)^{2\alpha_2}} &= -2\alpha_2 (k_{1\mu} - k_{2\mu}) \mathbf{2}^+ \frac{1}{(k_1 - k_2)^{2\alpha_2}}. \\
\frac{\partial}{\partial k_1^\mu} \frac{1}{(k_1^2 + 2p \cdot k_1)^{\alpha_4}} &= -2\alpha_4 (k_{1\mu} + p_\mu) \mathbf{4}^+ \frac{1}{(k_1^2 + 2p \cdot k_1)^{\alpha_4}}. \\
\frac{\partial}{\partial p^\mu} \frac{1}{(k_1^2 + 2p \cdot k_1)^{\alpha_4}} &= -2\alpha_4 k_{1\mu} \mathbf{4}^+ \frac{1}{(k_1^2 + 2p \cdot k_1)^{\alpha_4}}. \\
\frac{\partial}{\partial p^\mu} \frac{1}{(k_2^2 + 2p \cdot k_2)^{\alpha_5}} &= -2\alpha_5 k_{2\mu} \mathbf{5}^+ \frac{1}{(k_2^2 + 2p \cdot k_2)^{\alpha_5}}. \tag{6.8}
\end{aligned}$$

The above formulas contain four-vectors which we will contract with $k_{1\mu}$, $k_{2\mu}$ and p_μ . The resulting scalars in the numerator of the integrand can be cancelled with similar scalars in the denominator, so their appearance is equivalent to the action of following operators:

$$\begin{aligned}
k_1^2 &\sim \mathbf{1}^- \\
k_2^2 &\sim \mathbf{3}^- \\
2k_1 \cdot p &\sim \mathbf{4}^- - \mathbf{1}^- \\
2k_2 \cdot p &\sim \mathbf{5}^- - \mathbf{3}^- \\
2k_1 \cdot k_2 &\sim \mathbf{1}^- + \mathbf{3}^- - \mathbf{2}^- \tag{6.9}
\end{aligned}$$

In the following we derive relations M_1 and M_7 . The relations M_2 and M_3

can be found in the same way, and the remaining ones - by a change of indices $1 \leftrightarrow 3, 4 \leftrightarrow 5$, which is a consequence of a symmetry of $M(\alpha_1, \alpha_2, \alpha_3, \alpha_4, \alpha_5)$.

6.2.1 Relation M_1

For this relation equation (6.6) reads:

$$\begin{aligned} 0 &= \iint d^D k_1 d^D k_2 \frac{\partial}{\partial k_1^\mu} [k_1^\mu f(k_1, k_2, p, \{\alpha_i\})] \\ &= D \pi^D (p^2)^{D-\sum \alpha_i} M(\alpha_1, \alpha_2, \alpha_3, \alpha_4, \alpha_5) \\ &\quad + \iint d^D k_1 d^D k_2 k_1^\mu \frac{\partial}{\partial k_1^\mu} f(k_1, k_2, p, \{\alpha_i\}) \end{aligned} \quad (6.10)$$

The action of $k_1^\mu \frac{\partial}{\partial k_1^\mu}$ is equivalent to

$$\begin{aligned} &k_1^\mu [-2\alpha_1 k_{1\mu} \mathbf{1}^+ - 2\alpha_2 (k_{1\mu} - k_{2\mu}) \mathbf{2}^+ - 2\alpha_4 (k_{1\mu} + p_\mu) \mathbf{4}^+] \\ &\quad \rightsquigarrow -2\alpha_1 \mathbf{1}^+ \mathbf{1}^- - \alpha_2 \mathbf{2}^+ (\mathbf{21}^- - \mathbf{1}^- - \mathbf{3}^- + \mathbf{2}^-) - \alpha_4 \mathbf{4}^+ (\mathbf{21}^- + \mathbf{4}^- - \mathbf{1}^-) \end{aligned}$$

Thus we obtain:

$$\begin{aligned} &\left[D - 2\alpha_1 - \alpha_2 - \alpha_4 - \alpha_2 \mathbf{2}^+ (\mathbf{1}^- - \mathbf{3}^-) - \alpha_4 \mathbf{4}^+ \mathbf{1}^- \right] \cdot \\ &\quad \cdot M(\alpha_1, \alpha_2, \alpha_3, \alpha_4, \alpha_5) = 0. \end{aligned} \quad (6.11)$$

6.2.2 Relation M_7

This time we begin with

$$\iint d^D k_1 d^D k_2 k_1^\mu f(k_1, k_2, p, \{\alpha_i\}) = p^\mu \pi^D (p^2)^{D-\sum \alpha_i} \mathcal{O} M(\alpha_1, \alpha_2, \alpha_3, \alpha_4, \alpha_5). \quad (6.12)$$

where \mathcal{O} is an operator which we determine by contracting both sides of (6.12) with $2p_\mu$:

$$\mathcal{O} = \frac{1}{2} (\mathbf{4}^- - \mathbf{1}^-). \quad (6.13)$$

Now we differentiate (6.12) with respect to p^μ and get:

$$\begin{aligned} k_1^\mu \left(-2k_{1\mu}\alpha_4 4^+ - 2k_{2\mu}\alpha_5 5^+ \right) M(\alpha_1, \alpha_2, \alpha_3, \alpha_4, \alpha_5) \\ = \frac{1}{2} \left(D + 2D - 2 \sum a_i \right) (4^- - 1^-) M(\alpha_1, \alpha_2, \alpha_3, \alpha_4, \alpha_5) \end{aligned} \quad (6.14)$$

or

$$\begin{aligned} \left[-2\alpha_4 4^+ 1^- - \alpha_5 5^+ (1^- + 3^- - 2^-) - \frac{3D - 2 \sum a_i}{2} (4^- - 1^-) \right] \\ \cdot M(\alpha_1, \alpha_2, \alpha_3, \alpha_4, \alpha_5) = 0. \end{aligned} \quad (6.15)$$

6.3 Integrals $N(\alpha_1, \alpha_2, \alpha_3, \alpha_4, \alpha_5)$ and a summary of recurrence relations

In the same manner as described in the last section we can derive eight recurrence relations $N_{1,\dots,8}$ for integrals $N(\alpha_1, \alpha_2, \alpha_3, \alpha_4, \alpha_5)$.

It turns out that it is convenient to use certain linear combinations of the recurrence relations. Tables 6.2 and 6.3 summarize these combinations which turned out to be the most useful.

6.4 Analytic formulas for some of the integrals

It turns out that the recurrence relations described so far are sufficient to reduce all the integrals of the type (6.2) to products of one-loop integrals and three types of two-loop integrals for which we have closed formulas:

$$\begin{aligned} M(0, \alpha, 0, \beta, \gamma) &= (-1)^{1+\alpha+\beta+\gamma} \\ &\cdot \frac{\Gamma(\alpha + \beta + \gamma - D) \Gamma\left(\frac{D}{2} - \alpha\right) \Gamma\left(\alpha + \beta - \frac{D}{2}\right) \Gamma\left(\alpha + \gamma - \frac{D}{2}\right)}{\Gamma(\beta) \Gamma(\gamma) \Gamma\left(\frac{D}{2}\right) \Gamma(2\alpha + \beta + \gamma - D)}, \\ M(\alpha, \beta, \gamma, \delta, 0) &= (-1)^{1+\alpha+\beta+\gamma+\delta} \frac{\Gamma\left(\frac{D}{2} - \beta\right) \Gamma\left(\frac{D}{2} - \gamma\right) \Gamma\left(\beta + \gamma - \frac{D}{2}\right)}{\Gamma(\beta) \Gamma(\gamma) \Gamma(\delta)} \\ &\cdot \frac{\Gamma(2D - 2\alpha - 2\beta - 2\gamma - \delta) \Gamma(\alpha + \beta + \gamma + \delta - D)}{\Gamma(D - \beta - \gamma) \Gamma\left(\frac{3D}{2} - \alpha - \beta - \gamma - \delta\right)}, \end{aligned}$$

Table 6.2: Useful relations for integrals N

N_1 :	$[D - 2\alpha_1 - \alpha_3 - \alpha_5 - \alpha_3 3^+ 1^- + \alpha_5 5^+ (4^- - 1^-)] N = 0$
$N_1 + N_2 + N_3$:	$[D - \alpha_1 - \alpha_3 - 2\alpha_5 + \alpha_1 1^+ (4^- - 5^-)$ $+ \alpha_3 3^+ (2^- - 5^- - 2) - 2\alpha_5 5^+] N = 0$
$N_1 + N_3 + N_5$:	$[2D - \alpha_1 - 2\alpha_2 - 2\alpha_3 - \alpha_4 - 2\alpha_5 - \alpha_1 1^+ 3^-$ $- \alpha_4 4^+ 2^- - 2\alpha_3 3^+ - 2\alpha_5 5^+] N = 0$
$N_4 + N_5 + N_6$:	$[D - \alpha_2 - \alpha_4 - 2\alpha_5 + \alpha_2 2^+ (3^- - 5^-)$ $+ \alpha_4 4^+ (1^- - 5^- - 2) - 2\alpha_5 5^+] N = 0$
N_5 :	$[D - 2\alpha_2 - \alpha_4 - \alpha_5 - \alpha_4 4^+ 2^- + \alpha_5 5^+ (3^- - 2^-)] N = 0$
$N_1 + N_5 + N_6$:	$[2D - 2\alpha_1 - \alpha_2 - \alpha_3 - 2\alpha_4 - 2\alpha_5$ $- \alpha_2 2^+ 4^- - \alpha_3 3^+ 1^- - 2\alpha_4 4^+ - 2\alpha_5 5^+] N = 0$
$N_7 - 2N_1$:	$[-2D + 4\alpha_1 + 2\alpha_3 + \alpha_4 + \alpha_5 - \alpha_4 4^+ (5^- - 3^-)$ $+ \alpha_5 5^+ (3^- - 4^-) - (3D/2 - \sum \alpha_i) (3^- - 1^-)] N = 0$
$N_8 - 2N_5$:	$[-2D + 4\alpha_2 + \alpha_3 + 2\alpha_4 + \alpha_5 - \alpha_3 3^+ (5^- - 4^-)$ $+ \alpha_5 5^+ (4^- - 3^-) - (3D/2 - \sum \alpha_i) (4^- - 2^-)] N = 0$

Table 6.3: Useful relations for integrals M

M_1 :	$[D - 2\alpha_1 - \alpha_2 - \alpha_4 + \alpha_2 2^+ (3^- - 1^-) - \alpha_4 4^+ 1^-] M = 0$
$M_2 - M_1$:	$[-D + \alpha_1 + 2\alpha_2 + \alpha_4 + \alpha_1 1^+ (2^- - 3^-)$ $+ \alpha_4 4^+ (-5^- + 2^-)] M = 0$
$M_1 + M_3$:	$[D - \alpha_1 - \alpha_2 - 2\alpha_4 - \alpha_1 1^+ 4^- + \alpha_2 2^+ (5^- - 4^-)$ $- 2\alpha_4 4^+] M = 0$
$M_5 + M_6$:	$[D - \alpha_2 - \alpha_3 - 2\alpha_5 + \alpha_2 2^+ (4^- - 5^-) - \alpha_3 5^- 3^+$ $- 2\alpha_5 5^+] M = 0$
$M_4 - M_5$:	$[-D + 2\alpha_2 + \alpha_3 + \alpha_5 + \alpha_3 3^+ (-1^- + 2^-)$ $+ \alpha_5 5^+ (2^- - 4^-)] M = 0$
$M_1 + M_5$:	$[2D - 2\alpha_1 - 2\alpha_2 - 2\alpha_3 - \alpha_4 - \alpha_5 - \alpha_4 4^+ 1^-$ $- \alpha_5 3^- 5^+] M = 0$
M_7 :	$[-2\alpha_4 4^+ 1^- - \alpha_5 5^+ (1^- + 3^- - 2^-)$ $- (3D/2 - \sum \alpha_i) (4^- - 1^-)] M = 0$
M_8 :	$[-2\alpha_5 5^+ 3^- - \alpha_4 4^+ (3^- + 1^- - 2^-)$ $- (3D/2 - \sum \alpha_i) (5^- - 3^-)] M = 0$

$$N(1, 1, 1, 1, 1) \equiv I(\varepsilon), \quad (6.16)$$

where in the last formula only the value of $I(0)$ at $D = 4$ dimensions will be needed, for which case this integral has been calculated by Broadhurst [93].

For completeness we also give a formula for a single-loop integral:

$$\begin{aligned} S(\alpha, \beta) &\equiv \int \frac{d^D k}{k^{2\alpha} (k^2 + 2k \cdot p)^\beta} \\ &= i\pi^{\frac{D}{2}} (-1)^{\alpha+\beta} (p^2)^{\frac{D}{2}-\alpha-\beta} \frac{\Gamma(\alpha + \beta - \frac{D}{2}) \Gamma(D - 2\alpha - \beta)}{\Gamma(\beta) \Gamma(D - \beta - \alpha)}. \end{aligned} \quad (6.17)$$

6.5 Calculation of the anomalous magnetic moment

6.5.1 Vacuum polarization contribution

In this section the contribution of the vacuum polarization to the electron anomaly is calculated. The method of projecting the part which contributes to the interaction with the magnetic field is outlined.

Figure 6.1 depicts the diagram to be computed. The value of the correction to $g - 2$ due to this process has long been known, but its calculation required a complicated analytical integration which is avoided in the GBGS method. In the following a formula for the correction to the magnetic moment convenient for use in algebraic manipulation programs will be derived. Then the renormalization of the photon propagator is carried out in the way which allows easy incorporation into the framework of the GBGS method.

The question we want to address now is how to apply this method to the calculation of the anomalous magnetic moment. The diagram in Figure 6.1 corresponds to the following integral:

$$\int d^D k_1 \gamma^\mu \frac{1}{\not{p} + \not{k}_1 - m} \gamma^\rho \frac{1}{\not{p} + \not{k}_1 - m} \gamma^\nu \frac{1}{k_1^4} \left(g_{\mu\nu} - \frac{k_{1\mu} k_{1\nu}}{k_1^2} \right) \Pi_R^{(2)}(k_1^2) \quad (6.18)$$

where $\Pi_R^{(2)}(k_1^2)$ is the renormalized contribution of the vacuum polarization to the photon propagator. The trouble with the above integral is the presence of

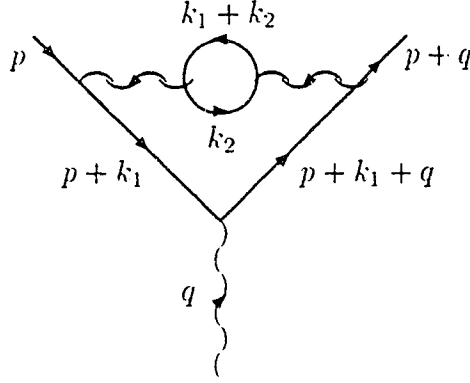


Figure 6.1: Vacuum polarization contribution to the anomalous magnetic moment

the q momentum in the denominator. However, for the anomalous magnetic moment we only need to consider infinitesimally small q for which the Taylor expansion can be used:

$$\frac{1}{\not{p} + \not{k}_1 - m} \approx \frac{\not{p} + \not{k}_1 + m}{k_1^2 + 2k_1 \cdot p} - 2k_1 \cdot q \frac{\not{p} + \not{k}_1 + m}{(k_1^2 + 2k_1 \cdot p)^2}. \quad (6.19)$$

All the denominators in the integral (6.18) depend now on k_1 , k_2 and p only (k_2 being hidden in $\Pi_R^{(2)}(k_1^2)$). We have reduced the problem to the calculation of propagator-type integrals.

We now have to express $\Pi_R^{(2)}(k_1^2)$ in such a form that all integrals to be done are of the type shown in (6.2). The unrenormalized vacuum polarization tensor is [94]:

$$\Pi_{\mu\nu}^{(2)}(k_1) = \frac{e^2}{(2\pi)^D} \text{Tr} \int \frac{\gamma_\mu (\not{k}_2 + m) \gamma_\nu (\not{k}_2 + \not{k}_1 + m)}{(k_2^2 - m^2) [(k_1 + k_2)^2 - m^2]} d^D k_2 \quad (6.20)$$

which can be expressed by:

$$\Pi_{\mu\nu}^{(2)}(k_1) = \left(g_{\mu\nu} - \frac{k_{1\mu} k_{1\nu}}{k_1^2} \right) \Pi^{(2)}(k_1^2) + g_{\mu\nu} A(k_1). \quad (6.21)$$

In the dimensional regularization $A(k_1) = 0$ and

$$\begin{aligned}\Pi^{(2)}(k_1^2) &= \frac{1}{D-1} \Pi_{\mu\mu}^{(2)}(k_1) \\ &= \frac{e^2}{(2\pi)^D} \frac{4}{D-1} \int \frac{Dm^2 + (2-D)k_2 \cdot (k_1 + k_2)}{(k_2^2 - m^2) [(k_1 + k_2)^2 - m^2]} d^D k_2. \quad (6.22)\end{aligned}$$

$\Pi^{(2)}(k_1^2)$ is divergent and we replace it by:

$$\Pi_R^{(2)}(k_1^2) = \Pi^{(2)}(k_1^2) - \Pi^{(2)}(0) - k_1^2 \left(\frac{\partial \Pi^{(2)}(k_1^2)}{\partial k_1^2} \right)_{k_1^2=0} \quad (6.23)$$

where $\Pi^{(2)}(0) = 0$, and

$$\left(-\frac{\partial \Pi^{(2)}(k_1^2)}{\partial k_1^2} \right)_{k_1^2=0} = \frac{e^2}{(2\pi)^D} \frac{4}{3} \int \frac{d^D k_2}{(k_2^2 - m^2)^2} \quad (6.24)$$

We shift the integration variable $k_2 \rightarrow k_2 + p$ so that the denominators in the above integrals become of the same form as in (6.2). The renormalized vacuum polarization is now:

$$\begin{aligned}\Pi_R^{(2)}(k_1^2) &= \frac{e^2}{(2\pi)^D} \int d^D k_2 \left[-\frac{4}{3} \frac{k_1^2}{(k_2^2 + 2p \cdot k_2)^2} \right. \\ &\quad \left. + \frac{4}{D-1} \frac{2m^2 + (2-D)(k_2^2 + k_1 \cdot k_2 + k_1 \cdot p + 2k_2 \cdot p)}{(k_2^2 + 2p \cdot k_2)((k_1 + k_2)^2 + 2p \cdot (k_1 + k_2))} \right] \quad (6.25)\end{aligned}$$

We now proceed to the actual calculation of the correction to the anomalous magnetic moment. The vertex function of an electron is parametrized by two formfactors:

$$\Gamma_\mu(p, p+q) = F_1(q^2) \gamma_\mu + F_2(q^2) \frac{i}{2m} q^\nu \sigma_{\mu\nu} \quad (6.26)$$

and the radiative correction to the magnetic moment is given by $\Delta g \equiv F_2(0)$. This means that we do not need the complete expression for the diagram in Figure 6.1 but only this part of it which contributes to $q^\nu \sigma_{\mu\nu}$.

In order to isolate this part we note that another vertex can be (artificially) constructed by taking a particular linear combination of γ_μ and $q^\nu \sigma_{\mu\nu}$

so that the interference term between the two interactions contains only $F_2(0)$, namely:

$$F_2(0)q^\rho = \frac{1}{16m^3(D-2)} \cdot \text{Tr}[(\not{p} + \not{q} + m)\Gamma_\mu(p, p+q)(\not{p} + m)(2m\sigma^{\mu\rho} - i(D-1)\gamma^\mu q^\rho)]. \quad (6.27)$$

This formula proves very useful for calculating contributions of various processes to the magnetic moment. In the case at hand we substitute for $\Gamma_\mu(p, p+q)$ the expression (6.18). The trace of gamma matrices is most easily calculated using the algebraic manipulation program FORM [32]. The next step is to perform the double integration over k_1 and k_2 . But in the framework of the GBGS method this only requires some algebra for which we employ Mathematica [64]. All scalar products in the numerator of the integrand can be expressed by combinations of scalar expressions in the denominator so that we are left with a sum of integrals $N(\alpha_1, \alpha_2, \alpha_3, \alpha_4, \alpha_5)$ and $M(\alpha_1, \alpha_2, \alpha_3, \alpha_4, \alpha_5)$. Using the GBGS recurrence relations we reduce all integrals to the following combinations of R_1 and R_2 , defined in the formula (6.5):

$$F_2(0) = \frac{\alpha^2}{216\pi^2} \left[(108 - 180\varepsilon + 183\varepsilon^2) R_1 + (144 - 240\varepsilon - 708\varepsilon^2) R_2 \right] + O(\varepsilon) \quad (6.28)$$

We expand R_1 and R_2 in Laurent series around $\varepsilon = 0$:

$$\begin{aligned} R_1 &= \frac{1}{\varepsilon^2} - \frac{2\gamma}{\varepsilon} + 2\gamma^2 + \frac{\pi^2}{6} + O(\varepsilon), \\ R_2 &= -\frac{3}{4\varepsilon^2} + \frac{3\gamma}{2\varepsilon} - \frac{3\gamma^2}{2} - \frac{5\pi^2}{8} + O(\varepsilon). \end{aligned} \quad (6.29)$$

The coefficients in the equation (6.28) are such that both poles and terms containing the Euler constant vanish and in the limit $\varepsilon \rightarrow 0$, $F_2(0) = \frac{\alpha^2}{\pi^2} \left(\frac{119}{36} - \frac{\pi^2}{3} \right)$. This is a well known result, derived first by Sommerfield [86], but we believe that the present method greatly facilitates the task shifting the labor (algebra!) to the computer. In the next section the remaining, two-photon diagrams, are calculated.

6.5.2 Two-photon contributions

To the fourth order in the coupling constant e the remaining contribution to the anomalous magnetic moment of the electron comes from diagrams shown in Figure 6.2. Diagrams 6.2(c-f) should be accompanied by their mirror reflections, not shown in the figure.

Diagrams of the types 6.2(b-d) contain infinite one-loop corrections to the propagator and vertex functions. In order to get a sensible finite result we carry out the renormalization procedure [94]. In the case of the vertex this consists in subtracting from it its value with electron legs taken on-shell and momentum transfer equal to zero. For example, the unrenormalized amplitude corresponding to the diagram 6.2(c) is, in the Feynman gauge (for simplicity we drop the four-spinors representing the electron):

$$M_c = -e^3 \int \frac{d^D k}{(2\pi)^D} \frac{1}{k^2} \gamma^\alpha \frac{1}{\not{p} + \not{k} + \not{A} - m} \gamma^\mu \frac{1}{\not{p} + \not{k} - m} \Lambda_\alpha(p, p+k; k), \quad (6.30)$$

where the unrenormalized vertex function is defined by:

$$\Lambda_\alpha(p, p+k; k) = -e^2 \int \frac{d^D k_2}{(2\pi)^D} \frac{1}{k_2^2} \gamma^\beta \frac{1}{\not{p} + \not{k}_1 + \not{k}_2 - m} \gamma_\alpha \frac{1}{\not{p} + \not{k}_2 - m} \gamma_\beta, \quad (6.31)$$

and the renormalized one is obtained by making the following subtraction:

$$\Lambda_\alpha^R(p, p+k; k) = \Lambda_\alpha(p, p+k; k) - \Lambda_\alpha(p_0, p_0; 0), \quad (6.32)$$

with $p_0^2 = m^2$.

Similarly, the renormalized propagator is defined by:

$$\Sigma^R(p) = \Sigma(p) - \Sigma(p_0) - (\not{p} - m) \frac{\partial \Sigma(p)}{\partial \not{p}} \Big|_{p=p_0}. \quad (6.33)$$

Thanks to the Ward-Takahashi identity:

$$\Lambda_\alpha(p_0, p_0; 0) = - \frac{\partial \Sigma(p)}{\partial p^\alpha} \Big|_{p=p_0}, \quad (6.34)$$

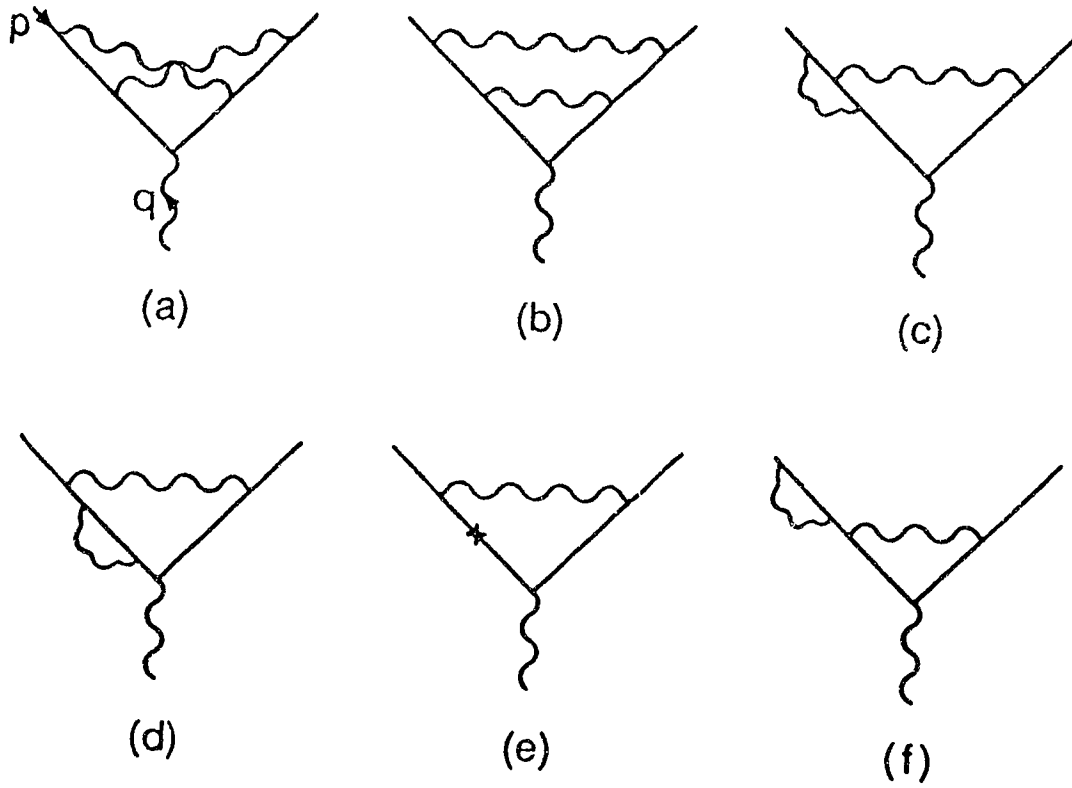


Figure 6.2: Two photon contributions to the anomalous magnetic moment

part of the infinities cancel after adding diagrams 6.2(c,d) and their mirror counterparts to the diagram 6.2(b). What remains are the mass counterterms $\Sigma(p_0)$, represented by 6.2(e), and half of the divergencies of the vertex functions 6.2(c), for which the subtraction is depicted by 6.2(f). We now briefly explain how these two diagrams are conveniently evaluated.

The mass counterterm is:

$$\begin{aligned}\Sigma(p_0) &= e^2 m^{1-2\varepsilon} \frac{3-2\varepsilon}{1-2\varepsilon} \frac{\Gamma(\varepsilon)}{(4\pi)^{\frac{D}{2}}} \\ &\equiv e^2 m \frac{3-2\varepsilon}{1-2\varepsilon} \int \frac{d^D k}{(2\pi)^D i} \frac{1}{(k^2 + 2k \cdot p)^2}\end{aligned}\quad (6.35)$$

which corresponds to a tadpole diagram inserted in place of the cross in the Figure 6.2(e), and this is just a product of one-loop integrals (6.18). The contribution symbolized by 6.2(f) is a product of the wave-function renormalization constant:

$$\left. \frac{\partial \Sigma(p)}{\partial \not{p}} \right|_{p=p_0} = -e^2 \frac{\Gamma(1+\varepsilon)}{(4\pi)^{\frac{D}{2}}} \left(\frac{3}{\varepsilon} + 4 \right) \quad (6.36)$$

and the one-loop correction to the magnetic moment, which in $(4-2\varepsilon)$ -dimensions is:

$$\frac{\alpha}{\pi} C_1(\varepsilon) = \frac{\alpha}{\pi} \frac{\pi^\varepsilon}{2^{1-2\varepsilon}} \Gamma(1+\varepsilon) \frac{1+2\varepsilon}{1-2\varepsilon} \quad (6.37)$$

After this discussion it is clear how the diagrams 6.2(a-e) are expressed in the form of integrals (6.2). To perform this calculation we have used symbolic manipulation programs FORM [32] and Mathematica [64].

In Table 6.4 the results of the calculation for each diagram in Figure 6.2 are summarized (together with their mirror counterparts, where applicable), in the limit $\varepsilon \rightarrow 0$. We have used the value of the integral $N(1,1,1,1,1) \equiv I(0) = \pi^2 \ln 2 - \frac{3}{2}\zeta(3)$, computed in [93]. For the sake of completeness the contribution from the vacuum polarization diagram is also listed in Table 6.4. The total correction is the same as the one computed by Sommerfield [85, 86] and Petermann [87, 88].

It can now be seen that the GBGS method greatly simplifies the calculation of the two-loop correction to the magnetic moment of the electron. In principle it can also be extended to calculations of three-loop diagrams

Table 6.4: Contributions of diagrams in Figure 6.2 to the anomalous magnetic moment of the electron.

Diagram	Coefficient of $\left(\frac{\alpha}{\pi}\right)^2$
1a	$\frac{1}{6} - \frac{5}{6}I(0) + \frac{13}{36}\pi^2$
1b	$\frac{3}{8\varepsilon} - \frac{3}{4}\gamma + \frac{107}{48} + \frac{1}{18}\pi^2$
1c	$\frac{1}{4\varepsilon} - \frac{1}{2}\gamma - \frac{19}{24} + \frac{1}{3}I(0) + \frac{1}{18}\pi^2$
1d	$\frac{1}{2\varepsilon} - \gamma + \frac{5}{24} - \frac{1}{18}\pi^2$
1e	$-\frac{3}{4\varepsilon} + \frac{3}{2}\gamma - \frac{7}{4}$
1f	$-\frac{3}{8\varepsilon} + \frac{3}{4}\gamma - 2$
Vac. pol.	$\frac{119}{36} - \frac{1}{3}\pi^2$
Total	$\frac{197}{144} + \frac{1}{12}\pi^2 + \frac{3}{4}\zeta(3) - \frac{1}{2}\pi^2 \ln 2$

and first steps in this direction have been made [95]. Calculation of two-loop corrections to the decay of a heavy quark can become another important application. This is worth studying both in the effective field theory approach [96] and in the exact QCD in the limit of the very large quark mass. The following section shows a calculation of one of relevant diagrams using traditional methods. The result suggests that GBGS method might also be applied to this case.

6.6 On the two loop corrections to top decay

In order to suggest a possible new application of the GBGS method I would like to discuss in this section one diagram contributing to two loop QCD corrections to the decay $t \rightarrow W^+ b$. A general calculation of these corrections has yet to be done, but the vacuum polarization effect in the gluon propagator is easy to evaluate. The topology of this diagram is the same as in the figure 6.1. We make the following approximation: the mass of the decaying quark is taken to be very large, so that we can neglect masses of the quarks in the vacuum polarization loop, as well as mass of the quark in the final state and of the W boson. The renormalization is not discussed: the sole purpose of this calculation is to demonstrate that the result turns out to be proportional to one of the three integrals on which the GBGS method is built – although the diagram in question is not of the propagator type.

Four-momenta of the initial quark, final quark and W boson are denoted by Q , q and W respectively, and we take $Q^2 = 1$, $q^2 = W^2 = 0$. To the leading order in m_W/m_Q we only have to retain the term $W_\mu W_\nu/m_W^2$ in the sum over polarizations of the W boson. In this approximation the amplitude of the process under consideration is proportional to:

$$\Lambda \bar{u}_q (1 - \gamma_5) u_Q \equiv \bar{u}_q \int \frac{d^D k}{(2\pi)^D i} \frac{1}{k^4} \Pi^{\alpha\beta}(k^2) \left[\gamma_\alpha \frac{-1}{\not{q} + \not{k}} (\not{Q} - \not{q}) (1 - \gamma_5) \frac{1}{1 - \not{Q} - \not{k}} \gamma_\beta \right] u_Q. \quad (6.38)$$

where the quark contribution to the vacuum polarization is

$$\Pi^{\alpha\beta}(k^2) = C k^{-2\epsilon} (k^2 g^{\mu\nu} - k^\mu k^\nu), \quad (6.39)$$

and C is a constant independent of the gluon momentum k . The calculation is considerably simplified by the fact that $k^\mu k^\nu$ part of the vacuum polarization does not contribute to Λ . The integration over k can be done exactly and the result is ¹:

$$\Lambda = -\frac{4(-1)^{-2\varepsilon}}{3(4\pi)^D} \frac{\varepsilon(1-\varepsilon)(-2+9\varepsilon-23\varepsilon^2+30\varepsilon^3-16\varepsilon^4)}{(1-2\varepsilon)(1-3\varepsilon)(3-2\varepsilon)(1-2\varepsilon)(2-3\varepsilon)} \frac{\varepsilon\Gamma^2(-\varepsilon)\Gamma(-4\varepsilon)\Gamma(2\varepsilon)\Gamma(\varepsilon)}{\Gamma(-2\varepsilon)\Gamma(-3\varepsilon)}. \quad (6.40)$$

We see that the result is proportional to the integral structure R_2 introduced in eq. 6.5. It is quite surprising that a diagram with non-zero momentum transfer (W) gives a result very similar to massive propagator type integrals. The reason might be that the integral considered here depends on a single mass scale, set by the decaying heavy quark [97]. An application of the GBGS method to general 2-loop corrections to the top decay is under investigation.

¹I am very grateful to Dr. Q.P. Xu for checking this formula.

Chapter 7

Conclusions and Outlook

In this thesis we have presented and discussed various aspects of quantum corrections to decays of heavy quarks. Here I would like to list the main problems examined in this thesis and point out some new directions of studies suggested by the results obtained.

Typical size of QCD corrections to the width of the top quark was shown to be of the order of 10% for both Standard Model decay channels and for the decays involving a charged Higgs boson. Corrections to the energy spectrum of hadronic products in semileptonic decays were also of this order, which will make it hard to test them experimentally using hadronic calorimeters.

The analysis of the angular distribution of charged leptons in semileptonic decays is of greater practical importance. The fact that the QCD corrections leave the shape of the distribution characteristic of a spin one-half particle essentially unmodified is important for future observation of possible CP violating effects in $t\bar{t}$ production at hadron supercolliders. It would be interesting to examine the corresponding effect of electroweak corrections in decays of polarized top quarks.

Electroweak corrections were presented here for the partial width of top quark decaying into bottom quark and a charged Higgs. A number of interesting features were observed in the dependence of the corrections on the ratio of expectation values of the two Higgs doublets, as well as on the mass of the charged Higgs boson. Although the size of corrections to this particular decay mode was rather small (typically of the order of 5%), some important problems in this area were noticed and should be solved in future. The currently popular renormalization scheme based on the condition of vanishing of

radiative corrections to one particular vertex (e.g. the interaction of charged Higgs with τ lepton and its neutrino) is very cumbersome in a calculation which takes into account full electroweak corrections. On the other hand, recently proposed scheme of calculations of neutral Higgs bosons decays [98] could probably be successfully applied to the charged Higgs boson decays as well. If the two Higgs doublet model is confirmed experimentally and the decays of charged Higgs bosons are to be studied in future precision experiments, it will be important to have a simple and natural renormalization scheme for calculations of radiative corrections to their decays. Work on this is now in progress.

It would also be important to compare electroweak corrections to the charged Higgs channel of the top quark decay with the Standard Model process $t \rightarrow W^+b$. To this end the Equivalence Theorem should be applied: in consequence one could obtain an excellent check of the results, as was done in the case of QCD corrections.

Some technical aspects of calculations of radiative corrections to decays of the top quark were also discussed in this thesis. It was shown to be advantageous to employ dimensional regularization to the treatment of not only ultraviolet divergences, but also to the infrared ones occurring in the calculation of soft and collinear gluon radiation. The results obtained in this way for the total rate of the decay $t \rightarrow W^+b$ confirmed previously published formulas of Jeżabek and Kühn. The same method was successfully applied to the analysis $t \rightarrow H^+b$. Dimensional regularization is also essential in the algebraic method of doing two loop calculations, proposed by Broadhurst et al. This approach was discussed with an example of calculating the anomalous magnetic moment of an electron. We hope to apply this method to the problem of two loop QCD corrections to the decay of heavy quarks.

Bibliography

- [1] M. Jeżabek and J. H. Kühn. Lepton spectra from heavy quark decay. *Nucl. Phys.*, B320:20–44, 1989.
- [2] M. Jeżabek and J.H. Kühn. QCD corrections to semileptonic decays of heavy quarks. *Nucl. Phys.*, B314:1–6, 1989.
- [3] B. Grzadkowski and W. Hollik. Radiative corrections to the top quark width within two-Higgs-doublet models. *Nucl. Phys.*, B384:101–112, 1992.
- [4] A. Denner and A.H. Hoang. The top decay $t \rightarrow bW$ in the two Higgs doublet model. *Nucl. Phys.*, B397:483–501, 1993.
- [5] J. F. Gunion, H. E. Haber, G. Kane, and S. Dawson. *The Higgs Hunter's Guide*. Addison-Wesley, Redwood City, 1990. Errata: hep-ph/9302272.
- [6] A. Czarnecki, M. Jeżabek, and J. H. Kühn. Hadron spectra from semileptonic decays of heavy quarks. *Acta Phys. Pol.*, B20:961, 1989. Erratum: *ibid*, **B23**, 173 (1992).
- [7] A. Czarnecki, M. Jeżabek, and J.H. Kühn. Lepton spectra from decays of polarized top quarks. *Nuclear Physics*, B351:70–80, 1991.
- [8] A. Czarnecki. QCD corrections to the decay $t \rightarrow Wb$ in dimensional regularization. *Phys. Lett.*, B252:467–470, 1990.
- [9] A. Czarnecki and S. Davidson. On the QCD corrections to the charged Higgs decay of a heavy quark. *Phys. Rev.*, D47:3063–3064, 1992.
- [10] A. Czarnecki and S. Davidson. QCD corrections to the charged Higgs decay of a heavy quark. *Phys. Rev. D*, 1993. in press.

- [11] A. Czarnecki and S. Davidson. Equivalence theorem and two body top quark decays. In *Proc. of the 8th Lake Louise Winter Institute*, 1993. To appear.
- [12] A. Czarnecki and A. N. Kamal. On the two-loop calculation of the anomalous magnetic moment of the electron. *Acta Phys. Polonica*, B23:1063–1073, 1992.
- [13] A. Czarnecki. Electroweak corrections to decays involving a charged Higgs boson. preprint Alberta Thy-29-93, submitted for publication in Physical Review D, 1993.
- [14] T. Muta. *Foundations of Quantum Chromodynamics*. World Scientific, Singapore, 1987.
- [15] P. Pascual and R. Tarrach. *QCD: Renormalization for the Practitioner*. Springer-Verlag, Berlin, 1984.
- [16] W. Celmaster and R.J. Gonsalves. Renormalization-prescription dependence of the quantum-chromodynamic coupling constant. *Phys. Rev.*, D20:1420, 1979.
- [17] T.D. Lee. *Particle Physics and Introduction to Field Theory*. Harwood Academic Publ., Chur, Switzerland, 1988.
- [18] N. Nakanishi and I. Ojima. *Covariant operator formalism of gauge theories and quantum gravity*. World Scientific, Singapore, 1990.
- [19] L.D. Faddeev and A.A. Slavnov. *Gauge Fields: introduction to quantum theory*. Benjamin/Cummings, Reading, Mass., 1980.
- [20] J.C. Taylor. *Gauge theories of weak interactions*. Cambridge Univ. Press, Cambridge, 1976.
- [21] G. 't Hooft and M. Veltman. Combinatorics of gauge fields. *Nucl. Phys.*, B50:318–353, 1972.
- [22] G. 't Hooft and M. Veltman. Example of a gauge field theory. In C.P. Korthals-Altes, editor, *Colloquium on Renormalization of Yang-Mills Fields and Applications to Particle Physics*, pages 37–75, Marseille, 1972.

- [23] C. Becchi, A. Rouet, and R. Stora. The abelian Higgs-Kibble model. unitarity of the S-operator. *Phys. Lett.*, B52:344, 1974.
- [24] C. Becchi, A. Rouet, and R. Stora. Renormalization of gauge theories. *Ann. Phys.*, 98:287, 1976.
- [25] I.V. Tyutin. Gauge invariance in field theory and in statistical physics in the operator formulation. Lebedev preprint FIAN 39, in Russian, unpublished, 1975.
- [26] F.J. Yndurain. *Quantum Chromodynamics*. Springer-Verlag, New York, 1983.
- [27] L. Baulieu. Perturbative gauge theories. *Phys. Rep.*, 129:1–74, 1985.
- [28] J.C. Ward. An identity in quantum electrodynamics. *Phys. Rev.*, 78:182, 1950.
- [29] Y. Takahashi. On the generalized Ward identity. *Nuovo Cim.*, 6:371–375, 1957.
- [30] J.C. Taylor. Ward identities and charge renormalization of the Yang-Mills field. *Nucl. Phys.*, B33:436, 1971.
- [31] A.A. Slavnov. Renormalization of gauge-invariant theories. *Sov. J. Particles and Nuclei*, 5:303–317, 1975.
- [32] J. A. M. Vermaseren. *FORM 1.0*. Amsterdam, 1989.
- [33] Particle Data Group. Review of particle properties. *Phys. Rev.*, D45, Part II, 1992.
- [34] C.R. Schmidt and M.E. Peskin. Probe of CP violation in top quark pair production at hadron supercolliders. *Phys. Rev. Letters*, 69:410–413, 1992.
- [35] M. Jezabek and J.H. Kühn. Semileptonic decays of top quark. *Phys. Lett.*, B207:91–96, 1988.
- [36] J.H. Kühn. Topics in top quark physics. 1993. Karlsruhe preprint TTP 93-18.

- [37] G. Altarelli, N. Cabbibo, G. Corbò, L. Maiani, and G. Martinelli. Leptonic decay of heavy flavors: a theoretical update. *Nucl. Phys.*, B208:365–380, 1982.
- [38] A. Ali and E. Pietarinen. Semileptonic decays of heavy quarks in quantum chromodynamics. *Nucl. Phys.*, B154:519–534, 1979.
- [39] R.J. Finkelstein R. E. Behrends and A. Sirlin. Radiative corrections to decay processes. *Phys. Rev.*, 101:866, 1956.
- [40] S. Berman. Radiative corrections to muon and neutron decay. *Phys. Rev.*, 112:267, 1958.
- [41] T. Kinoshita and A. Sirlin. Radiative corrections to Fermi interactions. *Phys. Rev.*, 113:1652, 1959.
- [42] L. Lewin. *Polylogarithms and associated functions*. North Holland, New York, 1981.
- [43] J.H. Kühn. How to measure the polarization of top quarks. *Nucl. Phys.*, B237:77–85, 1984.
- [44] Q. Hokim and Xuan-Yem Pham. Exact one-gluon corrections for inclusive weak processes. *Ann. Phys.*, 155:202–227, 1984.
- [45] R. Gastmans and R. Meuldermans. Dimensional regularization of the infrared problem. *Nucl. Phys.*, B63:277–284, 1973.
- [46] W. J. Marciano and A. Sirlin. Dimensional regularization of infrared divergences. *Nucl. Phys.*, B88:86–98, 1975.
- [47] L. Pondrom. Results from hadron colliders: Rapporteur talk. In K.K. Phua and Y. Yamaguchi, editors, *Proc. of the 25th Int. Conf. on High Energy Physics*, Singapore, 1990.
- [48] R. Peccei. The Standard Model and beyond. In A. Astbury, B. A. Campbell, S. Godfrey, P. Kalyniuk, A. N. Kamal, and F. C. Khanna, editors, *Proc. of the 5th Lake Louise Winter Institute*, Singapore, 1990. World Scientific.

- [49] M. Mannelli. Precision electroweak physics at LEP. 1993. Talk given at the XXI Summer SLAC Institute.
- [50] Y.P. Yao. Radiative corrections to $t \rightarrow b + W$. In K.K. Phua and Y. Yamaguchi, editors, *Proc. of the 25th Int. Conf. on High Energy Physics*, Singapore, 1990.
- [51] G. 't Hooft and M. Veltman. Regularization and renormalization of gauge fields. *Nucl. Phys.*, B44:189–213, 1972.
- [52] J. Liu and Y. P. Yao. QCD correction to heavy top exclusive decays. preprint UM-TH-90-09, 1990.
- [53] J. Reid, G. Tupper, G. Li, and M.A. Samuel. Heavy top quark decay into a charged Higgs scalar and a photon (gluon). *Zeit. Phys.*, C51:395, 1991.
- [54] C.S. Li and T.C. Yuan. QCD correction to charged Higgs decay of the top quark. *Phys. Rev.*, D42:3088, 1990. Erratum: *ibid.* **D47**, 2156 (1993).
- [55] C.S. Li, Y.S. Wei, and J.M. Yang. The b quark mass effect in the QCD correction to charged-Higgs-boson decay of the top quark. *Phys. Lett.*, B285:137–140, 1992.
- [56] J.M. Cornwall, D.N. Levin, and G. Tiktopoulos. Derivation of gauge invariance from high-energy unitarity bounds on the S matrix. *Phys. Rev.*, D10:1145, 1974.
- [57] M.S. Chanowitz and M.K. Gaillard. The TeV physics of strongly interacting W 's and Z 's. *Nucl. Phys.*, B261:379–431, 1985.
- [58] H. Veltman. The Equivalence Theorem. *Phys. Rev.*, D41:2294, 1990.
- [59] J. Liu and Y.P. Yao. QCD corrections to the charged-Higgs-boson decay of a heavy top quark. *Phys. Rev.*, D46:5196–5199, 1992.
- [60] E. Braaten and J.P. Leveille. Higgs-boson decay and the running mass. *Phys. Rev.*, D22:715–721, 1980.

- [61] B. Guberina, R.D. Peccei, and R. R  ckl. Dimensional regularization techniques and their uses in calculating infrared safe weak processes. *Nucl. Phys.*, 171:333–361, 1980.
- [62] J. Liu and Y.P. Yao. One loop radiative corrections to a heavy top decay in the Standard Model. *Int. J. Mod. Phys.*, A6:4925–4948, 1991.
- [63] C. S. Li, R. J. Oakes, and T. C. Yuan. QCD corrections to $t \rightarrow W^+ + b$. *Phys. Rev.*, D43:3759–3762, 1991.
- [64] S. Wolfram. *Mathematica – A System for Doing Mathematics by Computer*. Addison-Wesley, Redwood City, 1991.
- [65] G.J. Gounaris, R. K  gerler, and H. Neufeld. On the relationship between longitudinally polarized vector bosons and their unphysical scalar partners. *Phys. Rev.*, D34:3257, 1986.
- [66] W.B. Kilgore. The equivalence theorem in the abelian Higgs theory. *Phys. Lett.*, B294:257–262, 1992.
- [67] J. Bagger and C.R. Schmidt. Equivalence theorem redux. *Phys. Rev.*, D41:264, 1990.
- [68] C. Becchi, A. Rouet, and R. Stora. Renormalization of the abelian Higgs-Kibble model. *Comm. Math. Phys.*, 42:127–162, 1975.
- [69] J.F. Gunion and H.E. Haber. Higgs bosons in supersymmetric models (I). *Nucl. Phys.*, B272:1–76, 1986. Errata: hep-ph/9301205.
- [70] C.S. Li, B.Q. Hu, and J.M. Yang. Electroweak radiative corrections to $t \rightarrow H^+ b$ for a heavy top quark. *Phys. Rev.*, D47:2865–2871, 1993.
- [71] M.A. D  az. Top quark and charged Higgs: linked by radiative corrections. Preprint VAND-TH-93-5.
- [72] A. M  ndez and A. Pomarol. t-quark loop corrections to the charged Higgs boson hadronic width. *Phys. Lett.*, B265:177–181, 1991.
- [73] A. M  ndez and A. Pomarol. t-quark loop corrections to neutral Higgs couplings in the two-Higgs-doublet model. *Phys. Lett.*, B279:98–105, 1991.

- [74] M. Böhm and A. Denner. Radiative corrections in the electroweak Standard Model. In A. Perez and Roberto Huerta, editors, *Proc. of the Workshop on High Energy Phenomenology, Mexico City*, pages 1–113, River Edge, N.J., 1991. World Scientific.
- [75] A. Denner. Techniques for the calculation of electroweak radiative corrections at the one-loop level and results for W-physics at LEP200. *Fortschr. Phys.*, 41:307–420, 1993.
- [76] A. Hoang. Tau- und Top-Zerfälle im Zwei-Higgs-Dublett-Modell. Master's thesis, Karlsruhe University, 1992. In German.
- [77] M. Veltman. The infrared-ultraviolet connection. *Acta Phys. Pol.*, B12:437–457, 1981.
- [78] M. Capdequi Peyranère, H.E. Haber, and P. Irulegui. $H^\pm \rightarrow W^\pm \gamma$ and $H^\pm \rightarrow W^\pm Z$ in two-Higgs-doublet models: large-fermion-mass limit. *Phys. Rev.*, D44:191–201, 1991.
- [79] J. Kühnbeck, M. Böhm, and A. Denner. Feyn Arts - computer-algebraic generation of Feynman graphs and amplitudes. *Comp. Phys. Comm.*, 60:165–180, 1990.
- [80] R. Mertig, M. Böhm, and A. Denner. Feyn Calc - computer-algebraic calculation of Feynman diagrams. *Comp. Phys. Comm.*, 64:345–359, 1991.
- [81] G.J. van Oldenborgh. FF - a package to evaluate one-loop Feynman diagrams. *Comp. Phys. Comm.*, 48:1, 1991.
- [82] G. Passarino and M. Veltman. One loop corrections for e^+e^- annihilation into $\mu^+\mu^-$ in the Weinberg model. *Nucl. Phys.*, B160:151, 1979.
- [83] T. Kinoshita and D.R. Yennie. High precision tests of quantum electrodynamics: an overview. In T. Kinoshita, editor, *Quantum Electrodynamics*, pages 1–14. World Scientific, Singapore, 1990.
- [84] J. Schwinger. On quantum-electrodynamics and the magnetic moment of the electron. *Phys. Rev.*, 73:416, 1948.

- [85] C.M. Sommerfield. Magnetic dipole moment of the electron. *Phys. Rev.*, 107:328, 1957.
- [86] C.M. Sommerfield. The magnetic moment of the electron. *Ann. Phys.*, 5:26–57, 1958.
- [87] A. Petermann. Magnetic moment of the electron. *Nucl. Phys.*, 3:689–690, 1957.
- [88] A. Petermann. Fourth order magnetic moment of the electron. *Helv. Phys. Acta*, 30:407–408, 1957.
- [89] J. Schwinger. *Particles, sources and fields*, volume III. Addison-Wesley, Redwood City, 1988.
- [90] R. Z. Koskies, M. J. Levine, and E. Remiddi. Analytic evaluation of sixth order contributions to the electron’s g factor. In T. Kinoshita, editor, *Quantum Electrodynamics*, pages 162–217. World Scientific, Singapore, 1990.
- [91] N. Gray, D. J. Broadhurst, W. Grafe, and K. Schilcher. Three-loop relation of quark $\overline{\text{MS}}$ and pole masses. *Zeit. Phys.*, C48:673, 1990.
- [92] K.G. Chetyrkin and F.V. Tkachov. Integration by parts: the algorithm to calculate β -functions in 4 loops. *Nucl. Phys.*, B192:159–204, 1981.
- [93] D. J. Broadhurst. The master two-loop diagram with masses. *Zeit. Phys.*, C47:115–124, 1990.
- [94] A. I. Akhiezer and V. B. Berestetskii. *Quantum Electrodynamics*. Interscience Publ., New York, 1965.
- [95] D. J. Broadhurst. Three-loop on-shell charge renormalization without integration: $\Lambda_{\overline{QED}}^{\overline{\text{MS}}}$ to four loops. *Zeit. Phys.*, C54:599–606, 1992.
- [96] D. J. Broadhurst and A. G. Grozin. Operator product expansion in static-quark effective field theory. large perturbative correction. *Phys. Lett.*, B274:421–427, 1992.
- [97] D. J. Broadhurst. Which Feynman diagrams are algebraically computable? 1992. Open University preprint OUT-4102-37.

- [98] P. Chankowski, S. Pokorski, and J. Rosiek. Complete on-shell renormalization scheme for the minimal supersymmetric Higgs sector. 1992. Preprint MPI-PH-92-117.